The role of the apoptosis and splicing associated protein Acinus during apoptotic nuclear changes

Inaugural-Dissertation

zur Erlangung des Doktorgrades der
Mathematisch-Naturwissenschaftlichen Fakultät
der Heinrich-Heine-Universität Düsseldorf

vorgelegt von
ALVIN PAUL JOSELIN
aus
Nagercoil, Indien
Düsseldorf, 2006

Aus dem Institut für Molekulare Medizin

der Heinrich-Heine Universität Düsseldorf

Gedruckt mit der Genehmigung der

Mathematisch-Naturwissenschaftlichen Fakultät der

Heinrich-Heine-Universität Düsseldorf

Referent: Prof. Dr. Klaus Schulze-Osthoff

Koreferent: Prof. Dr. Heinz Mehlhorn

Tag der mündlichen Prüfung:

09 Nov 2006

I. ACKNOWLEDGEMENTS

This work was performed at the Institut für Molekulare Medizin, Heinrich-Heine-Universität Düsseldorf.

I would like to thank Prof. Dr. Klaus Schulze-Osthoff for his support, encouragement and advise concerning the project.

I would also like to thank Dr. Christian Schwerk, my supervisor and mentor, for his invaluable discussions, criticisms and timely motivation, which helped me on to thinking independently and acquiring the skills that I needed to perform experimentation successfully.

I thank Prof. Dr. Heinz Mehlhorn for making it possible for me to present this thesis.

I am grateful to Fr. Dr. med. Grete Berns and Dr. Matthias Drechsler for their help with performing pulsed-field gel electrophoresis. Thanks also to Dr. Axel Schwerk for his help with the statistical analyses.

My gratitude and appreciation to all my colleagues at the Institut für Molekulare Medizin, especially Ute, Frank, Vilma and Stephan, for their support and assistance, not to mention the innumerable phone calls they made on my behalf.

Thanks to my mom and dad for giving me the opportunity to study. And finally, I'm thankful to my wife for her presence, patience and for proofreading and correcting the many passive voices in my dissertation.

II. INDICES

II.1. TABLE OF CONTENTS

II.2. ABBREVIATIONS

$\Delta\Psi_m$	mitochondrial membrane potential
A/T	adenine thymine
aa	amino acid
AIF	apoptosis inducing factor
Amp	ampicillin
Apaf-1	apoptotic protease activating factor-1
ASAP	apoptosis and splicing associated protein
ASF/SF2	alternative splicing factor/ splicing factor 2
ATP	adenosine triphosphate
Bak	Bcl-2 homologous antagonist/killer
Bax	Bcl-2 associated X-protein
Bcl-2	B cell leukemia-2
BSA	bovine serum albumin
CAD	caspase-activated DNase
CARD	caspase recruitment domain
CED	cell death-defective
CIDE	cell-inducing DFF45-like effector
CPAN	caspase activated nuclease
C-terminal	carboxy terminal
dATP	deoxy adenosine triphosphate
DFF	DNA fragmentation factor
DNA	deoxyribonucleic acid
dNTP	deoxynucleotide triphosphate
DR	death receptor
dsDNA	double-stranded DNA
dsRNA	double-stranded RNA
DTT	dithiothreitol
ECL	enhanced chemo luminescence
EDTA	ethylenediamine tetraacetic acid
EJC	exon junction complex

ER	endoplasmic reticulum
FACS	fluorescence-activated cell sorting
FADD	Fas associated protein with death domain
HDAC	histone deacetylases
HEPES	N- (2-hydroxyethyl) piperazine-N`-(2-ethanesulfonicacid)
HMGB	high mobility group protein
HMW	high molecular weight
HSP	heat shock protein
ICAD	inhibitor of CAD
kb	kilo base
kDa	kilo Dalton
LMW	low molecular weight
miRNA	microRNA
MMP	mitochondrial membrane permeabilization
mRNA	messenger RNA
NGFR	nerve growth factor receptor
NLS	nuclear localization signal
NMD	nonsense-mediated mRNA decay
NP-40	Nonidet P-40
N-terminal	amino terminal
NuMA	nuclear mitotic apparatus protein
OD	optical density
ORF	open reading frame
PAGE	polyacrylamide gel electrophoresis
PARP	poly (ADP-ribose) polymerase
PBS	phosphate-buffered saline
PCR	polymerase chain reaction
PMSF	phenylmethylsulfonylfluoride
PS	phosphatidylserine
PTC	premature termination codon
rasiRNA	repeat-associated small interfering RNA
RISC	RNA-induced silencing complex

RNA	ribonucleic acid
RNAi	RNA interference
rpm	rounds per minute
RT	room temperature
SAP18	Sin3-associated polypeptide of 18 kDa
SDS	sodium dodecyl sulfate
shRNA	short hairpin RNA
siRNA	small interfering RNA
SR	serine/arginine
ssDNA	single-stranded DNA
STS	staurosporine
Taq	Thermus aquaticus
TBE	Tris / boric acid / EDTA
TE	Tris / EDTA
TetR	Tet repressor
TNF-α	tumor necrosis factor alpha
TNFR	TNF receptor
TRAIL	TNF-related apoptosis inducing ligand
UV	ultraviolet

II.3. FIGURE INDEX

II.4. TABLE INDEX

III. INTRODUCTION

III.1. PROGRAMMED CELL DEATH: AN OVERVIEW

The term ‘apoptosis’ was first introduced in 1972 to describe the morphological processes that led to a controlled self-destruction of the cell (Kerr et al., 1972). Apoptosis is a morphologically distinct, genetically controlled form of cell death by which superfluous or abnormal cells are eliminated in multicellular organisms during embryonic development, immune system function and during the maintenance of tissue homeostasis (Wyllie et al., 1980).

The two most common types of cell death that have been described in vertebrate tissues are apoptosis and necrosis. During necrosis, cells endure a major insult resulting in swelling and rupture causing the release of cellular content into the cells environment. This elicits a strong inflammatory response in the surrounding tissue. In contrast, the changes occurring in apoptotic cells are a consequence of controlled and coordinated molecular and biochemical events resulting in cell shrinkage, cleavage of the cellular deoxyribonucleic acid (DNA) into oligonucleosomal fragments, condensation of the nuclear content, membrane blebbing and the eventual packing of the cellular content and the compacted chromatin into numerous membrane-enclosed structures called the ‘apoptotic bodies’ that are finally disposed by macrophages without inducing an inflammatory response (Kerr et al., 1972). Apoptosis is an active form of cell death and requires energy and protein synthesis (Wyllie et al., 1980).

In addition to ‘classical’ apoptosis, another type of programmed cell death, associated with autophagy, has also been described. Autophagy is non-apoptotic and non-necrotic but is similar to apoptosis in that it is also an active form of cell death. During autophagy, cells degrade their own organelles and cytoplasm (Dunn, 1994). Autophagy is characterized by early morphological changes such as the appearance of a double membrane-bound vacuole (autophagosome) throughout the cytoplasm, which is formed from the endoplasmic reticulum (Dunn, 1990a). During later stages of autophagy the autophagosome is converted into a single membrane-bound degrading vacuole,

the autolysosome, as it fuses with endosome, lysosome and Golgi elements containing acid hydrolases (Dunn, 1990b).

Apoptotic and autophagic cell death represent two distinct physiological processes that are commonplace during embryonic development (Oppenheim, 1991), formation and shaping of body parts (Haanen and Vermes, 1996), and mitochondrial turnover in non-proliferating tissues (Dunn, 1990a). Necrosis, on the other hand, occurs rapidly and has been defined as an accidental or an un-programmed form of cell death. However, chemically induced hypoxia, depending on the intensity of the insult, results in a form of cell death that shares molecular and morphological features of both apoptosis and necrosis and is sometimes referred to as aponecrosis (Formigli et al., 2000). This suggests that apoptosis may sometimes be re-programmed to the alternative form of cell death, necrosis. The switch in molecular mechanisms, such as inhibition of caspase-3, which is active in apoptotic cells but remains inactive in necrotic cells, could be a pivotal step in this transition of apoptosis to necrosis (Formigli et al., 2000). It follows therefore, that molecular processes are crucial for the completion of the apoptotic program.

III.2. MOLECULAR MECHANISMS DURING APOPTOSIS

Apoptotic cell death has been shown to occur in many different cell types. Due to their potential to induce death of the cell, components of the apoptotic machinery are tightly controlled within the cell until it receives appropriate stimuli. Apoptosis can be triggered in a cell by various signals, which could be either extracellular or intracellular in origin. The cell death process that follows can be categorized as either an extrinsic or intrinsic apoptotic pathway (Adams, 2003). Triggers that are extracellular in origin are mediated by the activation of the so called ‘death receptors’ which are cell surface receptors that transmit apoptotic signals after ligation with their corresponding ligand. Death receptors belong to the tumor necrosis factor receptor family (TNFR/NGFR) and include Fas/CD95/Apo1, TNFR1, TNFR2, DR3/Wsl-1/Tramp, DR4/TRAIL-R1 (TNF-related apoptosis-inducing ligand receptor-1), DR5/TRAIL-R2/TRICK2/Killer and DR6. Subsequent signaling is mediated by the cytoplasmic part of the death

receptor, which then transmits the death signal to the intracellular death machinery (Figure 2). This constitutes the extrinsic apoptotic pathway.

In addition to amplifying the death signals received from the extrinsic apoptotic pathways, the mitochondrion plays a central role in the mediation of the death signals that originate from within the cells (intrinsic pathway), such as DNA damage, oxidative stress, starvation as well as chemotherapeutic agents (Kaufmann and Earnshaw, 2000; Wang, 2001). Nevertheless, death signals of such diverse origin, extracellular or intracellular, seem to converge eventually to activate a common cell death machinery resulting in the characteristic molecular and morphological features of both the extrinsic and intrinsic pathways of apoptotic cell death (Figure 2).

III.2.A. ACTIVATION OF CASPASES

The most defining molecular feature of apoptosis is the activation of a family of cysteinyl aspartate-specific proteases, called caspases, which carry in their sequence the conserved pentapeptide active-motif, QACR(N/Q)G, with a catalytic cysteine (Cohen, 1997; Los et al., 1999; Patel et al., 1996; Thornberry and Lazebnik, 1998). In fact, strictly defined, cell death can only be classified as apoptosis if execution of cell death is by means of caspase activation (Leist and Jaattela, 2001). 14 Different members of the caspase-family have currently been identified in mammals. In addition to their role in apoptosis, a sub-group of caspases also act as pro-cytokine activators and are implicated in the process of inflammation (Tschopp et al., 2003). Caspases-1, -4, -5, -11 and -12, which belong to this sub-group, appear to be involved in the maturation of pro-inflammatory cytokines and their role in apoptosis is questionable (Denault and Salvesen, 2002).

The apoptotic caspases are further classified as either initiator (procaspase-2, -8, -9 and -10) or executioner caspases (procaspase-3, -6 and -7) depending on their point of entry into the apoptotic cascade. The initiator caspases are usually activated early in apoptosis, which then cleave and activate downstream executioner caspases (Boatright and Salvesen, 2003; Nicholson and Thornberry, 1997).

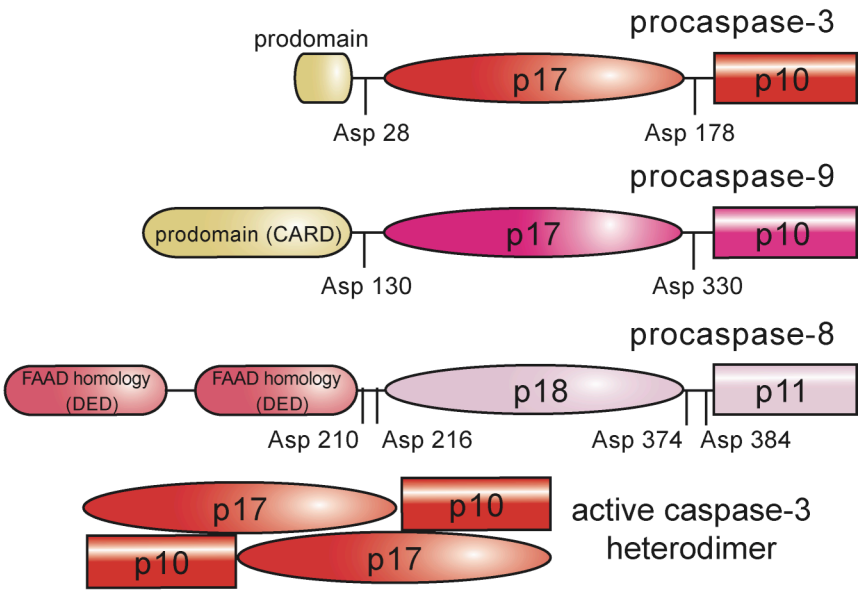

Figure 1: Schematic representation of caspase structure. A common feature of the caspase family of proteases is the presence of prodomains at their N-terminus that differ considerably in sequence. In general, executioner caspases such as procaspase-3 have shorter prodomains compared to the initiator caspases. Distinct sequences contained within the prodomain that determine the signaling pathway of caspase activation is indicated. The corresponding cleavage sites of the caspases are also indicated. Active caspases are a heterodimer of two small and two large subunits.

In the cells, caspases are synthesized as inactive zymogens called procaspases consisting of an N-terminal prodomain followed by one large and one small subunit separated by a spacer (Figure 1). Maturation of caspases consists of cleavage of the procaspase resulting in the generation of two subunits both of which are essential for the function of the mature enzyme. Active caspases are heterodimers of two large and two small subunits (Figure 1) (Cohen, 1997). Furthermore, all caspases specifically cleave their substrates at the Asp residue at the P_1 position of a conserved four amino acid sequence, which is also contained in all procaspases (Alnemri, 1997). Cleavage of procaspases is accomplished by autolysis or by upstream proteases, such as other caspases or granzyme B, which is the only mammalian serine protease that shares the caspase specificity for the Asp residue at the P_1 position.

Two prototypic mechanisms seem to regulate caspase activation. The end result of these distinct pathways is the activation of either caspase-8 or caspase-

9 (Budihardjo et al., 1999; Earnshaw et al., 1999). Activation of the extrinsic pathway by the ligation of a death ligand to its corresponding death receptor leads to receptor trimerization followed by recruitment of the adaptor protein FADD to the cytoplasmic domain of the receptor (Ashkenazi and Dixit, 1999). The multimeric protein FADD in turn recruits procaspase-8 molecules by virtue of their N-terminal prodomains, which contain a FAAD homology domain called death effector domain (DED). The prodomain, which has been hypothesized to maintain the procaspases in their inactive form, is also a necessary prerequisite for autoprocessing of the procaspases (Van Criekinge et al., 1996). Subsequent dimerization and autoprocessing of the procaspases at this complex, called the death inducing signaling complex (DISC), leads to the eventual activation and release of caspase-8 from the complex (Figure 2) (Medema et al., 1997).

Intrinsic apoptotic stimuli, such as treatment with the protein kinase inhibitor staurosporine (STS), activate downstream caspases through a pathway involving procaspase-9. These stimuli cause a change in the conformation and activity of proapoptotic Bcl-2 family members such as Bax and Bak (Desagher et al., 1999; Griffiths et al., 1999), which in turn results in the loss of mitochondrial membrane potential. Accumulation of Bax and Bak on the outer mitochondrial membrane causes them to di- or oligomerize. This increases their potential to form channels resulting in the release of cytochrome c and other apoptogenic factors from the mitochondria. The released cytochrome c binds to the cytoplasmic scaffolding protein Apaf-1 (apoptotic protease activating factor-1) that undergoes a conformational change and subsequent binding of ATP or dATP to its caspase recruitment domain (CARD) allows Apaf-1 multimerization and binding of procaspase-9 by virtue of its prodomain (Li et al., 1997). This cytochrome c:Apaf-1:caspase-9 complex called the apoptosome facilitates a conformational change in the procaspases and increases the proteolytic activity of procaspase-9 (Figure 2) (Rodriguez and Lazebnik, 1999; Stennicke et al., 1999). It has also been demonstrated that dimerization leads to a conformational change in the procaspases, which is sufficient to activate the procaspases independent of cleavage (Boatright et al., 2003; Stennicke et al., 1999).

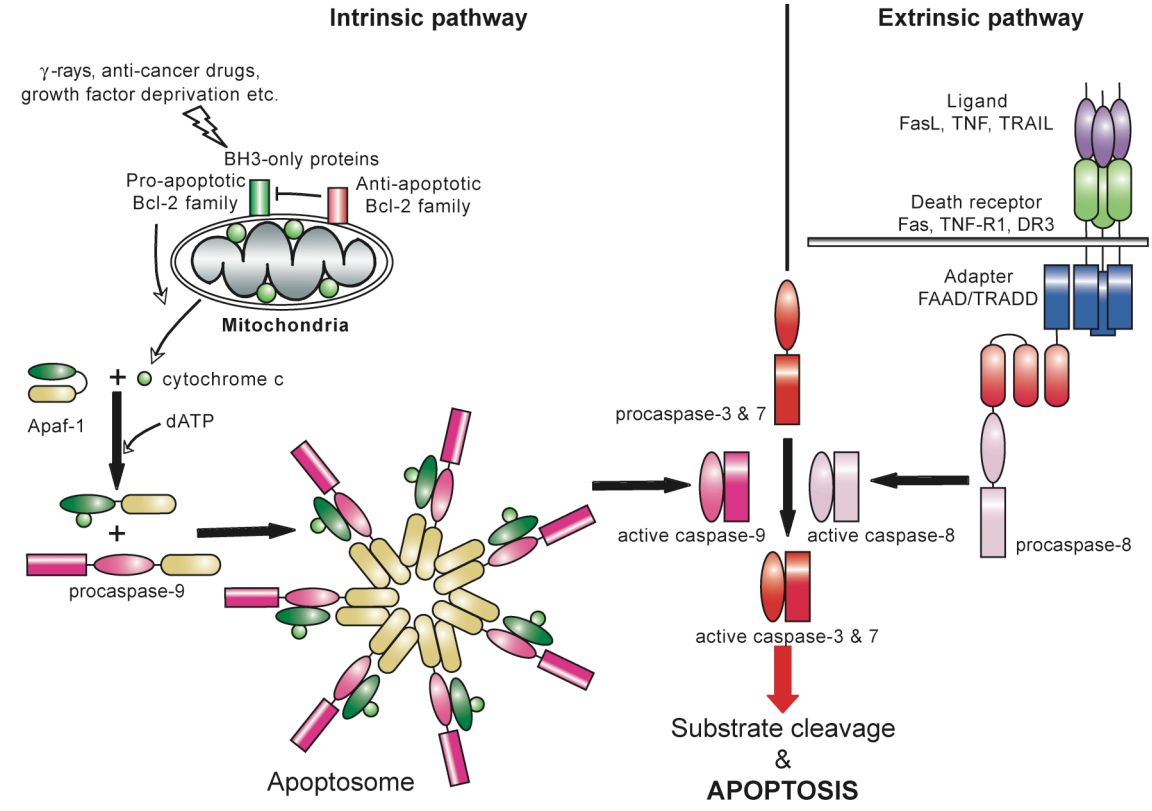

Figure 2: Intrinsic and extrinsic pathway of apoptosis induction. Two major caspase activation pathways resulting in the activation of either caspase-9 or caspase-8 are represented here (see text for details).

Interestingly, although the two prototypical mechanisms of caspase activation seem to run their separate courses, active caspase-8 can also lead to the activation of the mitochondrial pathway of apoptosis. Cleavage of the Bcl-2 family member Bid generates a 15 kDa fragment (tBid) that exerts its proapoptotic effects by inducing a conformational change in Bax and its translocation to the outer mitochondrial membrane (Desagher et al., 1999).

In contrast to the initiator caspases, executioners procaspase-3 and -7 exist as inactive dimers (Boatright et al., 2003) and are activated by cleavage within their linker regions by upstream caspases (Chai et al., 2001; Riedl et al., 2001), such as caspase-8 or caspase-9 and other proteases, such as the cytotoxic T-lymphocyte serine protease, granzyme B (Andrade et al., 1998; Greenberg, 1996). Activated executioner caspases cleave specific substrates, which lead to the characteristic molecular and morphological changes that typify apoptosis.

During apoptosis, more than 280 known proteins are cleaved by executioner caspases (Fischer et al., 2003; Stroh and Schulze-Osthoff, 1998), which ultimately results in the breakdown of the structural and functional components of the cell. Caspase-3, the major executioner caspase, has numerous cytoplasmic and nuclear targets. Certain caspase substrates can be cleaved by more than one caspase; for instance, poly (ADP-ribose) polymerase (PARP) is cleaved by both caspase-3 and caspase-7, while others are unique and can be cleaved by one specific caspase only (caspase-6 is the only caspase known to cleave lamins (Rao et al., 1996) although other proteases are also known to cleave lamins).

III.2.B. NUCLEAR CHANGES

Nuclear changes are one of the defining hallmarks and the first biochemical characteristic described for apoptotic cell death. Chromatin condensation and chromatinolysis, degradation of cellular DNA into fragments, have long been considered to be responsible for apoptotic cell death (Kerr et al., 1972; Wyllie et al., 1980). However, it has become apparent in recent times that nuclear condensation (pyknosis), advanced DNA cleavage into oligonucleosomal fragments and formation of apoptotic bodies are actually manifestations that occur well after the point-of-no-return has been reached and changes such as mitochondrial membrane permeabilization (MMP) and caspase activation has sealed the fate of the cell. Therefore, enucleated cells (cytoplasts) can be induced to undergo apoptosis, manifesting typical morphological features such as membrane blebbing, shrinkage of cytoplasm (karyorrhexis), phosphatidylserine (PS) exposure on plasma membrane and loss of mitochondrial transmembrane potential [$\Delta\Psi_m$] (Castedo et al., 1996; Jacobson et al., 1994; Schulze-Osthoff et al., 1994).

III.2.B.1. DNA fragmentation

Disintegration of the nuclear DNA into oligonucleosomal fragments represents a classical manifestation of apoptosis (Kerr et al., 1972; Wyllie et al., 1980). The observed pattern of DNA cleavage during apoptosis corresponds to

the higher-order packaging of nuclear DNA into heterochromatin.

Eukaryotic DNA is compacted within the cell nucleus by several hierarchical levels of chromatin folding. At the lowest level of chromatin folding, DNA is tightly bound to disc-like structures of histones that form repeating DNA-protein structures termed nucleosomes (Alberts, 2002). Nucleosomes are 11 nm in diameter and consist of an octameric histone core that comprises 2 copies each of histone H2A, H2B, H3 and H4 (Figure 3b). About two full turns of the double stranded DNA helix (83 base-pairs per turn) is wound around the nucleosome and a linker DNA, ranging up to 80 base-pairs, connects adjacent nucleosomes. Therefore, a stretch of 180-220 base-pairs of DNA is contained within adjacent nucleosomes resulting in a 'beads-on-a-string' chromatin structure (Figure 3b). Internucleosomal cleavage by DNA degrading enzymes can separate the DNA 'strings' from the nucleosomes.

The second order of heterochromatin organization consists of packing nucleosomes in 30 nm chromatin fibers, which requires the participation of one molecule of histone H1 per nucleosome (Figure 3c). The next higher order of structural organization of the chromatin is obtained by the formation of looped domains that extend from the chromosomal axis. DNA-binding proteins that recognize specific nucleotide sequences fasten the 30 nm chromatin fibers together forming looped domains (Figure 3d). Cleavage of the chromatin superstructure can lead to the generation of rosettes and chromatin loops. Rosettes contain six individual α-helical loops and correspond to about 300 kb in length whereas the loops are about 50 kb in length and correspond to individual looped domains (Filipski et al., 1990).

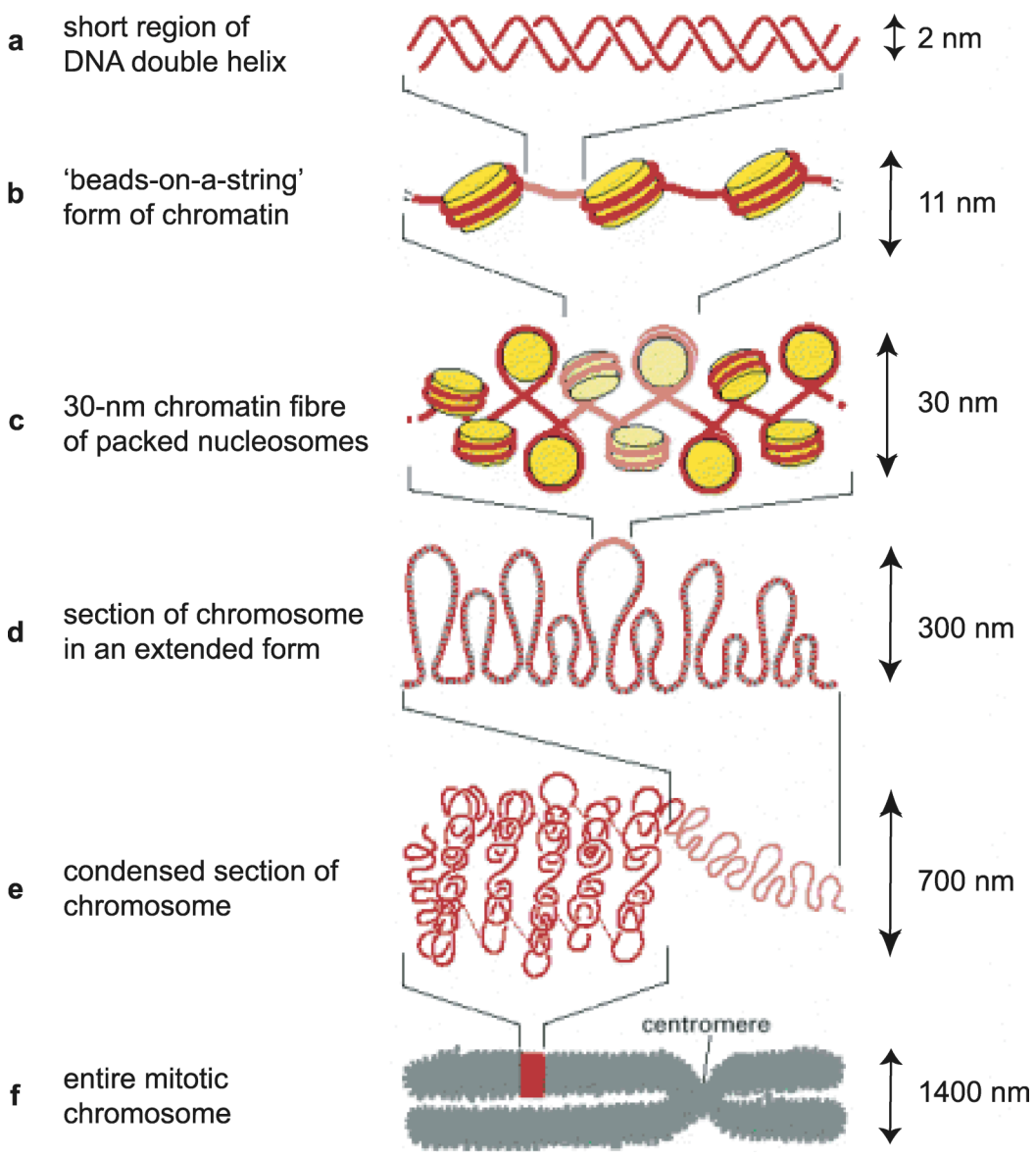

Figure 3: Schematic representation of eukaryotic chromatin organization. See text for details. (Adapted from Alberts, 2002)

Recent evidence suggests that DNA fragmentation is a two-step process. DNA is first cleaved into 50- 300 kb fragments, corresponding to looped domains and rosettes respectively, a process termed high molecular weight (HMW) fragmentation (Brown et al., 1993). Subsequently, HMW fragmented DNA is cleaved into smaller oligonucleosomal fragments, called low molecular weight (LMW) fragmentation, which can be observed as a ladder on a DNA gel and thus also called DNA laddering. The early HMW cleavage of DNA is associated with initial changes in nuclear morphology characterized by the

condensation of the chromatin at the nuclear periphery (stage I chromatin condensation). The later LMW fragmentation coincides with the appearance of more advanced chromatin condensation into highly compacted masses (stage II chromatin condensation) (Lecoeur, 2002; Susin et al., 2000). Furthermore, although HMW fragmentation is usually followed by LMW fragmentation, apoptosis can indeed proceed without oligonucleosomal DNA laddering while displaying HMW fragmentation (Boix et al., 1997; Formichi et al., 2006; Janicke et al., 1998; Oberhammer et al., 1993; Ucker et al., 1992; Walker et al., 1999; Woo et al., 1998; Yuste et al., 2001).

Activation of an endonuclease that preferentially cleaves DNA at the internucleosomal regions has long been considered a biochemical hallmark of apoptosis (Liu et al., 1997; Wyllie et al., 1980). Numerous proteins, including a few nucleases, have been reported to be involved in the nuclear changes that occur during apoptosis (Nagata, 2005; Samejima and Earnshaw, 2005; Zamzami and Kroemer, 1999). One of the first and best-characterized nuclease involved in major apoptotic nuclear changes is caspase-activated DNase/ DNA fragmentation factor-40 (CAD/DFF-40).

Table 1. Nucleases and co-factors involved in DNA fragmentation

	Type of cleavage	Location
Cell-autonomous nucleases and co-factors involved in apoptotic DNA fragmentation		
CAD/DFF40	HMW, LMW	Nuclei
Endonuclease G	HMW, LMW	Mitochondria
DNaseγ/DNAS1L3	HMW, LMW	Nuclei
L-DNase II	LMW	Cytoplasm
Topoisomerase II	HMW	Nuclei
Cyclophilins	HMW	Nuclei, cytoplasm
AIF (co-factor)	HMW	Mitochondria

Nucleases that are involved in apoptosis are classified into two broad categories (Nagata, 2005; Samejima and Earnshaw, 2005). The cell autonomous nucleases include those apoptotic nucleases that function within the dying cell and require direct access to the nucleoplasm. They are an inherent part of the apoptotic program and can actually contribute to the killing of

the cell. The major nucleases of this category, summarized in Table 1, include CAD/DFF-40, endonuclease G, apoptosis inducing factor (AIF), cyclophilins and NUC18. The waste management nucleases, on the other hand, are nucleases that are synthesized in the endoplasmic reticulum (ER) and are compartmentalized within the lysosomes or are released into the extracellular spaces. These nucleases, which include DNase I and II, play a major role in the eventual degradation of the DNA of the apoptotic cell within the macrophages (Samejima and Earnshaw, 2005).

The most important of the cell autonomous nucleases is the CAD/DFF-40, also known as caspase activated nuclease (CPAN). Within the cell, CAD exists as a heterodimeric complex with its specific chaperon/inhibitor DFF-45/inhibitor of CAD (ICAD) (Enari et al., 1998; Liu et al., 1998). Two different isoforms of ICAD are generated by alternative splicing. During CAD biosynthesis, only ICAD-L serves as a specific chaperon for the formation of a catalytically competent nuclease and once folding is accomplished it remains associated as a potent inhibitor of CAD activity. The isoform ICAD-S can inhibit CAD activity *in vitro* (Samejima and Earnshaw, 2005) but its role *in vivo* remains unknown. CAD and ICAD have an N-terminal homologous domain, the cell-death-inducing DFF45-like effector (CIDE) domain, which is responsible for the heterodimerization of CAD and ICAD (CAD/ICAD) (Aravind et al., 1999).

Human CAD carries a typical nuclear localization signal (NLS) at the C-terminus. An NLS-like region has also been identified in the C-terminal region of ICAD-L but not ICAD-S (Lechardeur et al., 2000; Samejima and Earnshaw, 2000). There is, however, contrasting evidence regarding the cellular localization of CAD/ICAD in proliferating cells. Two reports suggest that ICAD localizes to the nucleus (Lechardeur et al., 2000; Samejima and Earnshaw, 1998), whereas one report showed a cytoplasmic localization (Nagata et al., 2002). This localization paradox might be explained by the recent observation that CAD/ICAD is highly mobile in proliferating cells (Lechardeur et al., 2004).

Cleavage of ICAD by caspase-3, caspase-7 or granzyme B at two places dissociates it from the nuclease (Liu et al., 1997; Sakahira et al., 1998; Sharif-

Askari et al., 2001; Thomas et al., 2000; Wolf et al., 1999). The released nuclease forms either homodimers or oligomers by virtue of the N-terminal region, which becomes immobilized within the apoptotic nuclei. Although generally considered to be non-specific to particular sequences, CAD has been reported to display preference to A/T-rich regions (Nagata et al., 2003) and to purines (Rs) and pyrimidines (Ys) with rotational symmetry (5' R-R-R-Y/R-Y-Y-Y 3') (Widlak et al., 2000). Architectural chromatin proteins such as histone H1, heat shock protein 70 (HSP70), DNA topoisomerase II (topo II) and high mobility group protein (HMGB) 1 and 2 also enhance CAD activity. Furthermore, CAD directly binds to histone H1 suggesting recruitment of CAD to DNA linker regions where nucleosomal DNA fragmentation occurs (Liu et al., 1998; Widlak et al., 2000) resulting in the generation of DNA ladders which are characteristic of apoptotic cells. However, cells from ICAD deficient mice show residual DNA fragmentation suggesting the presence of alternative mechanisms of DNA degradation during apoptosis (Zhang et al., 1998).

Another apoptotic nuclease that is capable of inducing DNA cleavage in cells not expressing the CAD/ICAD system is endonuclease G (Endo G). Endo G is compartmentalized in the mitochondrial intermembrane space in normal cells, which protects genomic DNA from degradation. Caspase activation is not required for Endo G activation. However, in some cases, mitochondrial membrane permeabilization during apoptosis resulting in release of cytochrome c, which eventually results in caspase-3 activation, has been reported as a requirement for the release of Endo G into the cytosol. Endo G thus released then translocates to the nucleus and facilitates DNA degradation (Figure 4) (Arnoult et al., 2003; Samejima and Earnshaw, 2005). Whereas CAD is specific for double-stranded DNA (dsDNA), Endo G is sugar non-specific and can cleave either dsDNA, single-stranded DNA (ssDNA) or RNA. Both CAD and Endo G cleave DNA generating fragments possessing ends with 5'-phosphate and 3'-hydroxyl groups that are substrates for terminal deoxynucleotide transferase.

Mitochondrial membrane permeabilization during apoptosis also releases another protein, AIF, which has been implicated in DNA fragmentation (Lorenzo et al., 1999; Susin et al., 1999). AIF is a ubiquitously expressed flavoprotein with

significant homology to bacterial oxidoreductase and has NADH oxidase activity (Daugas et al., 2000). Although the role of AIF in the cells decision to die is controversial, evidence suggests that AIF contributes to the morphological and biochemical manifestations of nuclear apoptosis. Inhibition of the CAD system and the depletion of AIF is both required to block DNA loss in purified nuclei in an *in vitro* cell free system or for inducing chromatin condensation in intact cells treated with staurosporine or etoposide (Susin et al., 2000). AIF by itself lacks an intrinsic nuclease activity, suggesting that AIF presumably activates an yet unidentified nuclease responsible for DNA fragmentation (Susin et al., 1999). Many molecules of AIF bind DNA in a clustered fashion resulting in a caspase-independent HMW DNA degradation and promote stage I DNA condensation (Figure 3) (Modjtahedi et al., 2006).

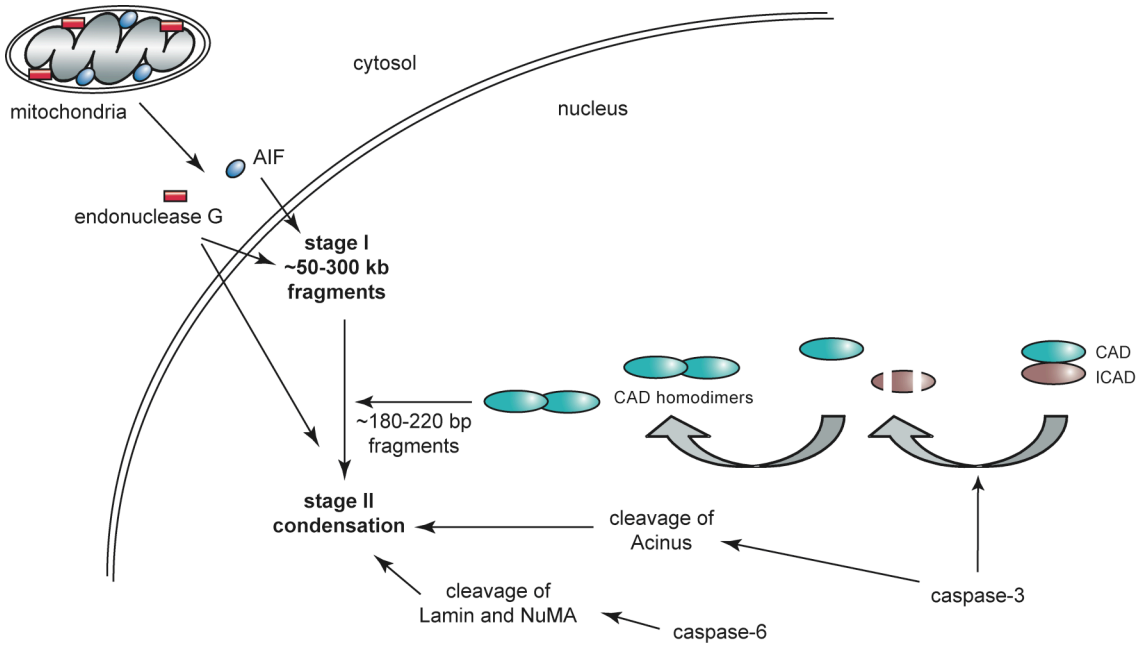

Figure 4: DNA degradation in apoptotic cells. Two distinctive pathways leading to nuclear apoptosis. Loss of mitochondrial membrane potential as a result of activation of the intrinsic pathway of apoptosis leads to a caspase-independent release of apoptogenic factors such as AIF and endonuclease G, which then translocate to the nucleus and fragment the DNA. In the caspase-dependent pathway, activated caspase-3 cleaves ICAD releasing active CAD resulting in the fragmentation of DNA into oligonucleosomal fragments and stage II chromatin condensation. Caspase-3 mediated cleavage of Acinus has been proposed to induce apoptotic chromatin condensation. Lamin and NuMA can be cleaved by caspase-6 resulting in chromatin condensation.

III.2.B.2. Apoptotic chromatin condensation

The process of apoptotic chromatin condensation, also known as pyknosis, remains controversial. Although nuclear pyknosis has been used as a definite hallmark of apoptosis, the molecular mechanisms leading to it remains poorly understood. As mentioned earlier, apoptotic chromatin condensation can be divided into two distinct stages. Stage I chromatin condensation is caspase-independent and is characterized by condensation of the chromatin at the nuclear periphery. Stage II chromatin condensation, however, is caspase-dependent and is characterized by condensation of the chromatin into highly compact masses. Stage I and stage II chromatin condensation coincides with HMW and LMW fragmentations respectively (Susin et al., 2000).

Two structural proteins that can be cleaved by caspases, lamin and nuclear mitotic apparatus protein (NuMA), have received considerable attention for their role during apoptotic chromatin condensation. Nuclear lamina, the structure underlying the inner nuclear membrane and supporting the nuclear architecture, is composed of four different intermediate filament proteins: lamin A, B1, B2 and C. Lamins A and C are generated by alternative splicing of the LMNA pre-mRNA and are absent from some cell types (Fisher et al., 1986; Guilly et al., 1987; Stewart and Burke, 1987). Proteolytic cleavage of lamin A and C by caspase-6 after a conserved Asp residue yielded 47 and 37 kDa products respectively, which accelerated nuclear changes during apoptosis (Rao et al., 1996; Ruchaud et al., 2002). Other proteases, including granzyme A, have also been reported to cleave lamin and might play a role during apoptosis in a caspase-independent manner (McConkey, 1996; Zheng et al., 1999; Zhivotovsky et al., 1997). NuMA, a 238 kDa protein, is a component of the nuclear matrix during interphase and redistributes to the spindle poles during mitosis (Lydersen and Pettijohn, 1980). NuMA can be cleaved by caspase-3 and -6 at distinct sites and has been reported to mediate DNA fragmentation and chromatin condensation during apoptosis (Hirata et al., 1998). In addition to caspases, granzyme B has also been reported to cleave NuMA (Andrade et al., 1998).

Many of the factors described in Table 1, have also been implicated in apoptotic chromatin condensation to varying degrees. Some of these factors such as CAD require caspase cleavage while others such as AIF do not. CAD and AIF induce chromatin condensation by virtue of their DNA cleavage abilities (Liu et al., 1998; Lorenzo et al., 1999). Another nuclear protein called Acinus (for 'apoptotic chromatin condensation inducer in the nucleus') was also identified as a key regulator of apoptotic chromatin condensation. Acinus is particularly distinct from the other factors in that it lacks an intrinsic nuclease activity and has been shown to induce chromatin condensation without DNA fragmentation (Sahara et al., 1999).

Acinus was isolated from bovine thymus as an inducer of apoptotic chromatin condensation (Sahara et al., 1999). Alternative splicing of Acinus pre-mRNA results in the generation of distinct isoforms of Acinus: Acinus-L, -S and -S' with an apparent molecular weight of 220, 98 and 94 kDa respectively. The long isoform of Acinus, Acinus-L, consists of 1341 amino acids while the shorter isoform, Acinus-S, has a unique sequence at the N terminus, which is followed by residues 767-1341 of Acinus-L. Acinus-S' corresponds to residues 767-1341 of Acinus-L. All isoforms of Acinus contain a specific caspase-3 cleavage site that is cleaved at Asp1093 within the characteristic DELD sequence. Mutation of the Asp to an Ala, DELA, prevents *in vitro* cleavage of Acinus by caspase-3. During apoptosis Acinus is cleaved by caspase-3 and an unidentified protease generating a 23 kDa fragment that has been recognized as the fragment responsible for chromatin condensation (Hu et al., 2005; Sahara et al., 1999). In a cell-free system, Jurkat cell lysates immunodepleted of Acinus failed to induce chromatin condensation though CAD activity was unchanged (Sahara et al., 1999). Moreover, reduction of Acinus using an antisense construct resulted in significant reduction of chromatin condensation during anti-Fas-induced apoptosis. It was suggested that Acinus, owing to its ubiquitous expression, might be a general chromatin condensation factor although CAD might be dominant in certain cell types. Furthermore, it has been recently reported that nuclear Akt might play a role in cell survival by phosphorylating Acinus which prevents cleavage of Acinus (Hu et al., 2005).

In a different study, a possible additional function of Acinus was identified in pre-mRNA splicing. Acinus was purified as a subunit of a novel protein complex involving two other proteins, RNPS1 and SAP18. On account of the diverse processes that the complex components are implicated in, namely apoptosis and splicing, the complex was accordingly named apoptosis and splicing associated protein (ASAP) complex (Schwerk et al., 2003).

III.3. APOPTOSIS AND SPLICING ASSOCIATED PROTEIN (ASAP) COMPLEX

The components of the ASAP complex include RNPS1, SAP18 and distinct isoforms of Acinus. Apart from its role in apoptotic chromatin condensation, Acinus has also been identified as a component of functional spliceosomes which facilitate intron removal during mRNA processing (Rappsilber et al., 2002; Zhou et al., 2002). Suggesting a possible role for Acinus in RNA metabolism is the presence of a region which shows considerable similarity to the Drosophila splicing regulator sex-lethal (Sxl) in all three known non-apoptotic isoforms of Acinus (Sahara et al., 1999). Furthermore, analysis of purified exon junction complex (EJC) by mass spectroscopy has revealed that Acinus, RNPS1 and SAP18 stably associate with each other and co-purify with other EJC components (Tange et al., 2005). The components of mammalian EJC includes numerous other splicing coactivators/alternative splicing factors, mRNA export factors and nonsense-mediated mRNA decay (NMD) factors (Tange et al., 2005). It follows from these results that Acinus and the other components of the ASAP complex, may bind to the core EJC as a trimeric complex. The multiprotein EJC is deposited on mRNAs upstream of exon-exon junctions as a result of pre-mRNA splicing. According to the currently accepted model, eukaryotic NMD is activated by the EJC core components and specifically degrades aberrant mRNAs in which the open reading frame (ORF) is truncated by the presence of the first in-frame premature termination codon (PTC) >25-30 nt upstream of any EJC deposition site (Ishigaki et al., 2001; Lejeune and Maquat, 2005; Lykke-Andersen et al., 2000).

RNPS1, also a component of the ASAP complex, is a well-known general activator of pre-mRNA splicing (Mayeda et al., 1999) with a possible role in

mRNA export and NMD (Le Hir et al., 2001; Le Hir et al., 2000; Loyer et al., 1998; Lykke-Andersen et al., 2000). Additionally, RNPS1, similar to Acinus, has also been shown to localize to nuclear factor compartments (Loyer et al., 1998; Mayeda et al., 1999). SAP18, the least characterized of the ASAP components, on the other hand, was originally identified as a component of a complex consisting of the mammalian transcriptional repressor Sin3 and histone deacetylases HDAC1 and 2 (Zhang et al., 1997). The Sin3-HDAC complex has been reported to cause transcriptional repression by deacetylating histones at promoter regions (Roopra et al., 2000; Sun and Hampsey, 1999).

Functionally, addition of ASAP complex to an *in vitro* splicing assay inhibited splicing even at conditions where RNPS1 would normally activate splicing. It was suggested that incorporation of RNPS1 into the ASAP complex could serve to regulate its general splicing activity. Furthermore, microinjection of purified ASAP complex into HeLa cells significantly enhanced tumor necrosis factor-α and cycloheximide-induced apoptosis. Subsequent analysis of extracts from apoptotic cells indicated that the complex dissociates, which is supported by the fact that Acinus is a caspase substrate and is cleaved during apoptosis (Schwerk et al., 2003). Interestingly, the possibility of ASAP complex as a novel protein complex, the first of its kind, participating in the regulation of splicing during apoptosis surfaced as a result of this study.

III.4. ALTERNATIVE SPLICING AND APOPTOSIS

In higher eukaryotes, the protein coding sequence (exons) of most messenger RNA precursors (pre-mRNAs) are interrupted by non-coding sequences called introns. Pre-mRNA splicing is the process by which these introns are removed from the intervening exons giving rise to a mature mRNA that can be translated into protein. Alternative splicing generates multiple mRNA transcripts from a common pre-mRNA resulting in the generation of different protein isoforms that can have altered or sometimes even opposite function. Isoforms generated by alternative splicing influence such diverse functions as apoptosis, sex determination, axon guidance, cell excitation and contraction (Black, 2003; Schwerk and Schulze-Osthoff, 2005).

Several proteins involved in the apoptotic cell death pathway are regulated by alternative splicing (Jiang and Wu, 1999; Schwerk and Schulze-Osthoff, 2005). The Bcl-2 family of proteins is one of the most complex sets of proteins involved in apoptotic regulation that are modulated by alternative splicing. The members of the family range from anti- to pro-apoptotic in nature and varying the balance between the opposing types of Bcl-2 family members could determine the fate of the corresponding cell. The significance of this balance is exemplified during certain disease states such as cancer and neurodegenerative diseases (Akgul et al., 2004).

The major players that influence splice site selection during alternative splicing include a group of serine/arginine-rich (SR) proteins that display diverse RNA binding specificities *in vitro*. A recent report provides evidence for the involvement of one such SR protein, alternative splicing factor/ splicing factor 2 (ASF/SF2), in the regulation of the process of apoptotic DNA fragmentation (Li et al., 2005). Data presented support the model that in normal cells, ASF/SF2 regulates the relative levels of the CAD regulatory factors ICAD-L to ICAD-S. ASF/SF2 depletion switches the ICAD pre-mRNA splicing pattern leading to a lowered level of ICAD-L and increases ICAD-S. Low ICAD-L levels translates to decreased amounts of properly folded CAD and increases the ability of ICAD-S to bind and inhibit CAD activation, thereby affecting oligonucleosomal DNA laddering in ASF/SF2 depleted cells (Li et al., 2005). Additionally, reversible modification of the phosphorylation status can post-transcriptionally regulate SR proteins. In fact, inactivation of certain SR protein kinases and modulation of the phosphorylation status of splicing factors are known to occur during the process of apoptosis (Schwerk and Schulze-Osthoff, 2005).

III.5. RNA INTERFERENCE

Regulation of eukaryotic gene expression occurs at various steps of protein biosynthesis including transcription, mRNA processing and translation and at the level of protein maturation and degradation. Post-transcriptional regulation of protein expression came into light with the discovery of gene silencing, which was first described in 1990 in plants. Overexpression of a pigment synthesis

enzyme in order to produce deep purple petunia flowers instead generated predominantly white flowers due to the repression of both the transgenic and the endogenous genes. This process was referred to as cosuppression (Napoli et al., 1990). A similar mechanism, termed gene quelling, was later described in the fungus *Neurospora crassa* (Cogoni et al., 1996) when amplification of the carotenoid pigment gene, also resulted in suppression of the endogenous gene. Based on the observation that both sense and antisense RNA could silence gene expression in the nematode *Caenorhabditis elegans* (Guo and Kemphues, 1995), Fire and colleagues determined that double-stranded RNA (dsRNA) was ten-fold more potent in silencing genes (Fire et al., 1998). With the discovery of gene silencing, the term RNA interference (RNAi) was coined (Fire et al., 1998). Subsequently, the occurrence of RNAi has been described in various eukaryotic organisms including mammals.

III.5.A. MECHANISM OF GENE SILENCING

In recent years, accumulating evidence has provided an increasing understanding of the mechanism of RNAi. One of the first pieces of evidence was the observation that a small 25 nucleotide dsRNA derived from the target mRNA sequence was involved in post-transcriptional gene silencing (PTGS) (Hamilton and Baulcombe, 1999). The major players of the RNAi machinery were discovered to be these small non-coding RNAs of 22-25 nt in length. The synthesis and function of these small RNAs require the participation of a vast number of proteins. These include dsRNA-specific endonucleases such as Dicer (Bernstein et al., 2001), dsRNA-binding proteins and small RNA-binding proteins called Argonaute proteins (Hammond et al., 2001; Tabara et al., 1999). The central component of all silencing pathways is a ribonucleoprotein complex called RNA-induced silencing complex (RISC). The complex consists of at least one Argonaute protein and a single strand of cleaved and processed small non-coding RNA. The RNA component guides the complex onto mRNAs bearing homologous antisense sequence, resulting in the cleavage and degradation of the specific mRNA target. These small non-coding RNAs are further subdivided into microRNAs (miRNAs), small interfering RNAs (siRNAs) and repeat-

associated small interfering RNAs (rasiRNAs) distinguished by their origins and not by their functions (Zamore and Haley, 2005).

miRNAs are encoded within the host genome as largely unstructured transcripts termed pri-miRNAs and contain stem-loop or hairpin structures ~70 nt in length (Ambros, 2003). In humans, the hairpins are cleaved out of pri-miRNA by a dsRNA-specific endonuclease, Drosha (Lee et al., 2003) along with its dsRNA-binding partner DGCR8 resulting in an ~30 nt dsRNA called the pre-miRNA (Figure 5) (Han et al., 2004). The pre-miRNA is translocated to the cytoplasm, aided by exportin-5, where it is further processed and cleaved by another dsRNA-specific endonuclease, Dicer (Bernstein et al., 2001), acting with its dsRNA-binding protein partner, the tar-binding protein (TRBP) (Haase et al., 2005). Subsequently, one strand of the mature miRNA is loaded onto RISC that then targets specific mRNAs. To date there are several known miRNAs reported in plants, animals and their viruses. rasiRNAs differ from miRNAs in that they are generated as overlapping sense and antisense RNAs from the same locus which then associate to form dsRNAs (Aravin et al., 2003). These dsRNAs are then processed and cleaved by Dicer and enter into the general RNAi pathway (Figure 5).

In contrast to miRNAs, siRNAs are derived from long, double-stranded RNAs that are either transcribed from endogenous genes or are introduced into the cells by viral infection or by transfection (Ambros et al., 2003; Elbashir et al., 2001b; Hammond et al., 2000; Zamore et al., 2000). Several siRNA duplexes of ~21-25 nt are produced as these long dsRNAs are processed by Dicer. One strand of the duplex that is less complementary, and thus less stable, at the 5' end, is incorporated into the RISC complex and as with miRNAs, the other strand is degraded. The RISC complex loaded with the siRNA carries out the silencing operation (Figure 5).

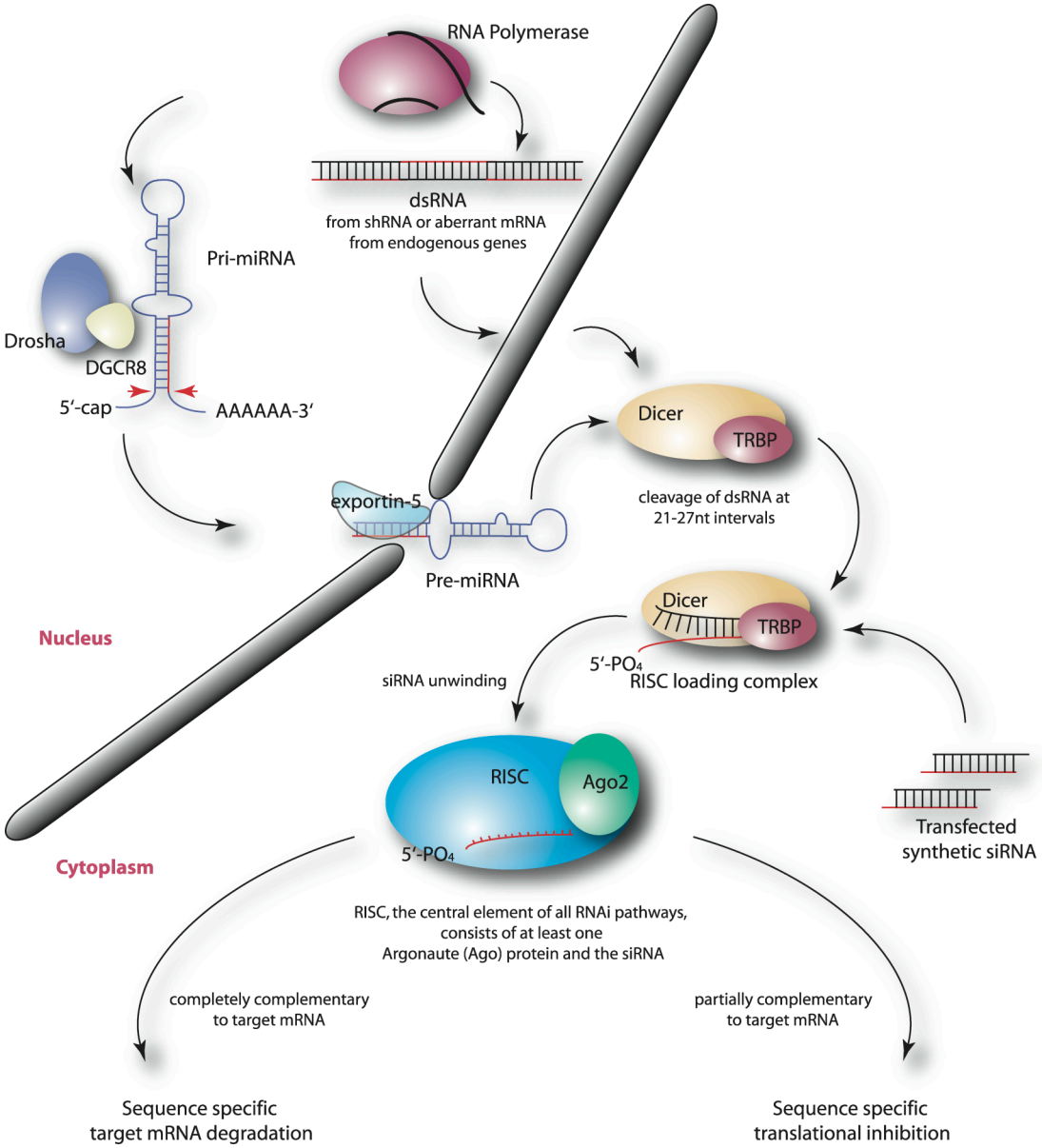

Figure 5: Distinct pathways of RNA interference. Generation of double-stranded RNA within the cell as a result of transcription of miRNA genes, synthesis of aberrant mRNA, replicating viruses or vector-based shRNA triggers the RNAi machinery. Alternatively, synthetic siRNAs can be transfected into the cell. dsRNA generated from distinct pathways all converge at Dicer, which is the major endonuclease involved in the RNAi process (see text for details). Dicer also serves as a platform for loading the siRNA onto the RNA-induced silencing complex (RISC). The siRNA is then unwound by RISC and one strand of the siRNA is degraded. RISC then mediates either target mRNA degradation or inhibition of protein synthesis depending on the complementarity of the siRNA to the target mRNA.

The outcome of the silencing process depends on the relative degree of homology of the small RNA compared to the RNA target sequence. In fact, a mere six or seven nucleotides within the miRNA or siRNA provide the binding

specificity for RISC. This relatively small sequence called the seed sequence subsequently enables the more 3' regions of the small RNA to bind the 5' regions of the target RNA (Bartel, 2004). It has been shown that the 5' end of the small RNA contributes disproportionately to target binding (Doench and Sharp, 2004; Haley and Zamore, 2004; Lai et al., 2005; Lewis et al., 2005). Extensive homology and pairing between the small RNA and its target sequence enables the Argonaute protein to cleave at a single phosphodiester bond in the target mRNA. This triggers the complete degradation of the mRNA target. On the other hand, partial pairing results in tethering of the Argonaute protein to the target mRNA. This tethering prevents translation of the target mRNA into proteins (Doench et al., 2003; Hutvagner, 2005; Zamore and Haley, 2005). The current model for RNAi argues that both the miRNA and siRNA pathways are functionally interchangeable and target specific mRNAs to either degradation or translational repression. Functionally, miRNAs are reported to be genetically programmed for the regulation of gene expression during processes as varied as embryogenesis, oncogenesis and haematopoiesis (Benard and Douc-Rasy, 2005; Chen and Lodish, 2005; Croce and Calin, 2005). In contrast, siRNAs are the first line of defense against dsRNAs generated during viral infections and by transposons (Hutvagner, 2005; Kanellopoulou et al., 2005).

III.5.B. VECTOR BASED, INDUCIBLE EXPRESSION OF SIRNAS

The resulting phenotype of RNAi is identical to that of a genetic null mutant (Kunath et al., 2003). For this reason, gene silencing is a powerful tool for loss-of-function studies. Two different approaches could be used to knockdown specific protein targets.

Preformed, synthetic siRNAs duplexes containing the sense and the antisense strand can participate in RNA interference when introduced into cells by transfection (Elbashir et al., 2001a). However, reduction of gene expression using synthetic siRNAs is transient and thus severely restricts its application. Secondly, with the generation of a stable expression system (Brummelkamp et al., 2002), it became possible to stably transfect a construct expressing the siRNA as a short hairpin RNA (shRNA) mimicking endogenous miRNAs. These

shRNA-expressing constructs can be used to establish stable RNAi based knockdown of a target protein in cells in culture or in transgenic mice (Chang et al., 2004).

Plasmid-based shRNA expression constructs utilize either the RNA polymerase III (pol III) promoter (including U6, human H1 and tRNA promoters) (Brummelkamp et al., 2002; Tuschl, 2002) or a pol II promoter with minimal poly (A) signal sequence (Xia et al., 2002). The major advantage of the pol III system is its high level of activity, producing ~4 $\times 10^5$ transcripts per cell, and the fact that it does not add additional nucleotides to the transcript which might affect functional activity. Within the cell, both pol II and pol III promoters control the synthesis of a large variety of non-coding, small nuclear RNAs (snRNAs) in higher eukaryotes (Hernandez, 2001). Additionally, the pol III H1 promoter has a well-defined start of transcription and generates a transcript lacking a poly-adenosine tail. The termination signal consists of a series of five consecutive thymidines (T5) and the transcript is cleaved after the second uridine (Baer et al., 1990) generating a transcript with a 2 nt 3' overhang which resembles synthetic siRNAs. This is important since synthetic siRNAs duplexes of 21-22 nt length containing a 19 nt duplexed region, 2-3 nt 3' overhangs and 5' phosphate (P) and 3' hydroxyl (OH) groups mimicking those generated by Dicer cleavage have been demonstrated to be functionally more efficient (Elbashir et al., 2002).

Several groups have reported the successful generation and use of inducible RNAi systems controlled by tetracycline (Tet) or its analog doxycycline (Dox) (Chang et al., 2004; Chen et al., 2003; Coumoul et al., 2004; Czauderna et al., 2003; van de Wetering et al., 2003). Most tetracycline-regulated systems consist of two components: a Tet repressor (TetR) protein and a Tet responsive promoter, the activity of which is regulated by the binding or the release of the TetR. In one such system, the TetR is a fusion of the TetR of the *Escherichia coli* Tet operon with the activation domain of virion protein 16 (VP16) of the Herpes simplex virus generating a Tet controlled transactivator. This chimeric TetR-VP16 protein strongly enhances transcription from minimal promoters on binding to the Tet operator (TetO) sequence (Gossen and Bujard, 1992; Gossen et al., 1995). Addition of Tet inhibits the binding of the TetR-VP16 chimera to the

TetO. Another system makes use of the physiological function of the TetR. In this case, the TetO is situated between the promoter and the coding region of the gene of interest (Yao et al., 1998). Binding of the TetR blocks transcription of the gene. In the presence of Tet, however, TetR binding to the TetO is interfered by Tet and transcription is allowed to proceed. This system more closely resembles the regulation of the native tet operon in bacteria (Hillen et al., 1983) and therefore avoids the potential toxic effects of the viral transactivating domains observed in some mammalian cells.

The pSUPERIOR group of vectors employs the benefits of the shRNA-based vectors in addition to the ease of inducible expression. The H1 promoter in pSUPERIOR vector carries a sequence modification between the TATA box and the RNA hairpin transcriptions start site (Figure 6). A 19 nt modification within the H1 promoter inserts a tetracycline operator 2 ($TetO_2$) site that binds TetR. TetR is expressed by pcDNA6/TR plasmid that is stably transfected into T-Rex cells and forms homodimers following synthesis. Binding of TetR homodimers results in transcriptional inhibition of shRNA synthesis. Upon tetracycline addition, TetR homodimers bind tetracycline and undergo a conformational change causing their release from the $TetO_2$ sites, subsequently allowing transcription of shRNA. shRNAs thus synthesized can enter into the RNAi pathway and enable target mRNA repression or degradation.

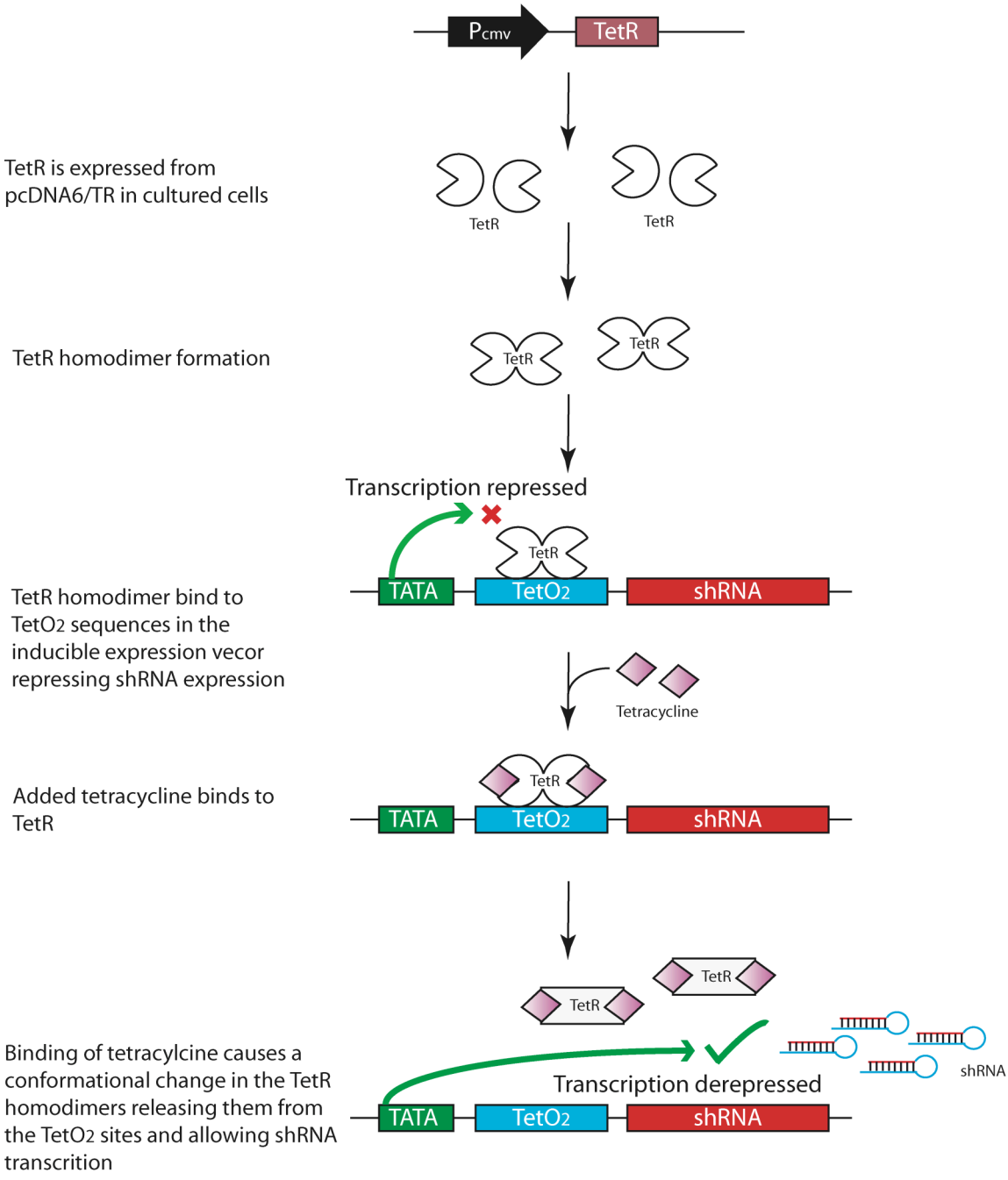

Figure 6: Tetracycline-inducible shRNA system.

IV. AIM OF THE STUDY

Although the molecular mechanisms during the early stages of apoptosis in a cell are well established, those transpiring at the later stages, including DNA fragmentation and chromatin condensation, are debated. Several factors and proteins have been implicated in these processes. Although most factors implicated induced both DNA fragmentation and condensation, the nuclear protein Acinus was proposed as an inducer of apoptotic chromatin condensation without DNA fragmentation (Sahara et al., 1999). This atypical inducer of apoptotic chromatin condensation and its isoforms, were later identified to exist predominantly in a complex with two other proteins, RNPS1 and SAP18 (Schwerk et al., 2003). Termed the apoptotic and splicing associated protein (ASAP) complex, this trimeric complex was detected as a functional component of spliceosomes (Rappsilber et al., 2002; Zhou et al., 2002).

The aim of the present study was to elucidate the role of the nuclear protein Acinus during nuclear changes occurring in the course of apoptosis. To this end, RNA interference was employed to knockdown Acinus in cells and its consequence on apoptotic chromatin condensation and DNA fragmentation was analyzed. The specific aims during the course of this study were:

- To determine whether upstream events during apoptosis, such as caspase activation and substrate cleavage, were affected by the absence of Acinus.
- To determine if the loss of Acinus influenced *in vivo* and *in vitro* apoptotic chromatin condensation.
- To elucidate whether knockdown of Acinus had an impact on apoptotic HMW and internucleosomal DNA fragmentation.

V. MATERIALS AND METHODS

V.1. GENERAL MATERIALS

V.1.A. CHEMICALS AND REAGENTS

Substance	Supplier
β-glycerophosphate	Sigma (München, Germany)
β-mercaptoethanol	Carl Roth GmbH (Karlsruhe, Germany)
Acrylamide 40%	Carl Roth GmbH (Karlsruhe, Germany)
Agarose	Carl Roth GmbH (Karlsruhe, Germany)
Ammonium peroxodisulfate (APS)	Carl Roth GmbH (Karlsruhe, Germany)
ATP	Roche (Mannheim, Germany)
Boric acid	Merck (Darmstadt, Germany)
Bovine serum albumin (BSA)	Sigma (München, Germany)
Bromophenol blue	Carl Roth GmbH (Karlsruhe, Germany)
Certified Megabase Agarose	Bio-Rad Laboratories (München, Germany)
CHAPS	Carl Roth GmbH (Karlsruhe, Germany)
Coomassie Brilliant Blue R-250	Carl Roth GmbH (Karlsruhe, Germany)
Creatine kinase	Sigma (München, Germany)
Crystal violet	Merck (Darmstadt, Germany)
Digitonin	Sigma (München, Germany)
Dimethylsulfoxide (DMSO)	Sigma (München, Germany)
Dithiothreitol (DTT)	Sigma (München, Germany)
Ethanol	Carl Roth GmbH (Karlsruhe, Germany)
Ethidium bromide	Carl Roth GmbH (Karlsruhe, Germany)
Ethlyleneglycol-bis-(2-aminoethyl) N, N, N', N'-tetra acetic acid (EGTA)	Carl Roth GmbH (Karlsruhe, Germany)
Ethylendiamine tetra acetic acid (EDTA)	Carl Roth GmbH (Karlsruhe, Germany)
FLAG M2-agarose	Sigma (München, Germany)
FLAG peptide	Sigma (München, Germany)
Glacial acetic acid	Carl Roth GmbH (Karlsruhe, Germany)
Glucose	Sigma (München, Germany)
Glutaraldehyde	Sigma (München, Germany)
Glycerol	Carl Roth GmbH (Karlsruhe, Germany)
Isopropanol	Merck (Darmstadt, Germany)
Magnesium acetate	Carl Roth GmbH (Karlsruhe, Germany)
Magnesium chloride (MgCl2)	Carl Roth GmbH (Karlsruhe, Germany)
Methanol	Carl Roth GmbH (Karlsruhe, Germany)
N, N', N' –Tetramethylethylenediamine (TEMED)	Carl Roth GmbH (Karlsruhe, Germany)

N-[2-hydroxyethyl]piperazine-N`-[2-ethanesulfonic acid] (HEPES)	Carl Roth GmbH (Karlsruhe, Germany)
Non-fat dry milk	Applichem (Darmstadt, Germany)
Nonidet P-40 (NP-40)	Calbiochem (La Jolla, USA)
Paraformaldehyde	Merck (Darmstadt, Germany)
Phenol:Chloroform:Iso-amyl alcohol	Sigma (München, Germany)
Phosphocreatine	Sigma (München, Germany)
Potassium acetate	Carl Roth GmbH (Karlsruhe, Germany)
Potassium chloride (KCl)	Merck (Darmstadt, Germany)
Potassium ferricyanide (FeK3(CN)6)	Sigma (München, Germany)
Potassium ferrocyanide (K4Fe(CN)6·3H2O)	Fluka Chemie GmbH
Propidium iodide (PI)	Carl Roth GmbH (Karlsruhe, Germany)
Protease inhibitor cocktail tablets	Roche (Mannheim, Germany)
Protein G-Sepharose	Amersham Pharmacia Biotech AB (Uppsala, Sweden)
Sodium Azide	Carl Roth GmbH (Karlsruhe, Germany)
Sodium chloride (NaCl)	Carl Roth GmbH (Karlsruhe, Germany)
Sodium citrate	Carl Roth GmbH (Karlsruhe, Germany)
Sodium dodecyl sulphate (SDS)	Merck (Darmstadt, Germany)
Sodium hydroxide (NaOH)	Carl Roth GmbH (Karlsruhe, Germany)
Sodium phosphate	Merck (Darmstadt, Germany)
Sucrose	Carl Roth GmbH (Karlsruhe, Germany)
Tris-(hydroxymethyl)-amino-methane (Tris)	Carl Roth GmbH (Karlsruhe, Germany)
Triton X-100	Carl Roth GmbH (Karlsruhe, Germany)
Tryptone	Carl Roth GmbH (Karlsruhe, Germany)
Tween-20	Carl Roth GmbH (Karlsruhe, Germany)
x-gal	Sigma (München, Germany)
Yeast extract	Carl Roth GmbH (Karlsruhe, Germany)

V.1.B. ENZYMES AND PROTEINS

Product	Manufacturer
Proteinase K	Sigma (München, Germany)
Recombinant human TNF-α (4×10^7 U/mg)	Knoll AG (Ludwigshafen, Germany)
Restriction enzymes	New England Biolabs GmbH (Frankfurt, Germany) and Fermentas GmbH, Germany
RNase A	Sigma (München, Germany)

V.1.C. KITS

Product	Manufacturer
CHEF Mammalian Genomic DNA plug kit	Bio-Rad Laboratories (München, Germany)
Cytotoxicity Detection Kit	Roche (Mannheim, Germany)
ECL Western blotting detection reagent	Amersham (Braunschweig, Germany)
QIAgen HiSpeed Plasmid maxi kit	Qiagen (Hilden, Germany)
QIAquick gel extraction kit	Qiagen (Hilden, Germany)
QIAquick PCR purification kit	Qiagen (Hilden, Germany)
RNeasy kit	Qiagen (Hilden, Germany)
TITANIUM One-Step RT-PCR kit	BD Pharmigen

V.1.D. CONSUMABLES

Product	Manufacturer
Bacterial culture tubes	Greiner Bio-One GmbH (Essen, Germany)
Hyperfilm™ MP	GE Healthcare UK Ltd (Buckinghamshire, UK)
Cryotubes	Nalgene (Rochester, NY, USA)
Disposable plastic cuvettes	Sarstedt (Nümbrecht, Germany)
Eppendorf tubes (1,5 and 2 ml safe-lock)	Eppendorf (Hamburg, Germany)
Falcon tubes (sterile, 5 ml, 15 ml and 50 ml)	Greiner Bio-One GmbH (Essen, Germany)
PCR tubes	Eppendorf (Hamburg, Germany)
Polyvinylidene difluoride (PVDF) membranes	Amersham Pharmacia (Braunschweig, Germany)
Quartz cuvette	PerkinElmer LAS GmbH (Jügesheim, Germany)
Tissue culture dishes	Greiner Bio-One GmbH (Essen, Germany)

V.1.E. EQUIPMENT

Product	Manufacturer
Autoclave-Varioklav	Thermo Electron corporation (Waltham, MA, USA)
Axiovert135 microscope	Zeiss, Germany
Certomat® BS-1 (Bacterial shaker)	Sartorius AG (Göttingen, Germany)
Lambda Fluoro 320 Plus plate reader	MWG Biotech (Ebersberg, Germany)
Cell culture hood	Heraeus Holding GmbH (Hanau, Germany)
CO_2 incubator	Heraeus Holding GmbH (Hanau, Germany)
Deep freezer (-80°C)	Heraeus Holding GmbH (Hanau, Germany)
Hypercassette™ (Developing cassettes)	GE Healthcare UK Ltd (Buckinghamshire, UK)
Curix 60 (Developing machine)	Agfa (Köln, Germany)
Horizon 58- Horizontal gel electrophoresis tank	Life technologies (Gaithersburg, MD, USA)

FACSCalibur	Becton Dickinson (Heidelberg, Germany)
LAS-3000 (Gel documentation system)	Fuji Photo Film Europe GmbH (Düsseldorf, Germany)
Gene Path System	Bio-Rad Laboratories (München, Germany)
Millipore H_2O-production unit	Millipore GmbH (Schwalbach, Germany)
pH meter-Thermo Orion 555A	Thermo Electron corporation (Waltham, MA, USA)
Pipettes (p-10, p-20, p-200, p-1000)	Eppendorf (Hamburg, Germany)
Power packs-EPS 1000	GE Healthcare UK Ltd (Buckinghamshire, UK)
Sartorius CP64-OCE and CP324S	Sartorius AG (Göttingen, Germany)
Sorvall RC5B Plus centrifuge	Thermo Electron corporation (Waltham, MA, USA)
Lambda 20, UV/VIS Spectrometer	PerkinElmer LAS GmbH (Jügesheim, Germany)
Epperndorf Concentrator 5301	Eppendorf (Hamburg, Germany)
GeneAmp PCR System 9700	Applied Biosystems (Foster City, CA, USA)
Ultracentrifuge-Optima LE-80K	Beckman Coulter GmbH (Krefeld, Germany)
UV illuminator	Carl Roth GmbH (Karlsruhe, Germany)
Wallac Victor 1420-Multilabel counter	PerkinElmer LAS GmbH (Jügesheim, Germany)
hp laserjet 4200 printer	Hewlett-Packard GmbH (Böblingen, Germany)

V.1.F. SOFTWARE

Program	Manufacturer
OpenLab software	Improvision (Tübingen, Germany)
BD CellQuest™	Becton Dickinson (Heidelberg, Germany)
Oligoengine	OligoEngine (Seattle, WA)

V.1.G. CELL LINES

Cell line	Description
HeLa T-Rex	HeLa cells stably expressing the tetracycline repressor protein
HeLa tet-off	HeLa cells stably expressing the tetracycline-controlled transactivator (tTA) protein
Sf9 cells	Spodoptera frugiperda insect cells
MCF7	Human breast adenocarcinoma cell line
MCF7/casp-3	Human breast adenocarcinoma cell line stably transfected with caspase-3 cDNA

V.1.H. CELL CULTURE REAGENTS

Product	Supplier
Blasticidin	Invitrogen (Karlsruhe, Germany)
Dulbecco's modified Eagle's medium with high glucose (DMEM)	PAA Laboratories GmbH (Pasching, Austria)
Fetal calf serum	PAA Laboratories GmbH
Geneticin (G418 solution)	PAA Laboratories GmbH
Penicillin/streptomycin	PAA Laboratories GmbH
RPMI 1640	PAA Laboratories GmbH
Sterile PBS	PAA Laboratories GmbH
Tetracycline	Sigma (München, Germany)
Tetracycline-reduced fetal bovine serum	PAA Laboratories GmbH
TNM-FH	BD Biosciences (San Diego, CA, USA)
Trypsin-EDTA	PAA Laboratories GmbH

V.1.I. OTHER REAGENTS

Product	Supplier
DEVD-AMC (N-acetyl-Asp-Glu-Val-Asp-aminomethylcoumarin)	Bachem (Heidelberg, Germany)
1 Mb DNA ladder	Bio-Rad Laboratories
6x DNA loading dye	Fermentas GmbH, Germany
Staurosporine	Sigma (München, Germany)
Fugene 6 reagent	Roche Diagnostics (Mannheim, Germany)

V.1.J. EXPRESSION VECTORS

Product	Description
pSUPER	shRNA vector driven by tet-inducible H1 RNA polymerase III promoter. Ampicillin resistance for selection in bacteria. No resistance marker for selection in mammalian cell lines
pSUPERIOR.neo	shRNA vector driven by H1 RNA polymerase III promoter. Ampicillin resistance for selection in bacteria. Neomycine (G418) resistance for selection in mammalian cell lines
pCAGGS-Acinus-L-FLAG	A general mammalian expression vector encoding full-length, FLAG-tagged, Acinus-L. Ampicillin resistance for selection in bacteria.

V.1.K. OLIGONUCLEOTIDES

shRNA Oligos

Name	Sequence
A3121 sense	GATCCCCGAGGCCTTCTGGATTGACATTCAAGAGATGTCAATCC AGAAGGCCTCTTTTTGGAAA
A3121 antisense	AGCTTTTCCAAAAAGAGGCCTTCTGGATTGACATCTCTTGAATGT CAATCCAGAAGGCCTCGGG
A3493 sense	GATCCCCTGGGATCGGGACAAAGTTCTTCAAGAGAGAACTTTGT CCCTAGCCCATTTTTGGAAA
A3493 antisense	AGCTTTTCCAAAAATGGGATCGGGACAAAGTTCTCTCTTGAAGAA CTTTGTCCCTAGCCCAGGG

PCR primer list

Name	Sequence
Acinus-Fwd	5’ -CAGATCGTTCAGAAAGAGG-3’
Acinus-Rev	5’ -CGGGGTGGGCGCCGC-3’
GAPDH-Fwd	5’ -GTGGAAGGACTCATGACCACAG-3’
GAPDH-Rev	5’ -CTGGTGCTCAGTGTAGCCCAG-3’

V.1.L. ANTIBODIES

Product	Source
Mcl-1	BD Pharmingen (Heidelberg, Germany)
PARP	BD Pharmingen (Heidelberg, Germany)
c-FLIP	Alexis Biochemicals (Lausen, Switzerland)
RNPS-1	a gift from Akila Mayeda
Acinus	Described before in Schwerk et al., 2003
Caspase-3	R&D systems (Wiesbaden, Germany)
SAP18	Santa Cruz Biotechnology (Santa Cruz, CA)
ICAD	Santa Cruz Biotechnology (Santa Cruz, CA)
phospho-H2A.X (Ser139)	Upstate Biotechnology (Lake Placid, NY)

Secondary antibodies, anti-mouse and anti-rabbit, coupled to horseradish peroxidase were purchased from Promega, Mannheim, Germany. Anti-goat antibody coupled to horseradish peroxidase was purchased from Molecular Probes, Leiden, The Netherlands.

V.2. METHODS

V.2.A. MAINTENANCE OF CELL LINES AND BACTERIAL CULTURES

V.2.A.1. Culturing bacteria and preparation of stocks

LB broth (per liter)

10g	Tryptone
5g	Yeast extract
10g	NaCl

To maintain bacterial stocks of plasmids and propagating plasmid constructs, competent *E. coli* DH5α strains were transformed with the plasmid and cultured overnight in LB medium, containing the appropriate concentrations of the respective antibiotic, at 37°C with shaking at 200 rpm. 16% glycerol stocks were prepared by adding 200 µl of sterile 80% glycerol to 800 µl of the overnight culture and stored at -80°C.

V.2.A.2. Growth and maintenance of insect cells

Sf9 cells derived from *Spodoptera frugiperda* ovarian cells were used for baculovirus infection and recombinant protein expression. Cells were propagated in TNM-FH media at 28°C initially as adherent cultures in tissue culture dishes but later adapted to suspension cultures. Cells were maintained at 2×10^6 cells/ml and seeded into 15 cm tissue culture dishes prior to infection with baculovirus.

V.2.A.3. Growth and maintenance of mammalian cell lines

HeLa tet-off cells were maintained in RPMI 1640 medium supplemented with 10% heat-inactivated fetal calf serum, 100 units/ml penicillin and 0.1 mg/ml streptomycin. Cells were subcultured every 3-4 days by dilution of the cells to a concentration of 1×10^5 cells/ml.

HeLa T-REx cells stably expressing the tetracycline repressor were obtained from Invitrogen. Cells were cultured in Dulbecco's modified Eagle's medium with high glucose, supplemented with 10% tetracycline-reduced fetal bovine serum, 100 units/ml penicillin, 0.1 mg/ml streptomycin (all from PAA Laboratories

GmbH, Pasching, Austria) and 5 µg/ml blasticidin (Invitrogen). Both HeLa tet-off and HeLa T-Rex cells were incubated at 37°C in a humidified incubator with 95% air and 5% CO_2.

V.2.A.4. Preparation of liquid nitrogen stocks

Cells cultured to approximately 70% confluence were harvested by trypsinization and resuspended in 4 ml growth medium. Cells were pelleted by centrifuging at 1000 rpm for 2 min at 4°C. The cell pellet resuspended in 2 ml freezing medium (growth medium containing 20% tetracycline-reduced fetal bovine serum and 10% DMSO) was aliquoted into cryotubes and then frozen at -80°C overnight. The following day the tubes were transferred to a liquid nitrogen tank.

V.2.B. CLONING AND ANALYSIS

V.2.B.1. Restriction digestion

Typically 10-50 µl digestion reactions were set up. All restriction enzymes were obtained from NEB or Fermentas and the digestions were performed in the supplied buffers at temperature conditions prescribed by the manufacturer. Digestions were set up for 2-4 hrs.

V.2.B.2. Agarose gel electrophoresis

0.5 × TBE buffer (per liter)

5.4 g	Tris base
2.75 g	Boric acid
2 ml	0.5 M EDTA, pH 8.0

Electrophoresis was performed in 0.8 to 2% (w/v) agarose gels in 0.5× TBE buffer depending on the expected fragment sizes. Agarose gels were typically electrophorosed in a horizontal electrophoresis tank submerged in 0.5× TBE buffer at 1-5 V/cm. Ethidium bromide stained gels were visualized and photographed.

V.2.B.3. Purification of DNA fragments form agarose gels

DNA fragments from restriction digestion or from PCR reactions were

separated by agarose gel electrophoresis. The gel pieces containing the desired DNA fragments were carefully excised using a scalpel under UV illumination. The DNA contained in the gel slices was then purified using the QIAgen gel extraction kit according to manufacturer's instructions.

V.2.B.4. Ligation and transformation

Typically 10 µl ligation reactions were set up for 2 hours at room temperature or for overnight ligation at 14°C. Annealed and gel eluted oligos were ligated with linearized vector DNA at a 3:1 equimolar ratio. T4 DNA ligase (Roche) and reaction buffer was added according to manufacturer's instructions.

Ligation reactions, pre-chilled on ice were added to 100 µl of chemically competent DH5α cells and left to stand on ice for 15 min. the cells were then heat-shocked at 42°C for 90 seconds and then immediately transferred to ice for a further 5 minutes. 900 µl of LB broth, pre-warmed to 37°C was added to the cells and incubated at 37°C for 40 to 60 minutes. Finally, the transformation mix, or an appropriate dilution, was plated onto selection plates containing the respective antibiotic and the transformants were allowed to grow overnight at 37°C.

V.2.B.5. Purification of plasmid DNA from bacteria

V.2.B.5.a. Small-scale plasmid isolation (Mini-prep)

Solution I

50 mM	Glucose
25 mM	Tris Cl, pH 8.0
10 mM	EDTA, pH 8.0
0.5 mg/ml	RNase A

Sterilized by autoclaving and stored at 4°C

Solution II

0.2 N	NaOH
1% (w/v)	SDS

Solution III

3 M	potassium acetate
11.5% (v/v)	glacial acetic acid

Fresh single colonies, picked from agar plates, were inoculated in 2 ml of LB broth, containing the respective antibiotic and incubated overnight at 37°C with constant shacking at 220 rpm. The bacterial cells were pelleted by centrifuging at 2000 rpm for 5 min at room temperature in a tabletop centrifuge (Biofuge fresco, Heraeus). Pellets were resuspended in 200 µl of solution I and lysed with 100 µl of solution II. Addition of 150 µl of solution III precipitated the proteins leaving the plasmid DNA in solution. The precipitate was pelleted by centrifugation at 13000 rpm for 15 min at 4°C and the supernatant was collected. 600 µl of isopropanol was added and the samples chilled at -80°C for 20-30 minutes to precipitate the DNA. Precipitated DNA was pelleted by centrifugation at 13000 rpm for 15 min at 4°C and was washed in 500 µl of ice cold 70% ethanol. The precipitated DNA was pelleted and dried in a speed vac. Finally, the dried pellet was resuspended in 40 µl of H_2O and the concentration of DNA determined spectrophotometrically.

V.2.B.5.b. Large-scale plasmid isolation (Maxi-prep)

A pre-inoculum was prepared by culturing a fresh single colony in 2 ml of LB broth, containing the respective antibiotic, at 37°C for 8 hours. This was used to subsequently inoculate 150 ml of LB broth containing the respective antibiotic. After overnight incubation in a bacterial shaker at 37°C, the cells were pelleted at 4000 rpm in a Sorvall GS3 rotor for 10 min at 4°C. Plasmid purification was subsequently carried out using the HiSpeed plasmid purification kit (Qiagen) according to manufacturer's instructions, finally eluted in 1 ml of H_2O and DNA concentration quantitated spectrophotometrically.

V.2.B.6. Quantification of DNA

Concentration of purified plasmid DNA was estimated using an UV spectrophotometer. Measurements were performed in quartz cuvettes using the standard conversion that 50 µg/ml DNA would give an OD of 1.0 at 260 nm. The ratio of OD_{260}/OD_{280} was determined to assess the purity of the sample.

V.2.C. TRANSFECTION OF MAMMLIAN CELL LINES AND GENERATION OF STABLES

Mammalian cells were transfected for transient assays or for the generation of stable cell lines using Fugene 6 reagent according to the manufacturer's instructions. For transient transfection, efficiency of transfection was monitored by transfecting a GFP construct in a separate well. Total cell extracts were collected after 24-36 hours of transfection.

To generate stable cell lines, transfection was performed similar to transient transfection. 24 hours after transfection, the cells were selected using the respective antibiotic. Geneticin (G418 solution), at 500 µg/ml was used to select for cells transfected with the various pSUPERIOR constructs. After 1-2 weeks of growth, single colonies were picked by trypsinization and propagated. Sufficient liquid nitrogen stocks were prepared before proceeding with experimentation.

V.2.D. RNA INTERFERENCE

V.2.D.1. shRNA design

siRNA target sequences were identified using the Oligoengine RNAi design software available on the internet. All sequences thus identified were searched in the National Center for Biotechnology Information's (NCBI) nucleotide BLAST using ''search for short nearly exact matches'' mode against all human sequences deposited in the GenBank, EMBL (European Molecular Biology Laboratory), DDBJ (DNA Data Bank of Japan) and PDB (Protein Data Bank) databases. Oligo sequences, which did not have significant homology to genes other than the targets, were chosen and synthesized as a 64-nt sense and antisense primer.

V.2.D.2. Plasmid generation and transfection

The 64-nt shRNA sense primer and the antisense primers were annealed, gel eluted and ligated into the pSUPER and pSUPERIOR vectors (Oligoengine) according to the manufacturer's instructions.

V.2.D.3. Induction of Acinus knockdown

Knockdown of Acinus in the HeLa-A3121 stable cell lines was induced by addition of 1 µg/ml tetracycline (Invitrogen). Cells transfected with the empty pSUPERIOR vector control were treated similarly. Maximal RNA interference and knockdown of Acinus in the A3121 cells were observed after 4 to 5 days of tetracycline treatment. For experimental analysis, A3121 and pSUPERIOR cells were maintained in tetracycline for 72 hrs or extended periods.

V.2.E. RNA METHODS

V.2.E.1. Purification of cellular RNA

Total cellular RNA was extracted from 6 x 10^5 cells seeded in 6 cm plates. Cells were harvested by scraping and washed once in cold PBS. Subsequently, RNA extraction was performed using the RNeasy Mini kit (Qiagen) according to the manufacturer's instructions. The amount of total RNA in the final eluate was spectrophotometrically determined.

V.2.E.2. Reverse transcriptase PCR (RT-PCR)

1 µg of RNA was reverse transcribed and amplified in a one-step reaction using the TITANIUM One-Step RT-PCR kit (BD Pharmigen) according to the manufacturer's instructions. For amplification of Acinus, primers targeting the following sequence at the C-terminal end of Acinus-L (product size: 326 bp) were used: forward primer 5´-CAGATCGTTCAGAAAGAGG-3´ and reverse primer 5´-CGGGGTGGGCGCCGC-3´. For the amplification of the housekeeping gene GAPDH (product size: 329 bp), the following primer pair was used: forward primer 5´-GTGGAAGGACTCATGACCACAG-3´ and reverse primer 5´-CTGGTGCTCAGTGTAGCCCAG-3´

V.2.F. SURVIVAL ASSAYS

V.2.F.1. Measurement of cell numbers

2 x 10^5 cells were seeded in 60 mm tissue culture dishes and counted in quadruplicates using a haemocytometer every 3 days. Each cell line was seeded in two separate dishes.

V.2.F.2. Crystal violet staining and quantification

For measurement of cell numbers, 1 x 10^4 cells were seeded into 96-well plates in triplicates and serially diluted 1:1. After 8 days cells were stained with 0.5% crystal violet and 20% methanol for 20 min and washed extensively with water. Stained cells were solubilized with 33% acetic acid and the absorbance was measured at 560 nm.

V.2.F.3. Senescence-associated β-galactosidase assay

SA-β-gal staining solution

2 mM	MgCl2
150 mM	NaCl
5 mM	Potassium ferricyanide ($FeK_3(CN)_6$)
5 mM	Potassium ferrocyanide ($K_4Fe(CN)_6 \cdot 3H_2O$)
40 mM/100 mM	sodium citrate/sodium phosphate, pH 6
1 mg/ml	x-gal

Cells, seeded in 6-well plates, were washed twice with PBS before fixation (2% paraformaldehyde, 0.2% glutaraldehyde prepared in 100 mM sodium phosphate, pH 6.0) for 5 min. The fixative was removed and 1.5 ml of the SA-β-gal staining solution was applied. Cells were incubated for up to 24h at 37°C. Finally, cells were washed with PBS before microscopy.

V.2.F.4. LDH assay

Cell viability after staurosporine treatment was determined by measurement of the release of lactate dehydroxygenase (LDH) employing a Cytotoxicity Detection Kit (Roche Diagnostics) following the instructions of the manufacturer. 10 µl of the overlaying medium after apoptosis induction was applied to 100 µl of freshly prepared LDH assay mix. Absorbance was measured at 495 nm every 10 min for a period of 30 minutes at room temperature.

V.2.G. Expression and purification of recombinant proteins

V.2.G.1. Infection of SF9 cells

High-titer virus stocks were used to infect 2 × 10^7 cells/plate SF9 cells in 15 cm tissue culture dishes. Infected plates were incubated at 27°C for 3 days before harvesting the cells.

V.2.G.2. Purification of recombinant FLAG-Acinus

Lysis buffer

20 mM	Tris, pH 7.9
500 mM	NaCl
4 mM	$MgCl_2$
0.4 mM	EDTA
20 mM	β-glycerophosphate
20%	glycerol

Cells from 15 tissue culture dishes, infected as described, with the appropriate baculovirus, were harvested by scraping. Harvested cells were washed twice in PBS before lysing with 8 ml of lysis buffer containing 1 mM DTT and Complete protease inhibitor cocktail. Complete lysis was accomplished by freezing and thawing 2-3 times. Subsequently, the cell debris was pelleted by centrifuging at 8000 rpm for 15 min at 4°C. 250 µl bed volume of FLAG M2-agarose, pre-equilibrated in lysis buffer, was added to bind the FLAG-tagged protein in the supernatant. Following incubation for 4 hours on a rotator at 4°C, the M2-agarose was washed 3-4 times with lysis buffer containing 0.5 mM DTT and Complete protease inhibitor cocktail. The bound FLAG-tagged proteins were eventually eluted in 250 µl lysis buffer containing 200 µg/ml FLAG-peptide, 0.5 mM DTT and Complete protease inhibitor cocktail on a rotator at 4°C for 30 min. All centrifugations of samples with M2-agarose were performed at 3000 rpm for 5 min at 4°C.

V.2.H. PROTEIN STUDIES

V.2.H.1. Preparation of cell extracts

High salt lysis buffer

350 mM	NaCl
20 mM	HEPES pH 7.9
1.0 mM	$MgCl_2$
0.5 mM	EDTA
0.1 mM	EGTA
0.5 mM	DTT
1.0%	NP-40
20%	glycerol

About 5×10^5 cells were collected from the cell culture dish by scraping and pelleted down at 2000 rpm at 4°C for 5 min. Cells were washed once in PBS and then lysed in a high-salt buffer containing Complete protease inhibitor cocktail and centrifuged at 13000 rpm for 15 min at 4°C to pellet the cell debris. The supernatant was collected and the protein concentration quantitated using Bio Rad Protein assay according to manufacturer's instructions.

V.2.H.2. Protein gel electrophoresis (SDS-PAGE)

Since the range of apparent molecular weights of proteins to be analyzed were between 18 and 220 kDa, 4-15% gradient SDS-PAGE gels were used to separate proteins. The composition of 4 and 15% gels as well as those of the stacking gel is given in Table 2.

Table 2. Composition of polyacrylamide gels

Stacking	Acrylamide (40%) (ml)	0.5M Tris/Cl pH 6.8 (ml)		H_2O (ml)	10% SDS (µl)	10% APS (µl)	TEMED (µl)
4%	1.35	1.25		7.15	100	100	10
Resolving	**Acrylamide (40%) (ml)**	**0.5M Tris/Cl pH 8.8 (ml)**	**50% glycerol (ml)**	**H_2O (ml)**	**10% SDS (µl)**	**10% APS (µl)**	**TEMED (µl)**
4%	0.666	1.25	-	3	50	33.3	3.3
15%	2.5	1.25	1	0.166	50	33.3	3.3

V.2.H.3. Western blotting

Laemmli's running buffer

0.25 M	Tris
1.92 M	glycine
1%	SDS

Transfer buffer

39 mM	glycine
48 mM	Tris base
0.037%	SDS
20%	methanol

5X SDS sample buffer

60 mM	Tris-Cl (pH 6.8)
24%	glycerol
2%	SDS
14.4 mM	β-mercaptoethanol
1%	bromophenol blue

Protein sample for SDS-PAGE was prepared by mixing an appropriate amount of cell extract with 5× SDS sample buffer with β-mercaptoethanol.

Samples were heated to 95°C for 3 to 5 min and cooled immediately on ice before loading. Equal amounts of proteins were separated under reducing conditions by SDS-PAGE on 4-15% gradient gels. Gels were run at 200V. The separated proteins were subsequently blotted onto a polyvinylidene difluoride membrane (Amersham Pharmacia) using a wet blot apparatus (Bio Rad).

Membranes were blocked for 1 hour with 5% non-fat dry milk in Tris-buffered saline with 0.05% Tween-20 and then immunoblotted overnight at 4°C using the respective primary antibody.

V.2.H.4. Immunoprecipitations

Buffer A		Buffer B	
10 mM	HEPES pH 7.9	10 mM	HEPES pH 7.9
5 mM	$MgCl_2$	25% (v/v)	glycerol
0.25 M	sucrose	1.5 mM	$MgCl_2$
10 mM	β-mercaptoethanol	0.1 mM	EDTA
		10 mM	β-mercaptoethanol

Buffer C	
20 mM	Tris-HCl pH 7.9
0.25 mM	EDTA
10% (v/v)	glycerol
0.5 mM	DTT
0.2 mM	phenylmethylsulfonyl fluoride

Extracts for immunoprecipitation were prepared as follows: 1 x 10^7 cells were collected and the cell pellets were resuspended in buffer A containing Complete protease inhibitor cocktail (Roche Diagnostics). NP-40 was added to a final concentration of 0.1%, and the cells were lysed by freezing and thawing followed by incubation on ice for 10 min. The supernatant or cytosolic fraction was collected after centrifugation in a microcentrifuge at 14,000 rpm for 5 min at 4°C. The pellet was dissolved in a buffer B containing Complete protease inhibitor cocktail. NaCl was added to a final concentration of 400 mM and the sample was incubated on ice for 30 min. The sample was freeze-thawed, centrifuged at 14,000 rpm for 15 min at 4°C and the supernatants used as input material for immunoprecipitations.

SAP18 antibodies were bound to 10 µl protein G-sepharose beads (Amersham Pharmacia Biotech AB) equilibrated in buffer C containing 100 mM KCl. The beads were incubated for 12 hrs with 100 µl of the input material at 4°C. Following four washes with buffer C containing 500 mM KCl and 0.05% NP-40, protein complexes were eluted from the beads with 2x SDS-sample buffer and analyzed by SDS-PAGE and Western blotting.

V.2.I. INDUCTION OF APOPTOSIS

Depending on the requirements of the particular experiment, appropriate numbers of cells were seeded into suitable culture dishes/plates. Following overnight growth, cells were washed once in fresh growth media and supplemented with fresh growth media containing the desired drug at the appropriate concentration.

V.2.J. CASPASE ASSAYS

Caspase assay buffer

50 mM	HEPES pH 7.3
100 mM	NaCl
10%	sucrose
0.1%	CHAPS
10 mM	DTT

Cell extracts were collected as described in section III.2.H.1. and the protein concentration determined. Lysates were diluted in high salt lysis buffer to obtain similar concentration of protein in all samples analyzed. Caspase-3 activity in apoptotic cells was determined by incubating cell lysates with 50 µM of a fluorogenic substrate DEVD-AMC (N-acetyl-Asp-Glu-Val-Asp-aminomethylcoumarin) in 200 µl caspase assay buffer. The release of aminomethylcoumarin was measured by fluorometry using an excitation wavelength of 360 nm and an emission wavelength of 475 nm. Data was collected every 5 minutes at 37°C over a period of 3 hours.

V.2.K. FACS ANALYSIS

About 2×10^5 cells were seeded in 12-well plates and allowed to grow overnight. After induction of apoptosis for the specified time duration, cells were

collected by scraping them from the tissue culture dish. Floating cells in the supernatant were also collected by centrifuging at 1200 rpm for 5 minutes at room temperature. Cell pellets were washed briefly in 1× PBS and lysed in a hypotonic lysis buffer (1% sodium citrate, 0.1% Triton X-100, 50 µg/ml propidium iodide). The nuclei were subsequently analyzed by flow cytometry after at least 10 minutes of lysis.

Percentage of hypodiploid nuclei was assessed by analyzing the FSC/FL-2 profile (Wesselborg et al., 1999) using a FACScalibur (Becton Dickinson). Apoptotic cells were determined by quantification of the sub-G_1 peak using the CELLQuest analysis software.

V.2.L. DNA LADDERING ASSAYS

Neutral lysing solution

0.5%	SDS
0.1 M	NaCl
5 mM	EDTA
10 mM	Tris-HCl pH 8.0
0.1 mg/ml	proteinase K

DNA for detection of apoptotic oligonucleosomal DNA fragmentation was prepared according to the protocol by Hirt (Hirt, 1967). 2 x 10^6 cells seeded in 60 mm dishes were washed with PBS and lysed in 1 ml neutral lysing solution followed by incubation at 37°C for 2 hrs. NaCl was added to a final concentration of 1 M and after overnight incubation at 4°C, the precipitated salt and SDS were pelleted at 25,000 rpm for 20 min in an ultracentrifuge. The supernatant was extracted with phenol:chloroform:iso-amyl alcohol (25:24:1) and the DNA was precipitated with ethanol. DNA laddering was then analyzed on 1% agarose gels.

V.2.M. PULSED-FIELD GEL ELECTROPHORESIS (PFGE)

Plugs for pulsed-field gel electrophoresis (PFGE) were prepared using the CHEF Mammalian Genomic DNA plug kit (Bio-Rad Laboratories) according to the manufacturer's instructions. PFGE was performed using the Gene Path System (Bio-Rad). 1% Certified Megabase Agarose (Bio-Rad) horizontal gels

were run at 14°C with program no. 18 for the separation of 50 kb to 1 Mb DNA fragments for 19.5 hours. Gels were stained with 0.5 µg/ml ethidium bromide in water for a period of 1 to 2 hours, washed 2-3 times in water to remove excess ethidium bromide and documented.

V.2.N. *IN VITRO* CHROMATIN CONDENSATION ASSAYS

Buffer A		Buffer B	
50 mM	HEPES pH 7.5	50 mM	HEPES pH 7.5
10 mM	potassium acetate	110 mM	potassium acetate
2 mM	magnesium acetate	2 mM	magnesium acetate
2 mM	EGTA	2 mM	EGTA

Cytoplasmic extracts for *in vitro* chromatin condensation assays were prepared as described (Adam et al., 1990) with slight alterations. Cells were washed with PBS and harvested by scraping from the tissue culture dishes. After one more wash with PBS cells were suspended with cold buffer B and resuspended in 1.5 vol of buffer A containing 2 mM DTT and protease inhibitor cocktail. After swelling on ice for 30 min the cells were lysed by douncing. Subsequently, nuclei and cell debris were spun down at 1500 g for 10 min. The supernatant was spun again at 100,000 g for 30 min. In the final supernatant the potassium acetate concentration was adjusted to 110 mM. For permeabilization cells were rinsed twice with buffer B and then treated with buffer B containing 2 mM DTT, 20 µg/ml digitonin and 1 µg/ml DAPI for 45 min at RT, followed by two washing steps with buffer B containing 2 mM DTT. 25 µl of reaction mixture were added to the permeabilized cells and sealed with a cover slip. The reaction mixture contained 300 µg of cytoplasmic extract, 5 µM phosphocreatine, 20 U/ml creatine kinase, 1 mM ATP and, where indicated, 1 µg recombinant caspase-3. Control reactions were performed in absence of cytoplasmic extract. The reactions were incubated for 3 hrs at 37°C and analyzed using an Axiovert135 microscope equipped with OpenLab software.

VI. RESULTS

VI.1. KNOCKDOWN OF ACINUS

RNA interference is a powerful tool to suppress gene expression for studying gene function. In order to characterize the physiological role of Acinus in apoptotic chromatin condensation, a vector based short hairpin RNA (shRNA) system for stable and inducible knockdown of Acinus in HeLa cells was employed. A 64-nt oligo, consisting of a 5' *Bgl*II site and a 3' *Hind*III site and a unique 19-nt sense and antisense target sequence, separated by a 9-nt spacer was cloned into the pSUPERIOR vector.

VI.1.A. SHRNA DESIGN

Numerous computational programs are available for target identification of potential shRNA targets. It is well documented that not all shRNAs designed against a particular target mRNA are functionally efficient. For this reason, two different target sequences (Table 3) against the Acinus mRNA were chosen.

Table 3: Acinus shRNA target sequences. Target sequences were selected based on criteria mentioned in the text. Sense and antisense oligos with the indicated target sequences were annealed and cloned into pSUPER or pSUPERIOR vector for transient and stable expression respectively.

shRNA	Target sequence on Acinus mRNA	GC content
Acinus 3121	GAGGCCTTCTGGATTGACA	53%
Acinus 3493	TGGGATCGGGACAAAGTTC	53%

Target sequences were identified using the Oligoengine RNAi design tool. The target sequences were 19-nt in length and consisted of a 2-nt 3' overhang. It has been reported that RNA duplexes with 2-nt 3' overhangs are more efficient in degrading target RNA than similar blunt-ended duplexes (Elbashir et al., 2002). Nucleotide BLAST searches were performed to ensure the specificity of the target sequences. Furthermore, sequences on Acinus were selected such that all known non-apoptotic isoforms of Acinus would be targeted. Figure 7

shows a schematic representation of the different Acinus isoforms with their distinctive domains. Since the RNA recognition motif (RRM) is common to all Acinus isoforms, target sequences from around this region were chosen (Figure 7). The shRNAs were named corresponding to the first nucleotide of the target sequence.

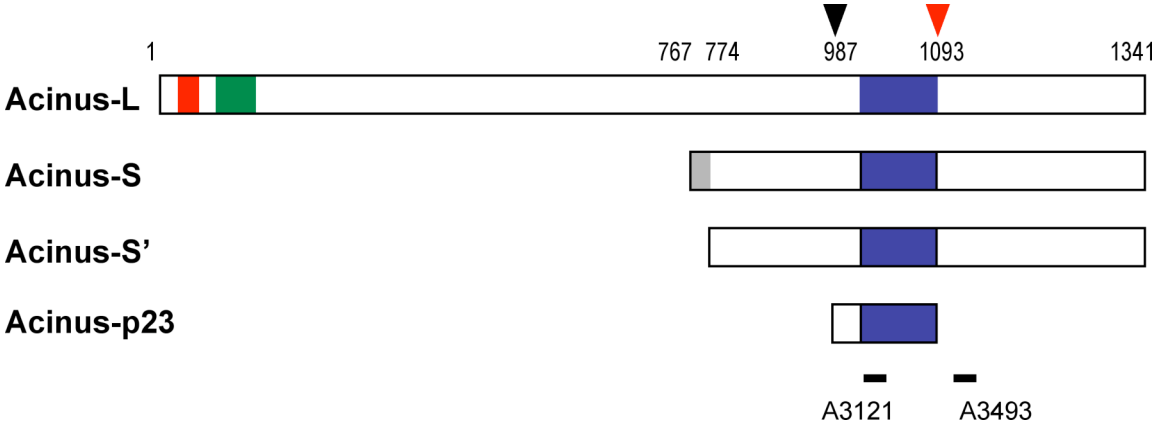

Figure 7: Schematic representation of Acinus isoforms and the location of the shRNA targeting sequences. Represented are the described protein domains of Acinus and the location of cleavage sites with their corresponding amino acids (Aravind and Koonin, 2000; Sahara et al., 1999). Red box, P-loop; green box, SAP domain; dark blue box, region homologous to the RNA-recognition motif of *Drosophila* Sxl. The grey box represents a unique eight amino acid sequence at the N terminus of Acinus-S followed by residues 767 to 1341 of Acinus-L. Acinus-S' corresponds to residues 774 to 1341 of Acinus-L. The black arrowhead represents the cleavage site of an unknown protease and the red arrowhead that of caspase-3. Positions of the targeting sequences are indicated by a small dash at the bottom of the figure.

VI.1.B. Evaluation of the silencing potency of the various shRNA

To evaluate the silencing potency, the two shRNA were cloned into pSUPER vectors (A3121-pSUPER and A3493-pSUPER) and were individually co-transfected with a mammalian expression construct encoding FLAG-tagged Acinus-S into HeLa tet-off cells. An empty pSUPER vector served as a negative control. Whole cell extracts were collected 12, 24 and 36 hours after transfection and were analyzed by Western blotting using an antibody targeted against the FLAG epitope (Figure 8).

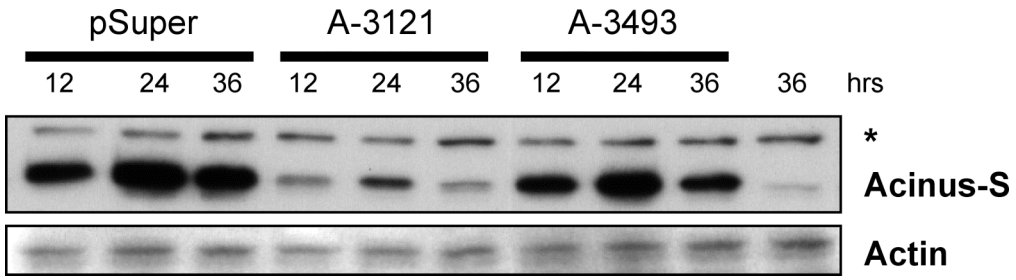

Figure 8: Evaluation of silencing potency of two different Acinus shRNA. HeLa tet-off cells were co-transfected with either the empty vector or the shRNA construct and a construct expressing FLAG-tagged Acinus-S. Western blotting using a FLAG monoclonal antibody detects a band corresponding to Acinus-S. An unspecific band recognized by the FLAG antibody is indicated by an *asterisk*.

In comparison to the untransfected control (last lane), considerable Acinus-S expression was observed after 12 hours of transfection, peaking at 24 hours in the pSUPER empty vector transfected cells. Significant knockdown of Acinus could be observed in cells co-transfected with A3121-pSUPER at all time points analyzed. The A3493-pSUPER co-transfected cells, however, did not exhibit any significant reduction in the level of Acinus-S-FLAG. An antibody directed against β–actin was used as a control to monitor equal loading. Based on the results of the co-transfection experiments, the A3121 shRNA was chosen for cloning into pSUPERIOR vector containing a tetracycline-regulated element for subsequent experiments.

VI.1.C. STABLE AND INDUCIBLE KNOCKDOWN OF ACINUS

To achieve an inducible knockdown of Acinus, HeLa T-Rex cells were transfected with a pSUPERIOR vector expressing A3121 shRNA and were subjected to geneticin selection to obtain individual clones that have the plasmid stably integrated. HeLa T-Rex cells stably expressing an empty pSUPERIOR vector served as experimental control. Clones thus selected were treated with or without tetracycline for 24 or 48 hours and were analyzed for knockdown of Acinus by Western blotting (Figure 9). Significant knockdown of both the long and short isoforms of Acinus was detected in all the analyzed clones at the protein level after 48 hours of tetracycline treatment. Analysis of two such clones is shown in Figure 9.

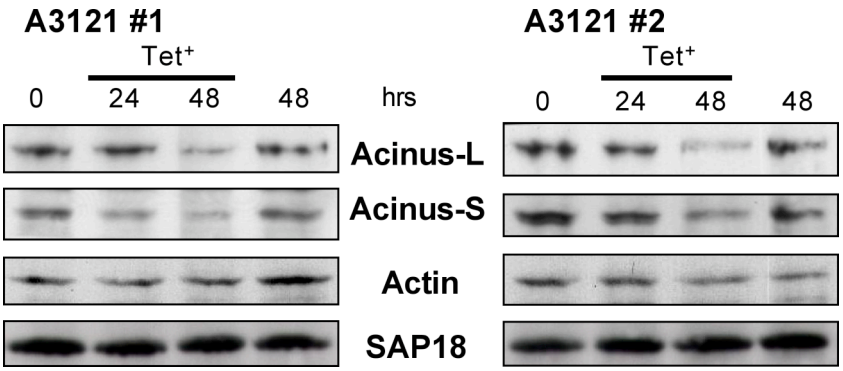

Figure 9: Inducible knockdown of Acinus in stable clones. Time course of Acinus knockdown in two different stable clones A3121 #1 and A3121 #2 after 0, 24 and 48 hours of induction with tetracycline (*Tet+*). Western blotting was performed on whole cell extracts using an antibody specifically recognizing both isoforms of Acinus. Levels of SAP18 and β-actin were also analyzed.

To determine the efficiency of Acinus knockdown in the stable clones at the mRNA level, total mRNA was isolated from uninduced A3121 cells or cells induced with tetracycline for 24, 48 and 72 hours and analyzed by reverse transcriptase PCR (RT-PCR) (Figure 10). A pSUPERIOR clone, treated similarly with tetracycline, served as an empty vector control. In comparison to the vector control, significant reduction in the level of Acinus mRNA was observed after 48-72 hours of induction of RNAi. Amplification of the housekeeping gene Glyceraldehyde-3-phosphate dehydrogenase (GAPDH) was performed to monitor the amount of RNA in the different lanes.

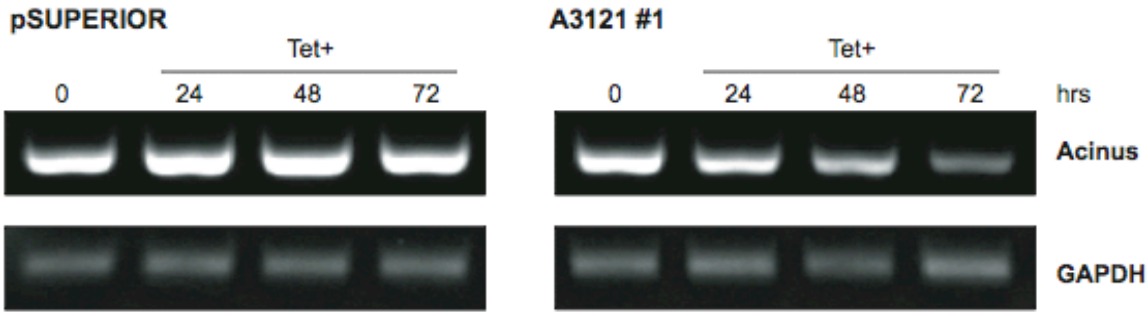

Figure 10: RT-PCR analysis of Acinus knockdown cells. Total RNA was isolated from pSUPERIOR and A3121 cells after 0, 24, 48 and 72 hours of tetracycline treatment (*Tet+*) and reverse transcriptase PCR was performed using Acinus specific primers. GAPDH was amplified as an internal control.

VI.1.D. ACINUS HAS A SLOW PROTEIN TURNOVER RATE

It is not uncommon that some proteins exhibit notable knockdown after 24- 48 hours of RNAi induction. However, efficient reduction of a target protein by RNAi is directly related to its protein turnover rate. To analyze the relative protein turnover rate of Acinus, total cell extracts of HeLa cells either untreated or treated with cycloheximide were analyzed by Western blotting (Figure 11). In comparison to the Bcl-2 protein Mcl-1 or the caspase-8 inhibitor FLIP-s that displayed significant degradation after 2 hours of cycloheximide treatment, Acinus as well as the ASAP subunit SAP18 were virtually unaffected even after 8-10 hours of cycloheximide treatment.

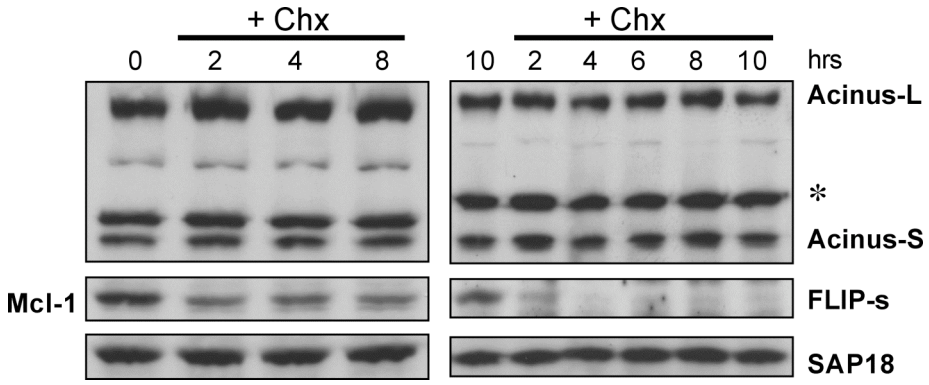

Figure 11: Acinus has a slow protein turnover rate. Whole cell extracts of HeLa cells treated with cycloheximide (*Chx*) for the indicated periods of time were analyzed for the indicated proteins by Western blotting. Mcl-1 is significantly reduced and FLIP-s is completely degraded after 2 hours of Chx treatment. In comparison, levels of Acinus and SAP-18 are not affected by 8-10 hours of Chx treatment. *Asterisk* indicates an unspecific band recognized by the Acinus antibody.

VI.1.E. KNOCKDOWN OF ACINUS IS REVERSIBLE

Because Acinus is a protein with relatively slow turnover rate, the Acinus knockdown clones were induced for longer periods of time, which allowed for > 95% knockdown of Acinus isoforms. Western blot analysis of three HeLa-A3121 clones after long-term tetracycline treatment (8 days) is shown in Figure 12. Notably, levels of Acinus in all three A3121 clones not treated with tetracycline were slightly lower than that of control HeLa-pSUPERIOR cells. This could be due to the fact that some background RNAi occurs in these cells even in the absence of tetracycline induction.

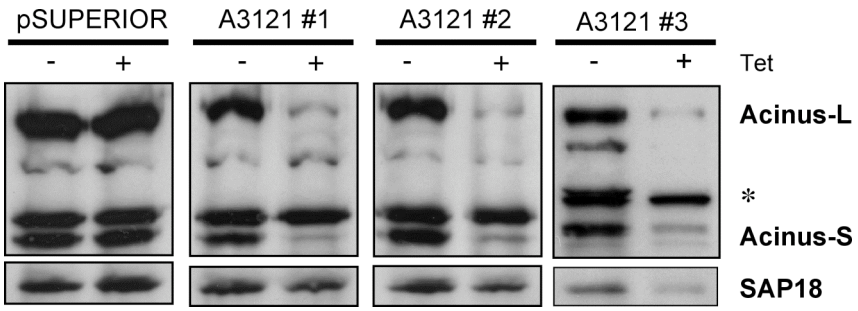

Figure 12: Long term knockdown in three independent Acinus knockdown clones. Western blot analysis of whole cell extracts from HeLa-pSUPERIOR and three different HeLa-A3121 clones after 8 days of tetracycline treatment using Acinus and SAP-18 specific antibodies. Significant knockdown of Acinus can be seen in tetracycline-treated (+) lanes but not in tetracycline untreated lanes (-). Asterisk indicates an unspecific protein recognized by the Acinus antibody.

It was observed repeatedly that upon knockdown of Acinus, levels of SAP18 were slightly reduced in all three clones analyzed (Figure 12). Reduction in the levels of one component of a multi-protein complex due to the knockdown of another component of the complex has been described before. Knockdown of the major scaffolding subunit (Aα) of the multiprotein complex protein phosphatase 2A (PP2A), resulted in the subsequent reduction of component subunits, such as the catalytic subunit (C) and the two regulatory subunits (B and B') at the protein level (Strack et al., 2004). It was suggested that this could reflect the differences in the half-life of the monomeric subunits and/or that complex involving subunit Aα may be protected from degradation. Similarly, it is possible that, in the absence of Acinus excess complex components not maintained in the complex are prone to degradation, resulting in the observed reduction in SAP18 levels.

Moreover, removal of tetracycline from the growth medium allowed for complete reversal of the phenotype. As can be seen in Figure 13, removal of tetracycline and recovery for several days resulted in re-expression of both long and short isoforms of Acinus in levels comparable to the uninduced control.

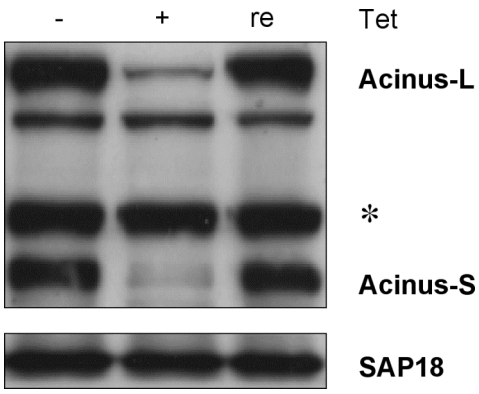

Figure 13: Acinus knockdown is completely reversible. Whole cell extracts from HeLa-A3121 cells uninduced (-), induced for knockdown (+) or released from knockdown (re) were analyzed for the indicated proteins by Western blotting. *Asterisk* indicates an unspecific band recognized by the Acinus antibody.

VI.2. EFFECT OF ACINUS KNOCKDOWN ON ASAP COMPLEX

VI.2.A. SAP18 AND RNPS1 LOCALIZE TO THE NUCLEUS

To determine if the knockdown of Acinus has any effect on the nuclear localization of the other ASAP complex subunits SAP18 and RNPS1, nuclear and cytoplasmic fractions of HeLa-pSUPERIOR and HeLa-A3121 cells, untreated or long-term treated with tetracycline were separated and analyzed by Western blotting. As shown in Figure 14, the individual components of the ASAP complex localize exclusively in the nucleus in the control cells since they were only detected in the nuclear and not in the cytoplasmic fraction. Notably, knockdown of Acinus had no influence on their localization. A tetracycline-treated pSUPERIOR control was included to rule out any potential effect of tetracycline by itself.

VI.2.B. ACINUS IS NOT REQUIRED FOR THE MAINTENANCE OF SAP18-RNPS1 INTERACTION

The ASAP complex was originally purified in six consecutive steps over various chromatographic columns (Schwerk et al., 2003), indicating a relatively strong interaction between the individual components of the complex. To determine the integrity of the remaining subunits of the complex in the absence of Acinus, immunoprecipitation experiments were performed using an antibody

directed against SAP18 (Figure 14). Notably, Acinus and RNPS1, both components of the ASAP complex, could be co-immunoprecipitated with SAP18 in the control cells as detected by Western blot analysis. More importantly, comparable amounts of RNPS1 were co-immunoprecipitated in the absence of Acinus (Figure 14, lower panel) indicating that Acinus is not required for the maintenance of a nuclear SAP18 and RNPS1 complex.

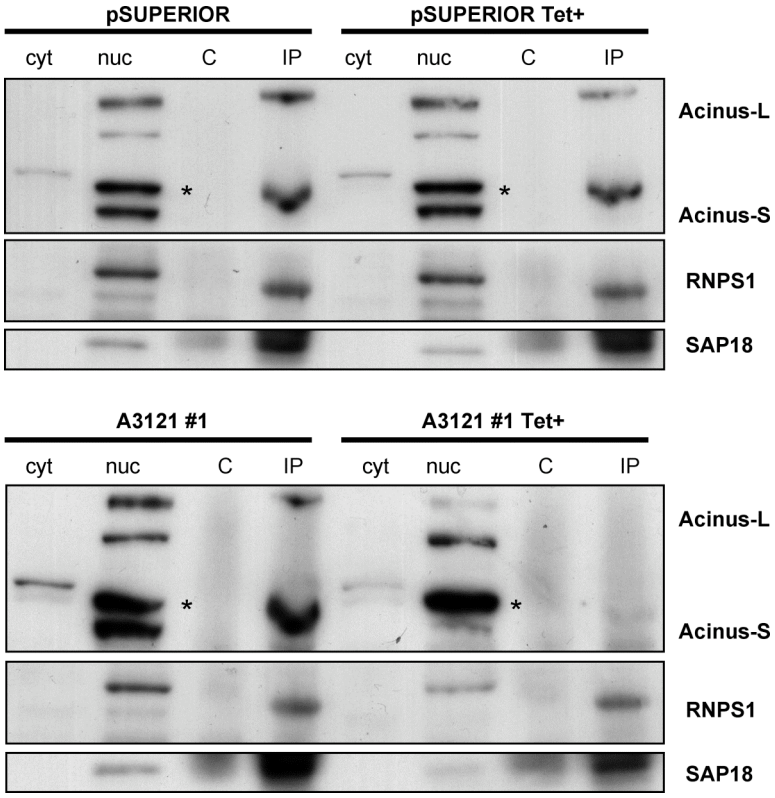

Figure 14: Acinus is not required for nuclear localization and interaction between ASAP components. Nuclear (nuc) and cytoplasmic (cyt) extracts were prepared from untreated or long-term tetracycline-treated (Tet+) pSUPERIOR and A3121 cells (clone #1). Nuclear extracts were immunoprecipitated using an antibody directed against SAP18 (IP) or with empty beads (C). Western blotting using Acinus, RNPS1 and SAP18 specific antibodies recognized the indicated proteins. The observed differences in mobility of the corresponding bands in some lanes are due to the differences in salt concentration. Unspecific bands recognized by the Acinus antibody are indicated with asterisks.

To rule out any potential artifacts developing due to the long-term absence of Acinus, nuclear and cytoplasmic fractions were generated from cells treated with tetracycline for 72 hours and analyzed similarly (Figure 15). As can be seen, the level of Acinus was considerably reduced after 72 hours of tetracycline

treatment of A3121 cells. However, significant amounts of RNPS1, comparable to the uninduced A3121 cells could still be co-immunoprecipitated with SAP18 in Acinus knockdown cells. It could be observed that residual Acinus-S, still persisting due to incomplete knockdown, was enriched after immunoprecipitation in the Acinus knockdown cells, although significantly less in comparison to that in the other control samples.

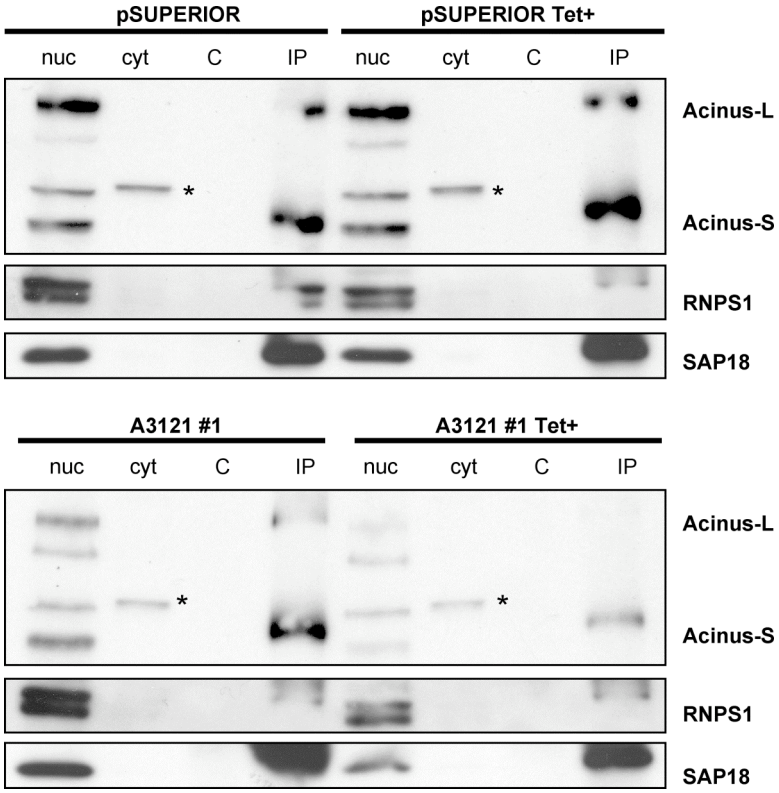

Figure 15: Immunoprecipitation 72 hours after induction of Acinus knockdown. Nuclear (nuc) and cytoplasmic (cyt) extracts were prepared from pSUPERIOR and A3121 cells (clone #1) untreated or tetracycline-treated (Tet+) for 72 hours. Nuclear extracts were immunoprecipitated using an antibody directed against SAP18 (IP) or with empty beads (C). Western blotting using Acinus, RNPS1 and SAP18 specific antibodies recognized the indicated proteins. An unspecific band recognized by the Acinus antibody is indicated with an asterisk.

VI.3. GROWTH SUPPRESSIVE EFFECT OF ACINUS KNOCKDOWN

VI.3.A. KNOCKDOWN OF ACINUS RESULTS IN A SLOW GROWTH PHENOTYPE

One of the first observations during the course of general maintenance of the RNAi clones was the relatively slow growth rate of the HeLa-A3121 clones after induction of RNAi by tetracycline treatment. Figure 16 shows the general growth

characteristic of HeLa-A3121 cells in the presence and absence of tetracycline after 9 days of growth. Though the addition of tetracycline had little or no effect on HeLa-pSUPERIOR cells, HeLa-A3121 cells displayed a substantial decrease in cell numbers after tetracycline addition indicating a reduced growth rate after Acinus knockdown. The reduced growth rate observed with the A3121 cells not induced for knockdown could be due to background RNAi in these cells (see Figure 12).

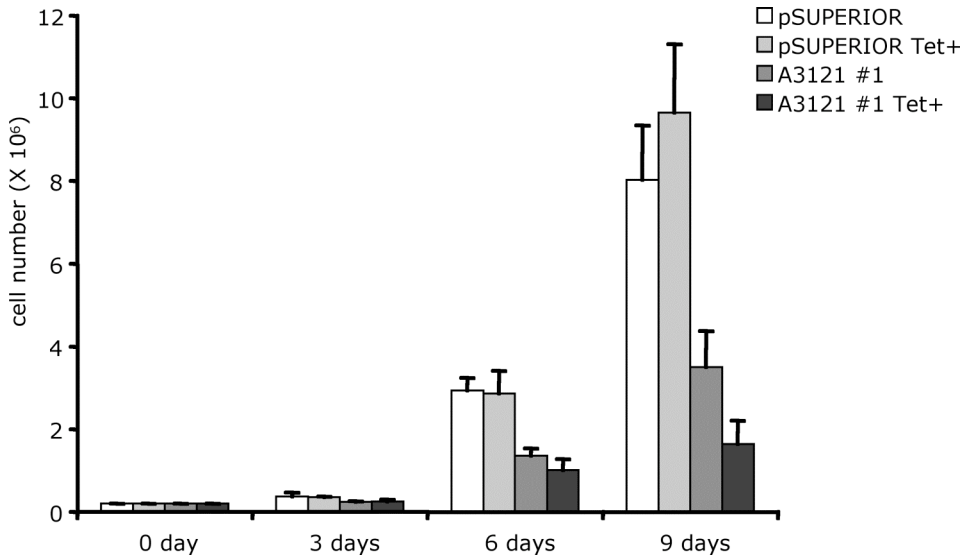

Figure 16: Analysis of growth characteristic of HeLa-A3121 clone #1. pSUPERIOR and A3121 cells were allowed to grow without treatment or after treatment with tetracycline (Tet+) for 9 days and cells counted every three days. Bars indicated are the mean ± s.d. of two independent experiments (*n*=2).

Furthermore, a crystal violet staining assay was performed to enable the quantification of the relative growth rates in Acinus knockdown clones as well as the HeLa-pSUPERIOR control cells. Cells were serially diluted and allowed to grow for 8 days in the presence or absence of tetracycline. Figure 17a shows the crystal violet staining of HeLa-pSUPERIOR and a HeLa-A3121 clone in triplicates. As can be clearly seen, knockdown of Acinus resulted in significant growth suppression in HeLa-A3121 cells. HeLa-pSUPERIOR cells treated or untreated with tetracycline had little or no growth effects.

Cells thus stained with crystal violet were solubilized and analyzed densitometrically. Figure 17b shows quantification of growth of three individual

HeLa-A3121 cells contrasted with HeLa-pSUPERIOR cells. Growth suppression was observed in all three HeLa-A3121 clones when Acinus was knocked down by the addition of tetracycline suggesting that the reduction in cell growth was not a clonogenic effect in one particular clone but rather a specific effect of Acinus knockdown.

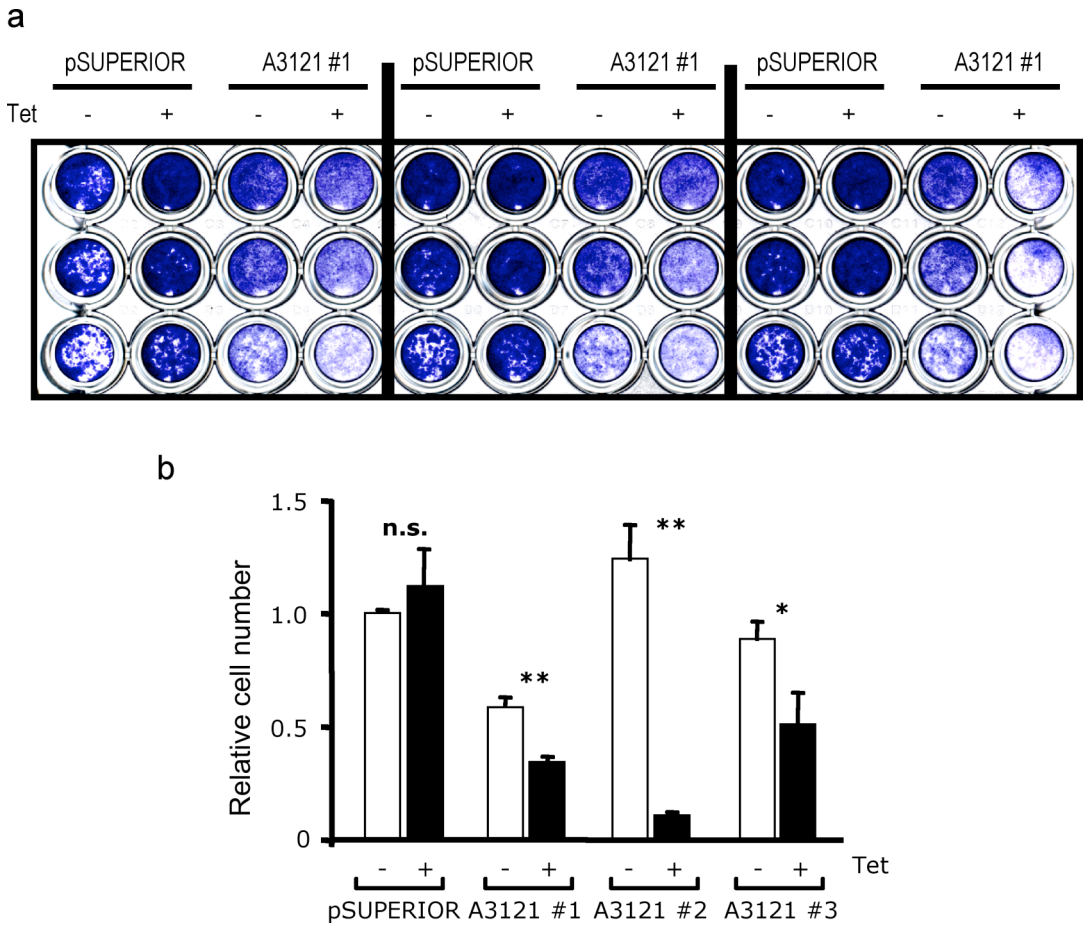

Figure 17: Acinus knockdown result in growth suppression. a. Crystal violet staining. pSUPERIOR and A3121 clone 1 cells were serially diluted and seeded into 96-well plates in triplicates. Cells were either left untreated (-) or treated with 1µg/ml tetracycline (+). Picture shows crystal violet staining of a portion of the 96-well plate after 8 days of growth. b. Quantification of crystal violet staining of pSUPERIOR and three independent A3121 clones by densitometric analysis. Bars represent the mean ± s.d. of three independent experiments (*n*=3). The cell number of untreated pSUPERIOR was set as 1. *n.s.*, not significant; *, $p < 0.005$; **, $p < 0.01$; *t* test for related samples.

VI.3.B. GROWTH SUPPRESSION IS NOT A RESULT OF SENESCENCE

Reduced growth rate in any cell population could be due to increased cellular senescence. Premature senescence in cultured cells (also referred to as 'stress'), as distinguished from replicative senescence in primary cell cultures, could be caused by one or more processes such as oxidative stress (Toussaint et al., 2000), epigenetic maintenance mechanisms (Jacobs et al., 1999), oncogenic stress (Bringold and Serrano, 2000; Serrano et al., 1997) and DNA damage (Di Leonardo et al., 1994). Senescent cells are metabolically active but are unable to divide further (Serrano and Blasco, 2001). Senescence-associated β-galactosidase (SA-βgal) has been shown to be a marker for cells undergoing senescence and/or stress (Dimri et al., 1995) probably reflecting the increased lysosomal content in these cells (Kurz et al., 2000). All cells express lysosomal β-galactosidase (βgal) that is optimally active at a pH of 4 (Morreau et al., 1989). Senescent cells on the other hand express βgal, which is also active at pH 6 and is referred to as senescence-associated β-galactosidase (SA-βgal) (Dimri et al., 1995). Staining cells with X-Gal, which is cleaved by βgal forming a localized blue precipitate at pH 6, distinguishes senescent from normal cells.

To determine if the growth suppression was a result of increased senescence in Acinus knockdown cells, a SA-βgal staining was performed. Figure 18 shows the results of light microscopic analysis of two HeLa-A3121 clones compared to the control pSUPERIOR cells. A slightly reduced but comparable amount of senescence-associated β-galactosidase staining was observed when cells were treated with tetracycline in both pSUPERIOR and A3121 cells, the effect being more pronounced in A3121 cells. This suggests comparable or even slightly lower background senescence in Acinus knockdown cells. However, it could be concluded from the analysis that the observed growth suppression in Acinus knockdown cells was not due to an enhancement of senescence in these cells.

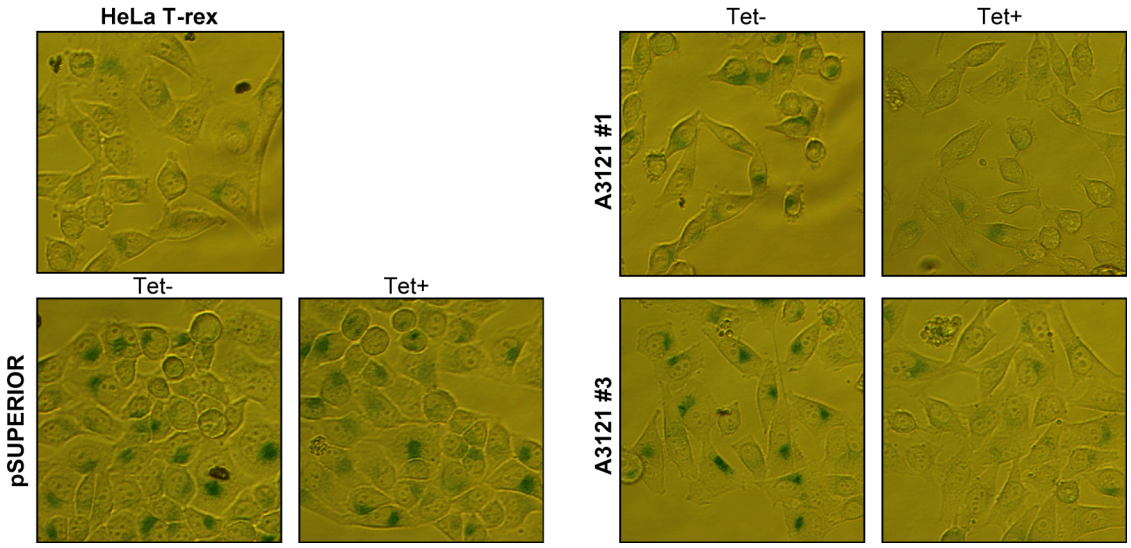

Figure 18: Senescence is not enhanced in Acinus knockdown cells. Phase contrast images of senescence-associated β-galactosidase staining. pSUPERIOR and two different clones of A3121 cells were grown in the absence of (Tet-) or presence of (Tet+) 1µg/ml tetracycline for 8 days and analyzed for senescence. HeLa T-rex parent cells were also analyzed for background senescence.

VI.4. APOPTOSIS IN ACINUS KNOCKDOWN CELLS

In its original description Acinus was identified as a protein involved in nuclear changes during later stages of apoptosis (Sahara et al., 1999). Furthermore, a recent study has provided evidence for regulation of apoptosis and cell survival by phosphorylation of Acinus by nuclear Akt (Hu et al., 2005). The effect of Acinus knockdown on the general progress of apoptosis was analyzed by different approaches.

VI.4.A. EARLIER CASPASE ACTIVATION IN ACINUS KNOCKDOWN CELLS

VI.4.A.1. Western blot analysis of caspase-3

In recent years it has become evident that a family of cysteinyl proteases, called caspases, are one of the major players during the process of apoptosis. In most cells, caspases are expressed as inactive zymogens and are activated by cleavage to give rise to active heterotetramers (Earnshaw et al., 1999). Analysis and detection of caspase cleavage by Western blotting can be used as an indication of processing and activation of caspases.

Caspase-3 is one of the downstream effector caspases that is activated later during the course of apoptosis. Inactive procaspase-3 is expressed as a 32 kDa protein that is processed by cleavage producing the active 17 kDa (p17) fragment. pSUPERIOR and A3121 cells cultured in the presence or absence of tetracycline were treated with the drug staurosporine, a broad-spectrum protein kinase inhibitor and an inducer of the mitochondrial pathway of apoptosis, for increasing durations of time. Whole cell extracts were collected and analyzed by Western blotting using a polyclonal antibody specifically recognizing procaspase-3 and the active p17 fragment. Results shown in Figure 19 indicate that caspase-3 is indeed activated in all cells analyzed. Furthermore, a closer inspection reveals a slight acceleration in the cleavage of caspase-3 in the A3121 cells treated with tetracycline as compared to their respective untreated controls.

VI.4.A.2. Cleavage of PARP

Cleavage of caspases is an essential event during the activation of caspases. However, reports suggest that caspases can indeed be activated by conformational changes without cleavage (Boatright et al., 2003; Stennicke et al., 1999). For this reason, cleavage of caspase substrates was analyzed as a more direct indication of caspase activity. Once activated, caspase-3 cleaves a number of downstream substrates. A specific nuclear target for caspase-3 is poly-(ADP-ribose)-polymerase (PARP), a 116 kDa protein that is cleaved during apoptosis resulting in two fragments of 84 and 32 kDa in size (Wieder et al., 1997). Western blot analysis was performed using an antibody specifically recognizing PARP to investigate whether cleavage and activation of caspases was accompanied by cleavage of specific caspase-3 target proteins in Acinus knockdown cells (Figure 19). Results of the analysis revealed that the kinetics of PARP cleavage indeed paralleled the cleavage and activation of caspase-3. As can be seen from Figure 19, after 2 hours of staurosporine treatment PARP was only partially cleaved in the control pSUPERIOR cells and in A3121 cells not induced for knockdown. However, knockdown of Acinus in the A3121 cells lead to an almost complete cleavage of PARP after only 1.5 hours of STS treatment,

further confirming that caspase-3 activation and thus apoptosis in general proceeded slightly faster in the Acinus knockdown cells.

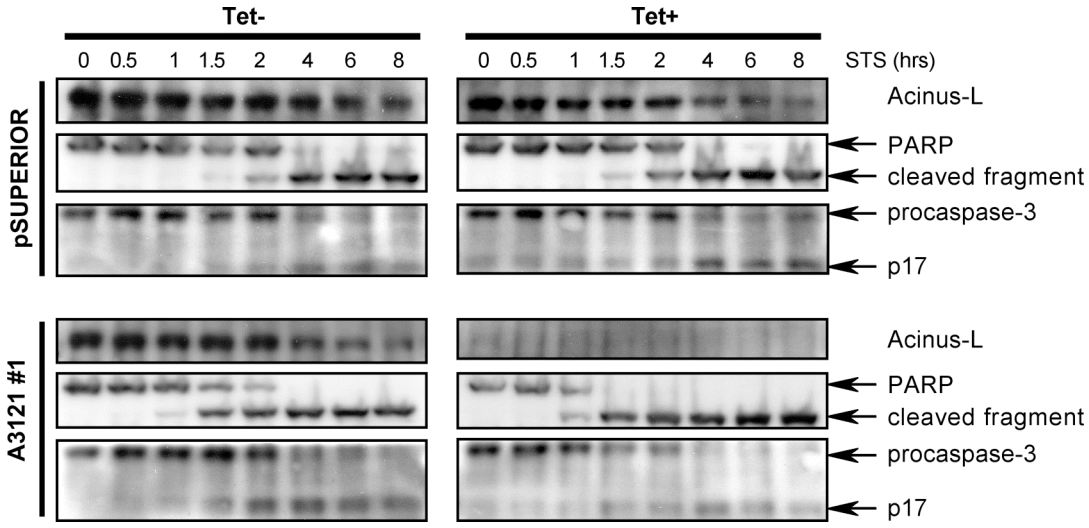

Figure 19: Accelerated caspase-3 and PARP processing in Acinus knockdown cells. pSUPERIOR and A3121 cells grown in the absence (Tet-) or presence (Tet+) of tetracycline were induced to undergo apoptosis with 1 µM staurosporine for the indicated amounts of time. Time course of caspase-3 cleavage was analyzed by Western hybridization using an antibody specifically recognizing procaspase-3 and the cleaved active caspase (p17). PARP cleavage was analyzed using a monoclonal antibody against PARP. Full length PARP and the cleavage product are indicated. Acinus levels in the cells were monitored by Western blot analysis of the long isoforms of Acinus (Acinus-L).

VI.4.A.3. Cleavage of ICAD

Human DNA fragmentation factor of 45 kDa (DFF45) and its mouse homologue, the inhibitor of caspase-activated DNase (ICAD) function as molecular chaperones for DFF40 or caspase-activated deoxyribonuclease (CAD) (Enari et al., 1998). Moreover, in normal cells, association of ICAD isoforms with CAD inhibits the nuclease activity of CAD (Enari et al., 1998; Gu et al., 1999; Sakahira et al., 1998; Wolf et al., 1999). During apoptosis, ICAD is cleaved primarily by caspase-3 inactivating its inhibitory function on CAD. The released CAD then cleaves DNA into oligonucleosomal fragments that are characteristic of the apoptotic nuclear changes (Liu et al., 1999; Zhang et al., 1999). To investigate cleavage of ICAD-L during apoptosis in Acinus knockdown cells, a Western blot analysis was performed using an antibody specific for human DFF45. Analysis of apoptotic lysates of control and HeLa-A3121 cells

induced or uninduced for knockdown (Figure 20) revealed that disappearance of DFF45 parallels the activation of caspase-3 and indeed occurred earlier in Acinus knockdown cells compared to any of the other controls. As can be observed from Figure 19 and Figure 20, background RNAi in A3121 cells contributes to an intermediate phenotype. This further emphasizes the significance of maintaining stoichiometric amounts of Acinus in cells.

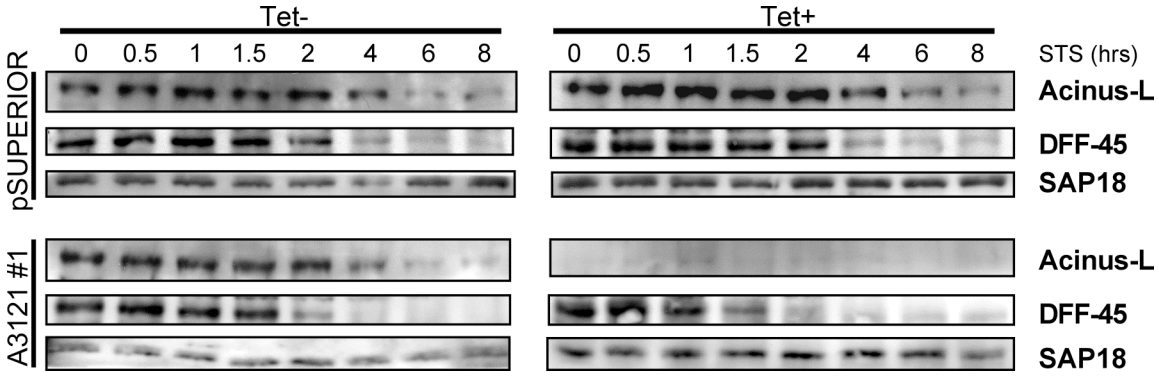

Figure 20: Time course of DFF-45 (ICAD) processing in Acinus knockdown cells. pSUPERIOR and A3121 cells, grown in the absence (Tet-) or the presence (Tet+), were treated with 1µM staurosporine (STS) for the indicated amounts of time. Whole cell extracts were analyzed for the indicated proteins by Western blotting.

VI.4.A.4. Caspase activity assay

Detection of caspase activity in extracts from apoptotic cells by *in vitro* fluorogenic substrate cleavage assays is also a direct indication of the activation of caspases. A relative advantage of the assay is that it allows for quantification of caspase activity.

Ac-DEVD-AMC was used as a substrate to assess caspase-3-like activity in extracts from control and HeLa-A3121 cells treated with staurosporine for the indicated amounts of time (Figure 21). Significant activation of caspase-3-like activity paralleling the cleavage of substrates was observed by Western blotting. Caspases were activated rapidly in Acinus knockdown cells with considerable substrate cleavage detectable already after 1.5 hours of apoptosis induction by staurosporine in all three clones analyzed. Thus, analysis of both *in vitro* caspase activity assay and *in vivo* caspase cleavage confirmed earlier activation of caspases in the absence of Acinus.

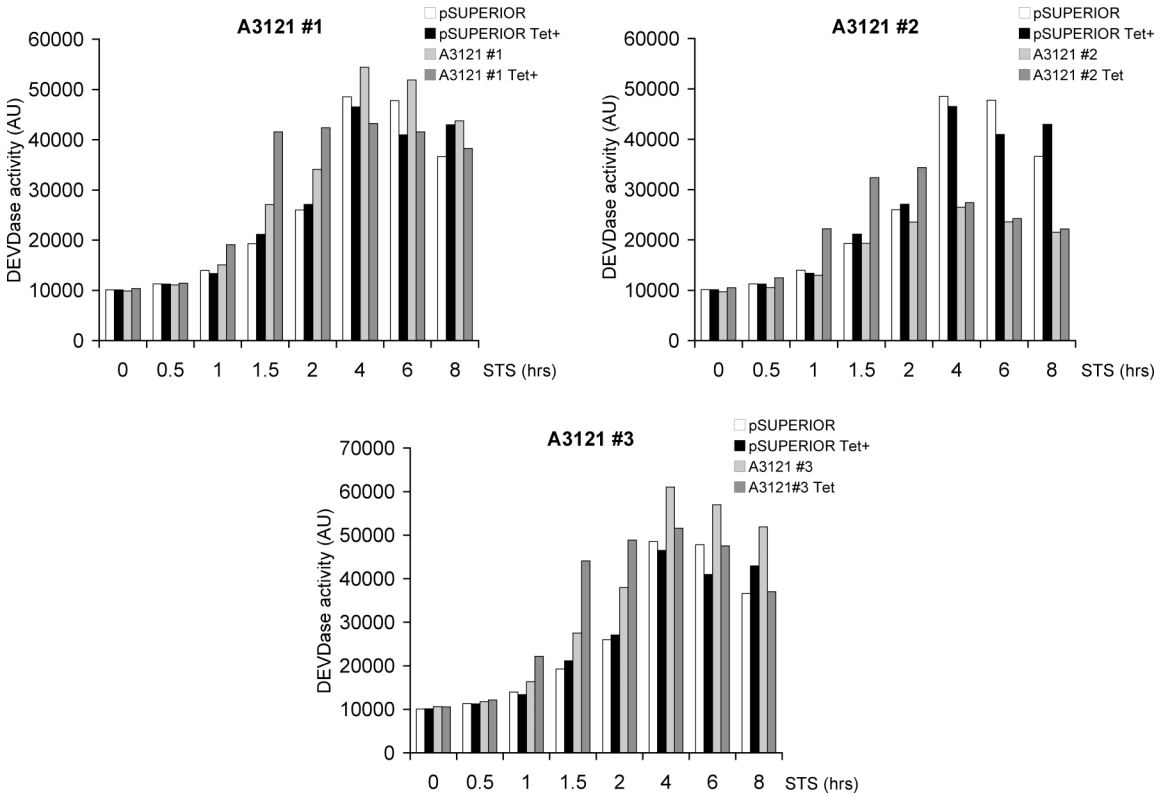

Figure 21: Earlier caspase activation in the absence of Acinus. pSUPERIOR and three independent A3121 clones (A3121 #1, #2 and #3), cultured in the absence or presence (Tet+) of tetracycline were induced for cell death with 1 µM staurosporine (STS) for the indicated periods of time. Equal amounts of cell extracts were used in a fluorogenic substrate cleavage assay as described. Cleavage of the fluorogenic substrate Ac-DEVD-amc is indicated as DEVDase activity (AU).

VI.5. APOPTOTIC CHROMATIN CONDENSATION IN ACINUS KNOCKDOWN CELLS

VI.5.A. *IN VIVO* CHROMATIN CONDENSATION ASSAY

In its original description, the p17 fragment of Acinus, generated by cleavage during apoptosis, was reported to be sufficient and necessary to induce chromatin condensation (Sahara et al., 1999). To evaluate the extent of apoptotic chromatin condensation in the absence of Acinus, apoptotic nuclei from control and knockdown cells were visualized by fluorescence microscopy after staining with DAPI. Different types of stained nuclei were observed after the induction of apoptosis and were categorized as non-condensed, partially condensed or completely condensed (Figure 22a). Nuclei thus classified were scored to assess the level of condensation at various time-points after staurosporine treatment (Figure 22b).

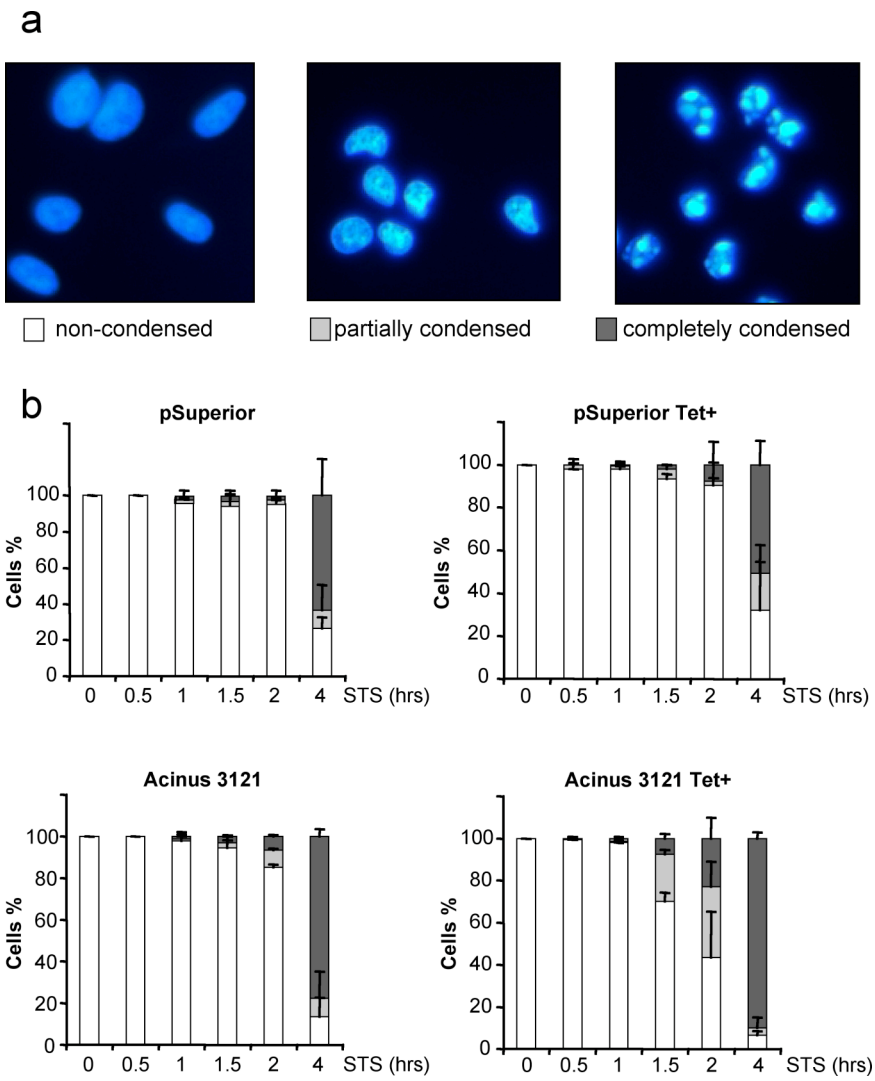

Figure 22: Apoptotic chromatin condensation occurs even in the absence of Acinus. a. Scoring of condensed chromatin. Fluorescence micrographs of DAPI stained apoptotic nuclei showing typical non-condensed, partially condensed and completely condensed nuclei. b. Quantification of condensed chromatin after 72 hours of induction with tetracycline. HeLa-pSUPERIOR and HeLa-A3121 cells uninduced or induced for Acinus knockdown (Tet+) for 72 hours were treated with kinase inhibitor staurosporine (STS) for the indicated time durations. Cells fixed and stained with DAPI were visualized using fluorescence microscope and were scored according to morphological criteria. Bars denote mean values ± s.d. from triplicates with an average of 150 nuclei counted per condition (*n*=3).

Results of quantification of chromatin after 72 hours of induction of Acinus knockdown (Figure 22b) and after long-term induction of Acinus knockdown (Figure 23), indicate that chromatin condensation was not affected in the absence of Acinus. Instead, a slight acceleration in the progress of condensation, probably as a result of earlier caspase activation, was detected in

Acinus knockdown cells. As can be seen from Figure 23 and Figure 24, considerable amounts of condensed nuclei could be observed after 2 hours of staurosporine treatment in Acinus knockdown cells as compared to the control cells.

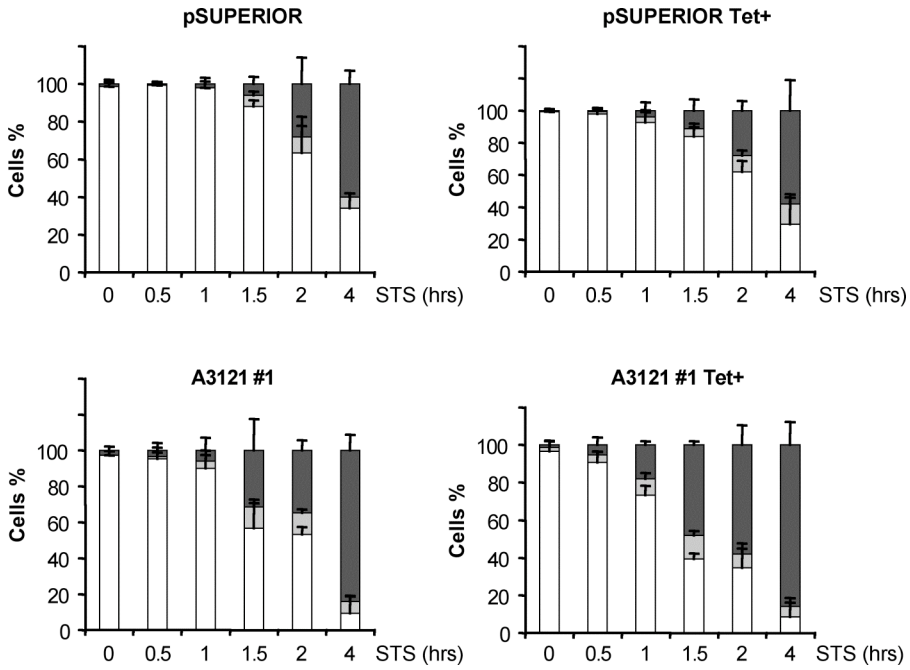

Figure 23: Quantification of chromatin condensation in long-term Acinus knockdown cells. Same as Figure 22 except that cells treated with tetracycline for extended periods were used for apoptosis induction. Data denote the mean values ± s.d. of quadruplicates (*n*=4) with 200 nuclei being counted for each condition.

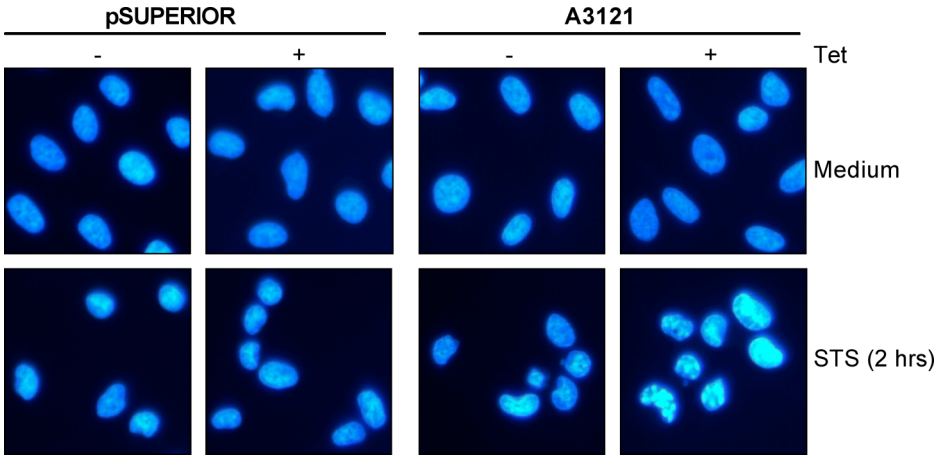

Figure 24: Fluorescence microscopic visualization of chromatin condensation. Micrographs of DAPI stained nuclei from long-term tetracycline untreated (-) and treated (+) HeLa-pSUPERIOR and HeLa-A3121 cells after no induction (Medium) and 2 hours of apoptosis induction with staurosporine (STS). Predominantly completely condensed chromatin are evidently observed in Acinus knockdown compared to control cells after 2 hours of apoptosis induction.

To determine if chromatin condensation in Acinus knockdown cells was dependent on the concentration of staurosporine used to induce apoptosis, a titration of staurosporine between concentration ranges of 0.25 to 1 µM was performed (Figure 25). Although apoptosis in general was delayed in all cells analyzed at lower concentrations of staurosporine, chromatin condensation in Acinus knockdown cells was always accelerated in comparison to the uninduced A3121 cells or control HeLa-pSUPERIOR cells.

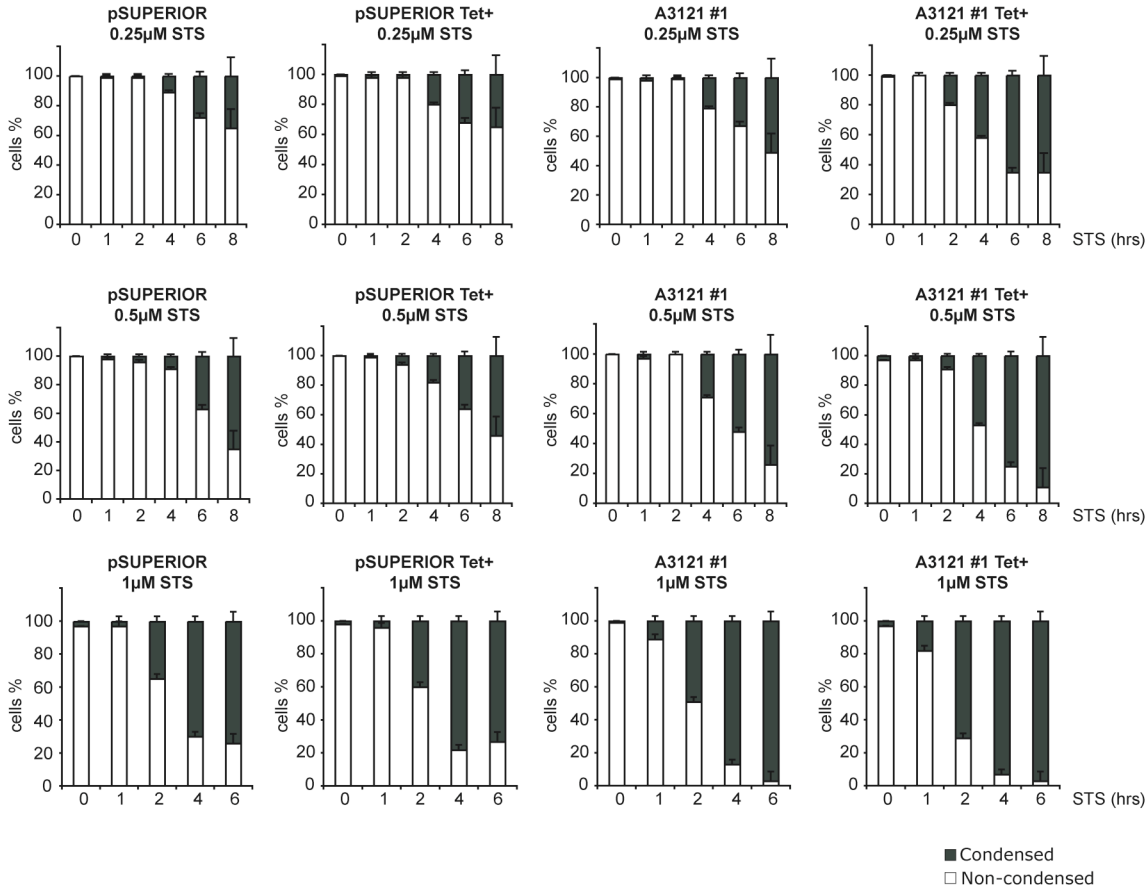

Figure 25: Chromatin condensation at different staurosporine concentrations. HeLa-pSUPERIOR and HeLa-A3121 cells cultured in the absence or presence (Tet+) of tetracycline for 8 days were induced with 0.25 µM, 0.5 µM and 1 µM staurosporine for the indicated amounts of time. Cells were fixed and stained with DAPI and visualized by fluorescence microscopy. Nuclei were classified as non-condensed (open bars) or condensed (filled bars) based on morphological criteria. Data represent mean values ± s.d. from triplicates with a total of 200 nuclei counted for each time-point.

Staurosporine is an inducer of the mitochondrial pathway of apoptosis. To investigate chromatin condensation during receptor-induced apoptosis, Acinus knockdown cells and control cells were treated with tumor necrosis factor alpha (TNF-α) and translation inhibitor cycloheximide. Fluorescence microscopic analysis and quantification shown in Figure 26 indicate that apoptotic chromatin condensation does indeed progress normally in Acinus knockdown cells further confirming that TNF-α mediated apoptotic chromatin condensation is not inhibited in Acinus knockdown cells.

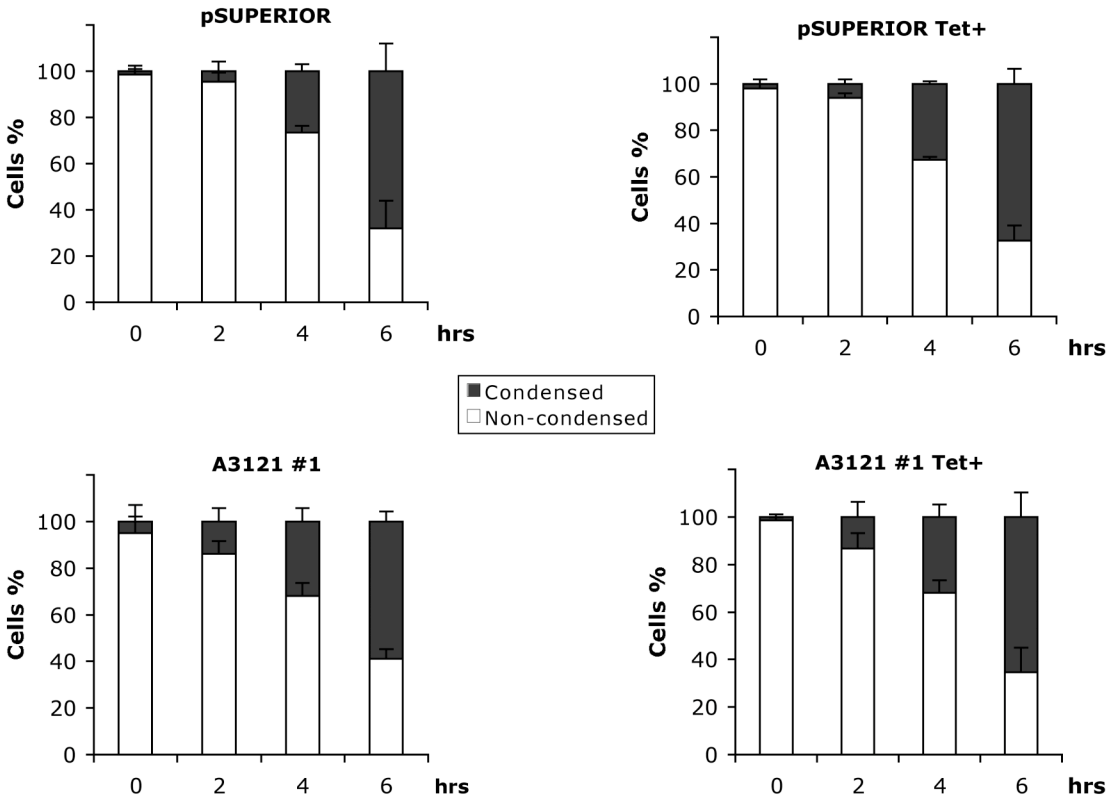

Figure 26: TNF-α mediated apoptotic chromatin condensation is unaffected in Acinus knockdown cells. HeLa-pSUPERIOR and HeLa-A3121 cells cultured without or with (Tet+) tetracycline for 7 days were induced to undergo apoptosis with 100 ng/ml TNF-α and 10 µg/ml cycloheximide for the indicated duration of time. Cells were fixed and stained with DAPI to be visualized using a fluorescence microscope. Condensed and non-condensed nuclei were classified based of morphological criteria as mentioned before. Bars represent the average of triplicates ± s.d. (*n*=3) with a total of 150 nuclei counted per condition.

VI.5.B. *IN VITRO* CELL-FREE APOPTOTIC CHROMATIN CONDENSATION ASSAY

In view of the fact that an *in vivo* assay did not indicate a role for Acinus in apoptotic chromatin condensation and because Acinus was originally implicated in chromatin condensation using an *in vitro* system utilizing permeabilized cells (Sahara et al., 1999), a similar *in vitro* cell-free system was employed to analyze chromatin condensation in Acinus knockdown cells. For this purpose, two independent clones of HeLa-A3121 cells induced or uninduced for Acinus knockdown and HeLa-pSUPERIOR cells treated or untreated with tetracycline were permeabilized with digitonin. Condensation was initiated by the addition of HeLa cell cytoplasmic extract supplemented with or without recombinant active caspase-3. Due to the nuclear localization of Acinus, HeLa cell cytoplasmic extracts are virtually devoid of Acinus as observed by Western blotting (Figure 27b), ruling out the possibility of significant amounts of Acinus being contributed by the cytoplasmic extract. The levels of Acinus in the cells employed were also similarly monitored by Western blot analysis (Figure 27a). It is evident from Figure 27c that neither the cytoplasmic extract nor active caspase-3 by itself induces condensation. On the other hand, chromatin condensation was detected in permeabilized cells only when cytoplasmic extract was supplemented with active caspase-3. However, chromatin condensation, comparable to that observed in HeLa-A3121 cells not induced for knockdown or HeLa-pSUPERIOR controls, was also observed in Acinus knockdown cells.

A similar *in vitro* condensation assay was also performed using HeLa-A3121 cells treated with tetracycline for 72 hours. Quantification of the relative amounts of condensed DAPI stained nuclei observed under a fluorescent microscope, shown in Figure 28, confirmed that *in vitro* chromatin condensation was indeed unaffected in Acinus knockdown cells.

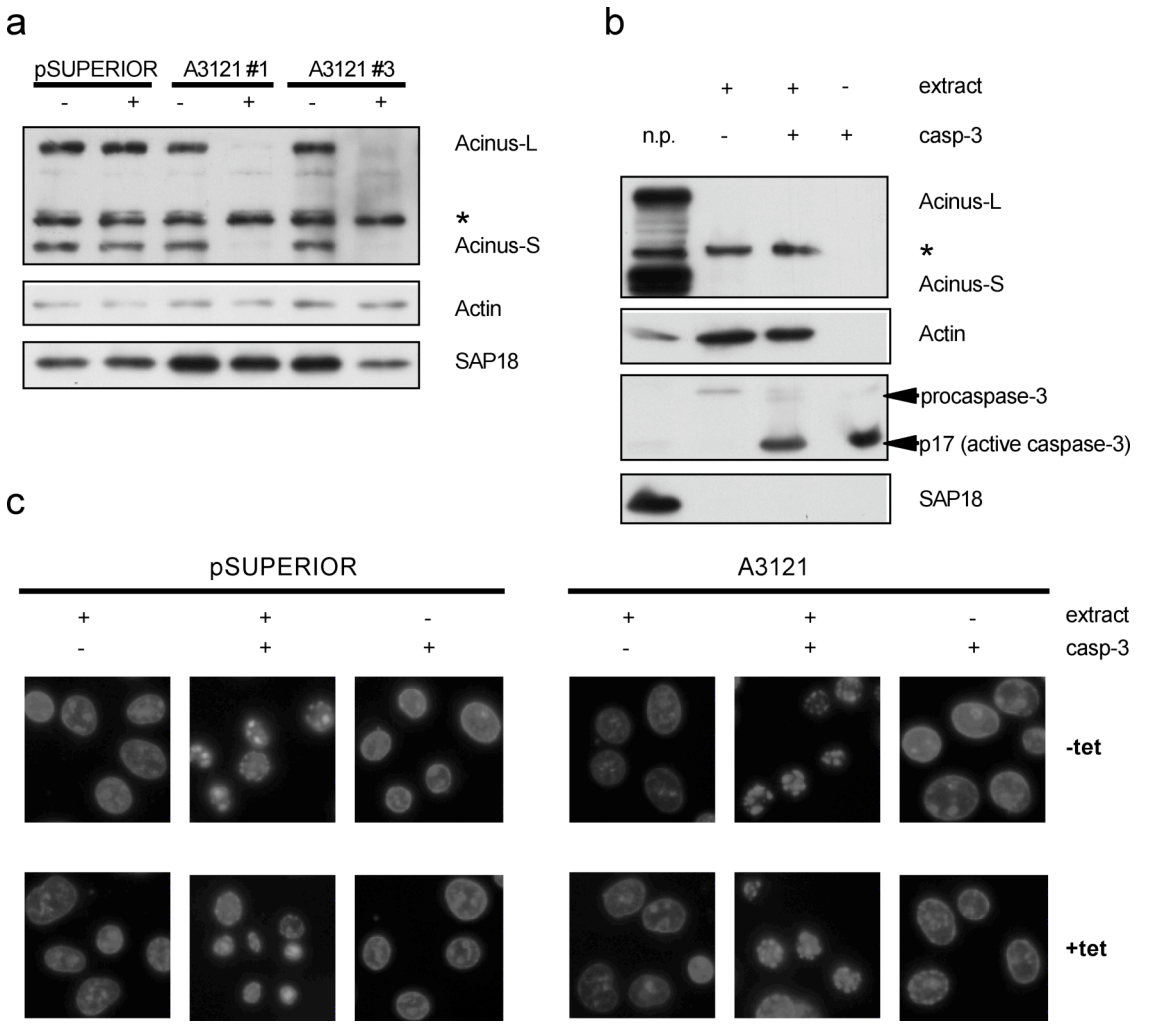

Figure 27: *In vitro* cell-free chromatin condensation in Acinus knockdown cells. a. Western blot analysis of pSUPERIOR, A3121 clone 1 and clone 3 cells employed in the assay. Total cell extracts were collected from untreated (-) and tetracycline-treated (+) cells and analyzed for the indicated proteins using their respective antibodies. Efficient Acinus knockdown was confirmed by the virtual absence of both Acinus isoforms in the tetracycline-treated A3121 cells. b. Western blot analysis of extracts used in the *in vitro* condensation assay. Cytoplasmic extract used in the assay was analyzed for its constitution. Acinus and SAP18, both predominantly nuclear proteins, can be detected only in the control nuclear pellet (n.p.) but not in the cytoplasmic extract (extract). Reaction mixtures of extract or buffer with added active recombinant caspase-3, indicated by an arrowhead, were also analyzed. Procaspase-3 recognized in the cytoplasmic extract is also indicated. Asterisks indicate an unspecific band recognized by the Acinus antibody. c. Fluorescence micrographs of pSUPERIOR and A3121 clone 1 nuclei after DAPI staining. Permeabilized cells were treated with cytoplasmic extracts with or without active caspase-3 for 3 hours. Chromatin condensation is observed only in the presence of both extract and caspase-3. Cells treated with active caspase-3 alone served as control.

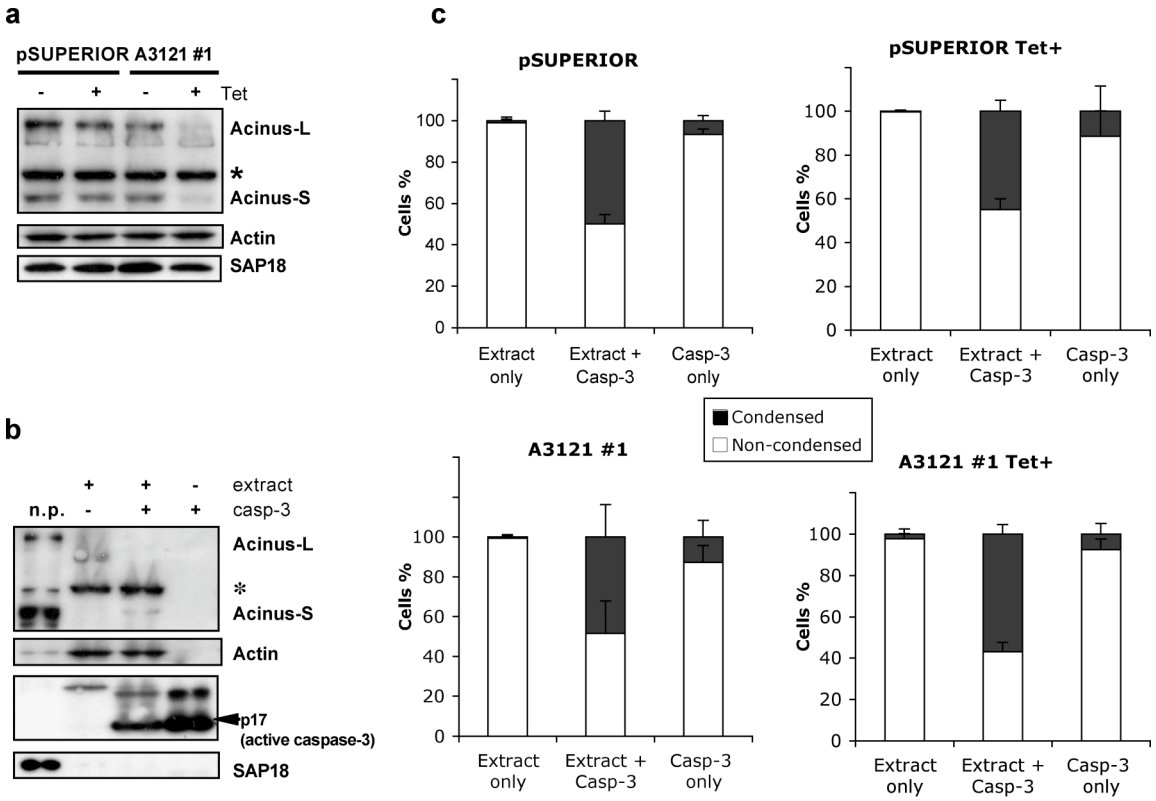

Figure 28: Quantification of *in vitro* chromatin condensation after 72 hours of tetracycline treatment. a. Western blot showing knockdown of Acinus. Whole cell extracts untreated (-) and 72 hours tetracycline-treated (+) pSUPERIOR and A3121 clone 1 cells were analyzed by Western blotting for the indicated proteins. b. Western blot analysis of the reaction mixes of cytoplasmic extracts and caspase-3 employed in the *in vitro* condensation assay. Proteins recognized by their respective antibodies are indicated on the right hand side. An arrowhead indicates the recombinant active caspase-3. c. Quantification of condensation. Permeabilized pSUPERIOR and A3121 tetracycline untreated and treated (Tet+) cells were incubated with HeLa cytoplasmic extracts in the absence or presence of active caspase-3 for 3 hours. DAPI stained nuclei were observed using a fluorescent microscope and scored as non-condensed (open bars) or condensed (filled bars) based on morphological considerations. Bars indicate the mean values ± s.d. of triplicates (*n*=3) with an average of 300 nuclei counted per condition.

VI.5.C. *IN VITRO* CHROMATIN CONDENSATION ASSAYS

VI.5.C.1. Caspase cleavage of recombinant Acinus

The active form of Acinus that induces chromatin condensation was reported to be generated as a result of cleavage by capsase-3 and an unidentified protease. The caspase-3 cleavage site was identified by microsequencing of the cleavage product to be at Asp 1093 of DELD 1093 (Sahara et al., 1999). Mutation of the Asp to an Ala (D/A) abolishes the caspase-3 cleavage site and renders Acinus uncleavable. Baculovirus expressing wild type Acinus-L and the caspase-3

uncleavable mutant Acinus-L DELA were used to infect insect cells to obtain the recombinant proteins. Purified FLAG-tagged Acinus-L wild type and mutant were analyzed in an *in vitro* caspase-3 cleavage assay followed by Western blotting to detect the cleaved fragments. As can be seen in Figure 29, an antibody directed against the N-terminal FLAG tag detected an ~170kDa cleavage fragment. Similarly, a ~50kDa C-terminal cleavage product was detectable by an Acinus antibody. Notably, cleavage was observable after just one hour of incubation with active recombinant caspase-3 whereas no cleavage product was detected when the non-cleavable Acinus mutant was incubated with caspase-3 for up to 3 hours.

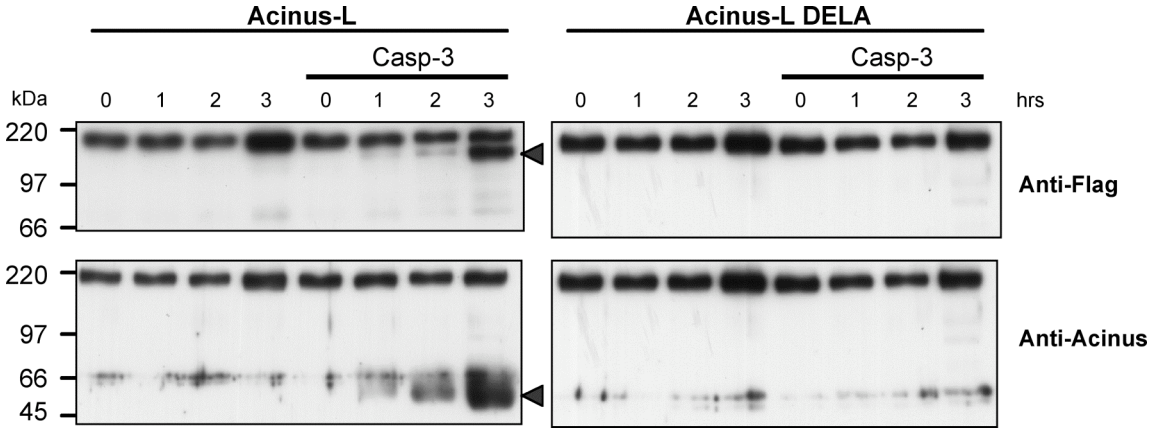

Figure 29: *In vitro* caspase-3 cleavage of recombinant Acinus. Baculovirus-expressed Acinus-L and Acinus-L DELA was incubated with (Casp-3) or without recombinant active caspase-3 at 37°C for the indicated amounts of time at the end of which a Western blot analysis was performed using a C-terminal Acinus antibody and an antibody recognizing the FLAG epitope. An arrowhead indicates the cleavage products generated as a result of caspase-3 cleavage.

VI.5.C.2. *In vitro* chromatin condensation assays with recombinant Acinus

To further substantiate the results obtained in *in vivo* and *in vitro* chromatin condensation assays, baculovirus-expressed recombinant Acinus-L was employed in an *in vitro* cell-free chromatin condensation assay. Wild-type or mutant Acinus-L was added to permeabilized HeLa-pSUPERIOR and HeLa-A3121 cells treated or untreated with tetracycline and were induced for condensation by the addition of active recombinant caspase-3 in the presence or absence of HeLa cytoplasmic extracts. As can be seen in Figure 30, neither the addition of wild-type nor mutant recombinant Acinus-L had any influence on the extent of chromatin condensation observed.

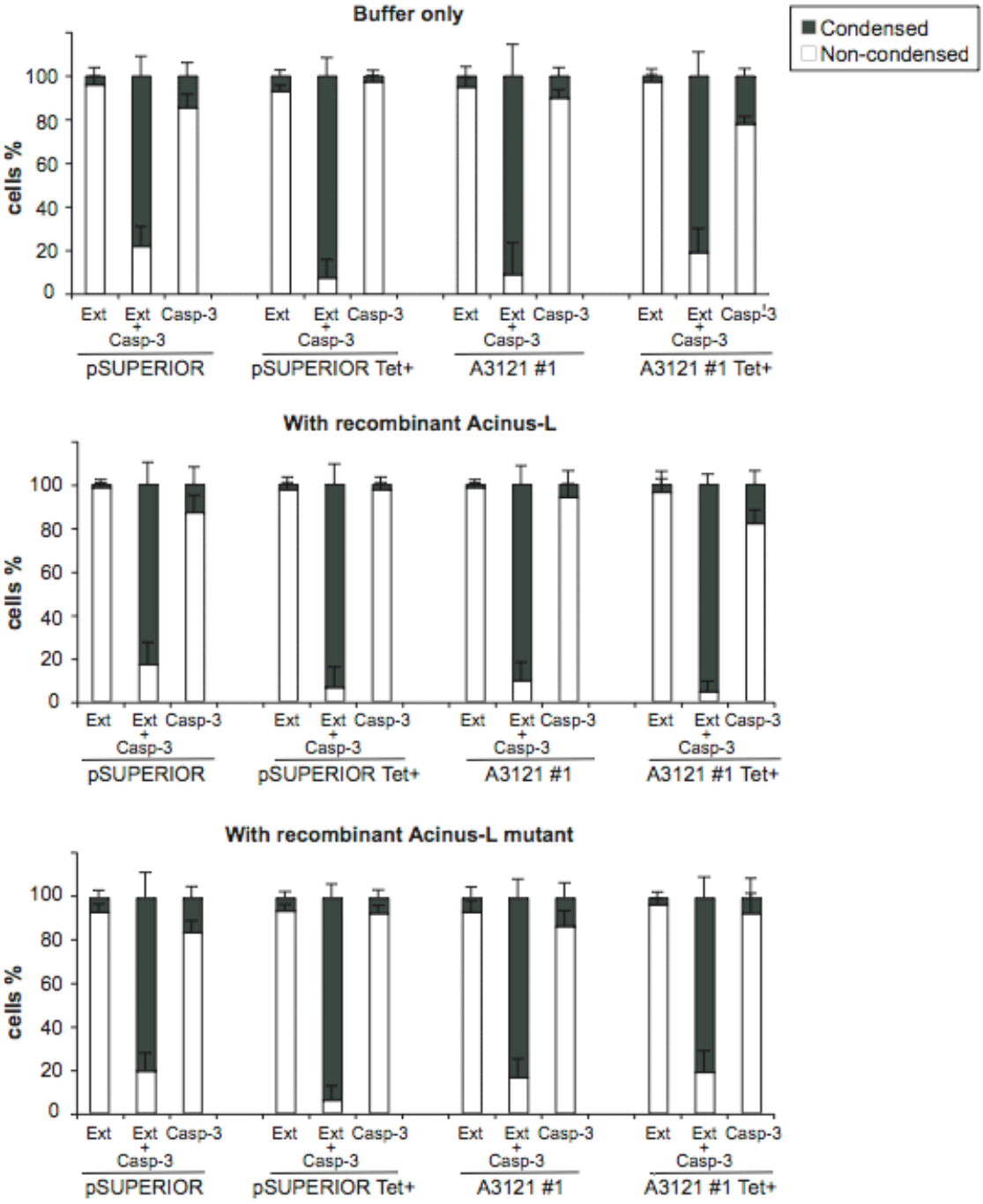

Figure 30: Chromatin condensation in an *in vitro* assay employing recombinant Acinus. In vitro chromatin condensation assays essentially similar to those described in Figure 27 and Figure 28 were setup. Permeabilized pSUPERIOR and A3121 cells, untreated or treated (Tet+) with tetracycline, were incubated with extract (Ext) in the absence or presence of caspase-3 (Casp-3). Chromatin condensation was analyzed in the absence (a) or presence of recombinant wild type Acinus-L (b) or in the presence of the caspase-3 uncleavable mutant Acinus-L DELA (c). After 3 hours of incubation, DAPI stained nuclei were observed by fluorescence microscopy and counted. Non-condensed (open bars) and condensed (filled bars) were classified based on morphological criteria. Data represent mean values ± s.d. of duplicates with a total of 200 nuclei counted per condition.

VI.6. APOPTOTIC DNA FRAGMENTATION IN ACINUS KNOCKDOWN CELLS

Nuclear morphological changes that occur during apoptosis include chromatin condensation and fragmentation of the nuclei (Robertson et al., 2000). DNA degradation is considered to be one of the defining hallmarks of apoptosis and can be analyzed using one of several different assays.

VI.6.A. FLOW CYTOMETRIC ANALYSIS OF APOPTOTIC HYPODIPLOID NUCLEI

During the course of apoptosis, several nucleases and other factors are activated by caspase-dependent and independent pathways, which result in the eventual disintegration of the cellular DNA in the apoptotic cell. In order to detect and quantitate the percentage of apoptotic cells present in a population by analysis of their DNA content, a flow cytometric method described by Nicoletti et al. (Nicoletti et al., 1991) was employed. Depending on the phase of cell cycle, distinct $G_{0/1}$ and $G_{2/M}$ peaks of DNA can be observed using this assay. Reduced DNA binding of propidium iodide (PI) dye in apoptotic cells due to cleavage and loss of oligonucleosomal DNA fragments results in the appearance of sub-G_1 peaks (hypodiploid DNA) in the DNA profile (Barbieri et al., 1992; Ettorre et al., 2003).

To investigate the involvement of Acinus in DNA fragmentation, apoptosis was induced in tetracycline-treated and untreated pSUPERIOR and HeLa-A3121 cells and analyzed by flow cytometry after PI staining. Representative histograms and the quantification of the hypodiploid DNA are shown in Figure 31. Quantification of the amount of hypodiploid DNA over a period of 10 hours, shown in Figure 32, indicates a significant reduction in the amount of hypodiploid DNA content in Acinus knockdown cells after 10 hours of induction of apoptosis in comparison to the untreated A3121 control. This suggests a repression of oligonucleosomal DNA fragmentation in the Acinus knockdown cells.

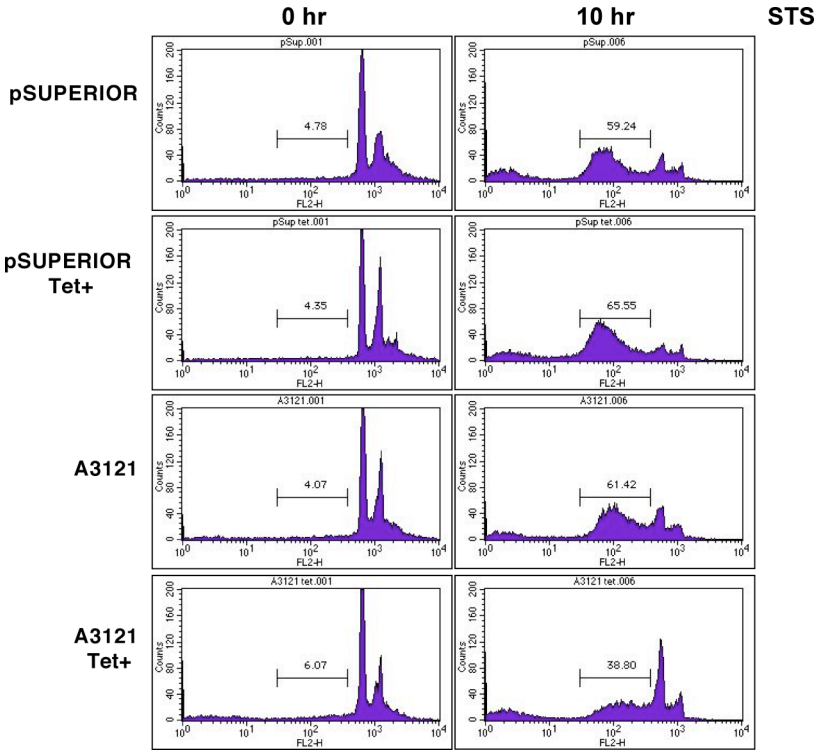

Figure 31: FACS analysis of DNA fragmentation in Acinus knockdown cells. Untreated and 8 days tetracycline-treated (Tet+) HeLa-pSUPERIOR and HeLa-A3121 cells were induced to undergo apoptosis by treatment with 1 µM staurosporine (STS). The amounts of hypodiploid nuclei in untreated (0 hr) and 10 hrs STS-treated cells were subsequently analyzed using a fluorescence activated cell sorter. Quantification of the hypodiploid nuclei for the respective samples is indicated.

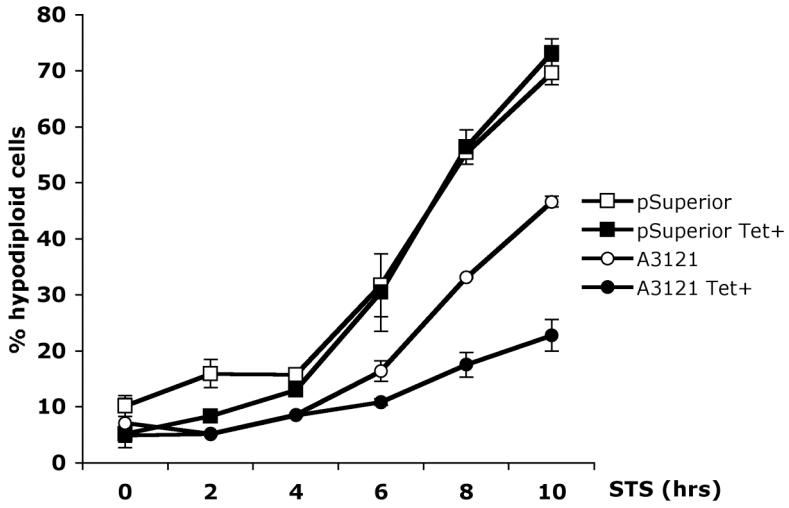

Figure 32: STS-induced apoptotic DNA fragmentation is inhibited in Acinus knockdown cells. HeLa-pSUPERIOR and HeLa-A3121 cells grown in the absence or presence (Tet+) of tetracycline for extended periods of time were treated with 1 µM staurosporine (STS). Quantification of hypodiploid nuclei after STS treatment for the indicated periods of time is shown. Results indicate mean ± s.d. of three independent experiments (*n*=3).

Furthermore, a similar repression of hypodiploid DNA was also observed in Acinus knockdown cells when the extrinsic pathway of apoptosis was induced using TNF-α in combination with cycloheximide (Figure 33). This indicated an inhibition of DNA degradation in Acinus knockdown cells. Notably, A3121 cells not induced for knockdown also displayed a small but reproducible reduction in the amount of hypodiploid nuclei, suggesting background RNAi in these cells.

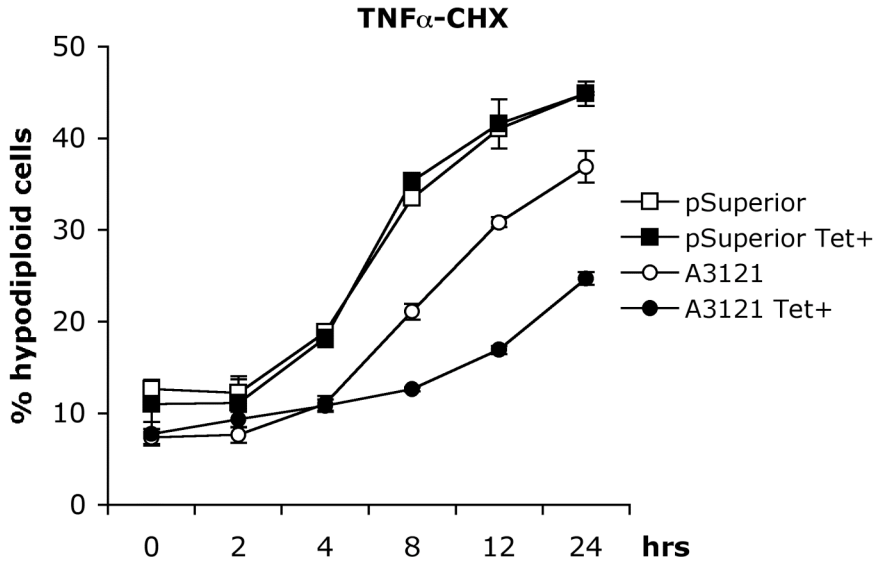

Figure 33: Time course of TNF-α-induced DNA fragmentation in Acinus knockdown cells. Untreated or tetracycline-treated (Tet+) cells were induced to undergo apoptosis by treatment with 100 ng/ml TNF-α and 10µg/ml cycloheximide for the indicated amounts of time. FACS analysis was subsequently performed to quantitate hypodiploid nuclei in the different samples. Results indicate mean ± s.d. of two independent experiments (*n*=2).

VI.6.B. LACTATE DEHYDROGENASE RELEASE ASSAY

Plasma membrane damage and the release of cytoplasmic contents occur as the ultimate outcome of cell death. Apoptosis, however, is characterized by the fact that cellular contents are not released *in vivo* and are instead retained in apoptotic bodies, which are eventually disposed by phagocytosis. Under cell culture conditions, however, in the absence of phagocytes, apoptotic bodies develop plasma membrane damage, after continued induction of apoptosis and can lead to release of cytoplasmic content. This can serve as an indicator of cytotoxicity of the dying cells.

To analyze if the impairment of DNA fragmentation in Acinus knockdown cells was due to a decreased susceptibility to cell death in general, a cytotoxicity assay was performed. Lactate dehydrogenase (LDH) is a stable cytoplasmic enzyme, present in all cells, which is rapidly released into the cell culture supernatant upon plasma membrane damage. Quantification of LDH release gives an estimate of the ability of the cells to die in general. LDH release was analyzed in cell culture supernatants from HeLa-pSUPERIOR and HeLa-A3121 cells in the presence or absence of tetracycline, after 24 hours of staurosporine treatment. As can be seen from Figure 34, comparable amounts of LDH release was observed in all samples analyzed indicating that all cells were equally cytotoxic.

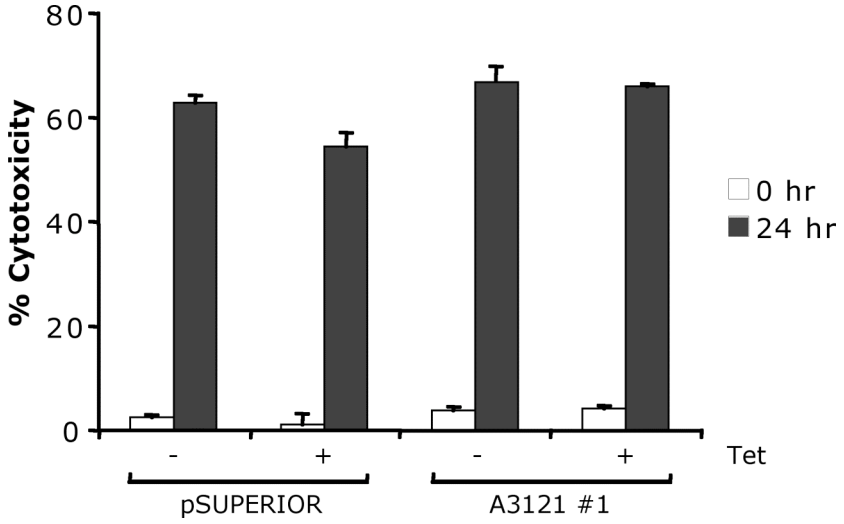

Figure 34: Acinus knockdown and control cells are equally susceptible to death. Apoptosis was induced in tetracycline untreated (-) or treated (+) HeLa-pSUPERIOR and HeLa-A3121 cells using 1 µM staurosporine for 24 hours. Growth medium was collected at the end of the treatment from induced (24 hr) or uninduced (0 hr) cells and assayed for LDH release. Cytotoxicity percentage was calculated from maximum LDH release from uninduced cells treated with 2% Triton-X 100.

VI.6.C. OLIGONUCLEOSOMAL DNA LADDERING ASSAY

Activation of CAD during apoptosis catalyzes internucleosomal cleavage of DNA strands, also referred to as low molecular weight (LMW) cleavage (Enari et al., 1998). This process leads to the generation of fragments of DNA ~180 bp or multiples of ~180 bp in size, which shows a distinctive laddering pattern when

analyzed by agarose gel electrophoresis. To confirm the results observed by the FACS analysis, DNA was extracted from HeLa-pSUPERIOR and HeLa-A3121 cells treated or untreated with tetracycline, which were induced to undergo apoptosis for different periods of time by treatment with staurosporine. DNA thus extracted was subjected to agarose gel electrophoresis.

As can be seen in Figure 35, significant DNA laddering could be observed after 2 to 4 hours of staurosporine treatment in pSUPERIOR and A3121 Tet- cells. The appearance of oligonucleosomal DNA ladders in HeLa-A3121 treated with tetracycline, however, was severely impaired during the complete course of staurosporine-induced apoptosis.

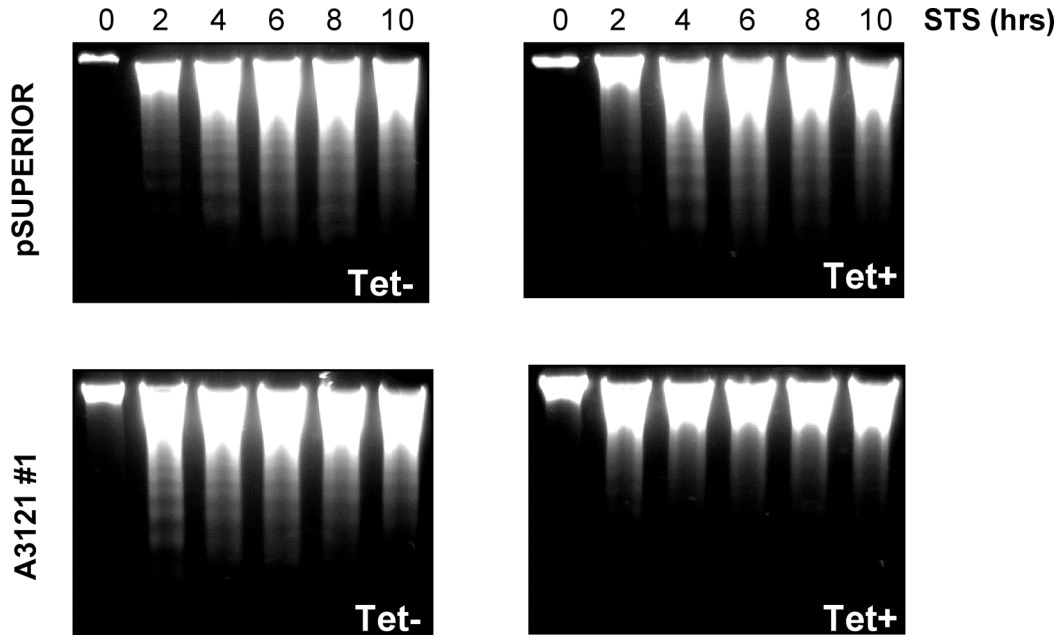

Figure 35: Oligonucleosomal DNA laddering during apoptosis. Genomic DNA was extracted from untreated and tetracycline-treated (Tet+) HeLa-pSUPERIOR and HeLa-A3121 cells induced with staurosporine (STS) for the indicated time durations. DNA was separated on a 1 % agarose gel by electrophoresis and gels documented after Ethidium Bromide staining.

Shown in Figure 36 are the results of a similar agarose gel electrophoresis of DNA extracted from two additional HeLa-A3121 clones. Both A3121 clones induced for Acinus knockdown displayed inhibition of DNA laddering. However, A3121 cells not induced for knockdown and pSUPERIOR cells treated or untreated with tetracycline did not show any impediment in DNA laddering during apoptosis.

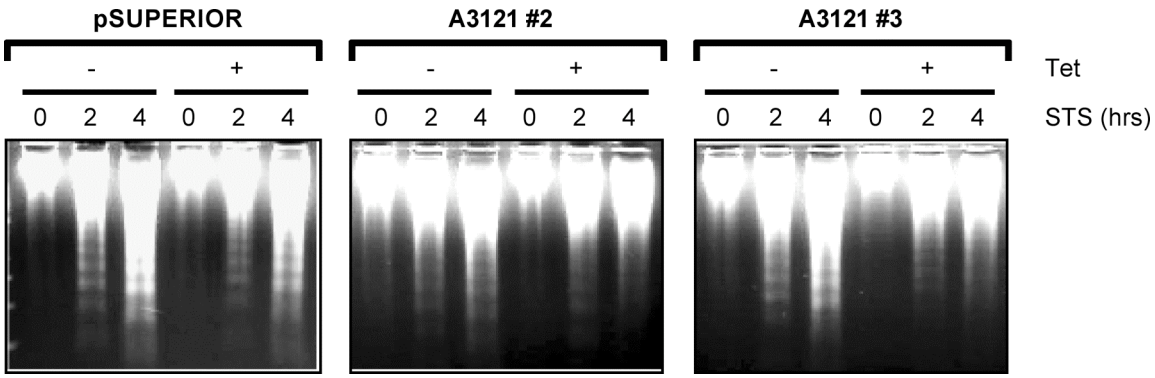

Figure 36: Apoptotic DNA laddering in different A3121 clones. DNA extracted from two independent Acinus knockdown clones (A3121 clone 2 and clone 3) was also analyzed by agarose gel electrophoresis after apoptosis induction with staurosporine for 0, 2 and 4 hours. Tetracycline untreated (-) pSUPERIOR and A3121 cells and tetracycline-treated (+) pSUPERIOR cells were also analyzed as controls.

VI.6.D. HIGH MOLECULAR WEIGHT DNA FRAGMENTATION

DNA degradation during apoptosis occurs in a two-step process. Early in the process, double strand breaks (DSB) occur in cellular DNA cleaving it into high molecular weight (HMW) fragments of about 50-300 kb in size. The executors of this process include factors such as AIF and other endonucleases as potential candidates (Susin et al., 2000).

VI.6.D.1. Pulse-field gel electrophoresis

To investigate whether Acinus knockdown cells displayed HMW cleavage even though oligonucleosomal cleavage was impaired, DNA from apoptotic Acinus knockdown cells, treated with STS for different durations, was subjected to pulsed-field gel electrophoresis (PFGE). Gels stained with ethidium bromide after PFGE, shown in Figure 37, revealed that HMW DNA fragments of ~50 kb were indeed generated in Acinus knockdown cells in amounts comparable to that of A3121 cells not induced for knockdown and pSUPERIOR controls.

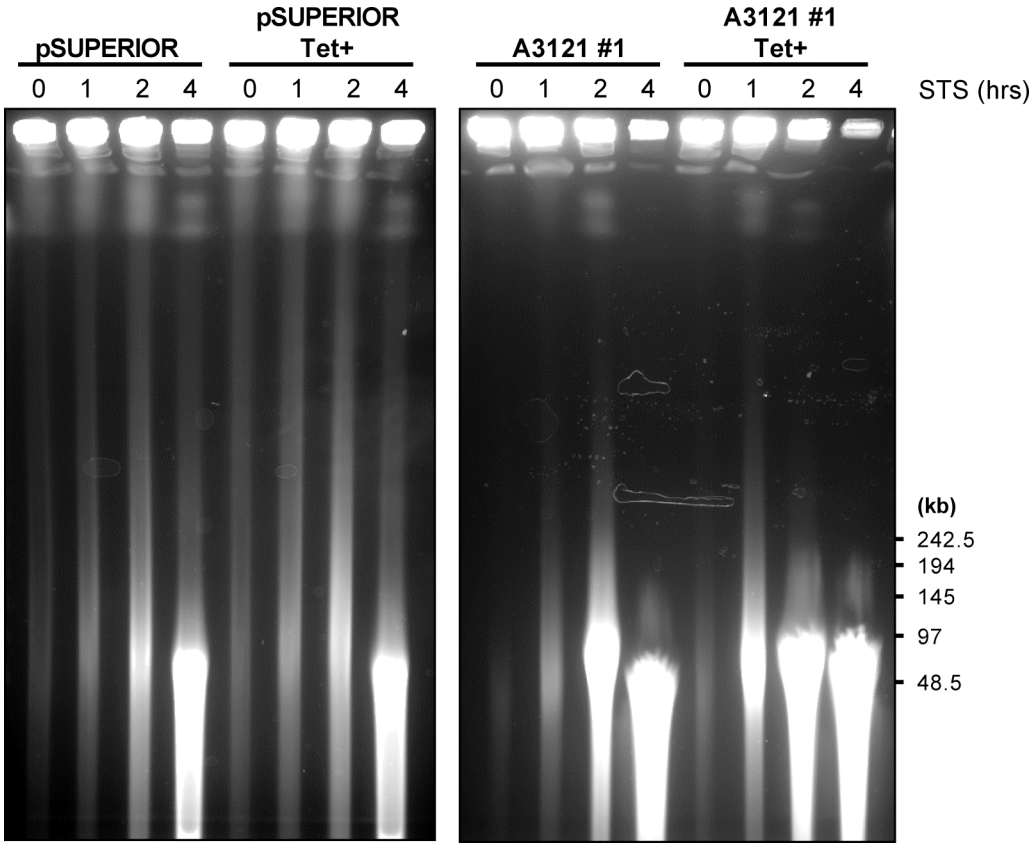

Figure 37: High molecular weight cleavage is unaffected by the absence of Acinus. HeLa-pSUPERIOR and HeLa-A3121 cells cultured in the absence or presence (Tet+) of tetracycline were treated with 1 µM staurosporine for the indicated amounts of time. Cells were subsequently immobilized into agarose plugs and treated as mentioned in 'Methods' and separated on a 1 % agarose gel by pulsed-field gel electrophoresis (PFGE). Sizes corresponding to the marker bands are indicated.

VI.6.D.2. Histone H2A.X phosphorylation

HMW fragmentation in apoptotic cells, as a result of activation of one or more nucleolytic factors and/or nucleases, is also indicative of DNA double strand breaks (DSBs) resulting in the generation of DNA rosettes and looped domains. One of the earliest responses to DSBs in eukaryotes is the serine phosphorylation of histone variant H2A.X at serine 139 giving rise to γ-H2A.X (Rogakou et al., 1998). For this reason H2A.X phosphorylation can also be used as a marker for detecting DSBs during apoptosis (Rogakou et al., 2000). To determine the phosphorylation status of H2A.X in Acinus knockdown cells during apoptosis, a Western blot analysis was performed using an antibody specifically recognizing the phosphorylated form of H2A.X. Extracts from pSUPERIOR and A3121 cells grown in the presence or absence of tetracycline were collected at different time

points after treatment with staurosporine. Similar kinetics of H2A.X phosphorylation could be detected in all four cell lines analyzed (Figure 38), confirming that DSB and thus H2A.X phosphorylation indeed occurred in Acinus knockdown cells.

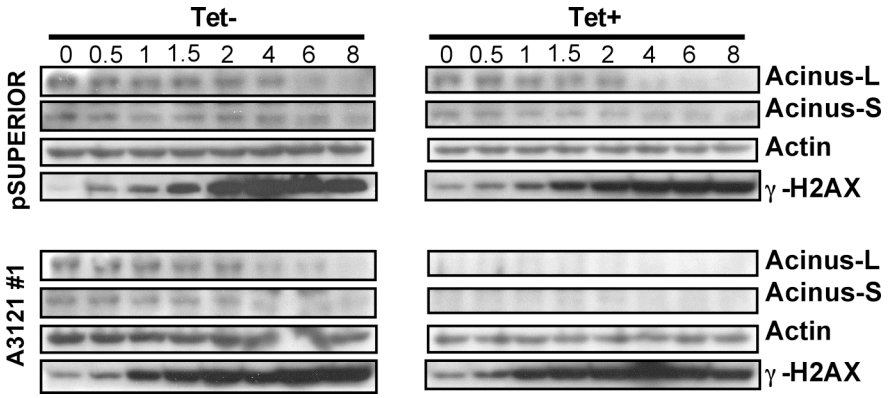

Figure 38: H2A.X phosphorylation as a marker for double strand breaks during apoptotic HMW cleavage. pSUPERIOR and A3121 cells uninduced (Tet-) or induced (Tet+) for RNAi were treated with staurosporine (STS) for the indicated lengths of time. Whole cell extracts were analyzed for H2A.X phosphorylation by Western blotting using a phospho-specific H2A.X antibody. The extent of Acinus knockdown was monitored by analyzing both the isoforms of Acinus. The level of actin served as a loading control.

VI.6.D.3. H2A.X phosphorylation and LMW in MCF7 cells

In MCF7 human breast carcinoma cells, one of the key enzymes involved in apoptosis, caspase-3, is not expressed owing to a 47 bp deletion in exon 4 of the procaspase gene (Janicke et al., 1998). Due to the absence of active caspase-3, MCF7 cells show severe impairment in oligonucleosomal DNA fragmentation during TNF-α/CHX or staurosporine-induced apoptosis. To further support the observed evidence that H2A.X phosphorylation and DSBs occur even in the absence of oligonucleosomal DNA fragmentation, extracts from apoptotic MCF7 and MCF7 caspase-3 retransfected cells were analyzed by Western blotting. As can be seen in Figure 39, H2A.X phosphorylation is virtually unaffected in both MCF7 and MCF7 caspase-3 retransfected cells, appearing 4 hours after staurosporine treatment, although caspase-3 is completely lacking in MCF7. It is noteworthy that PARP cleavage is significantly delayed (Figure 39) and oligonucleosomal DNA laddering is completely blocked (Figure 40) in MCF7 cells but not in the retransfected cells. The residual PARP cleavage observed in the

MCF7 cells is indicative of caspase-7-mediated cleavage, since many caspase-3 substrates, including PARP, are also well-known caspase-7 targets (Fischer et al., 2003).

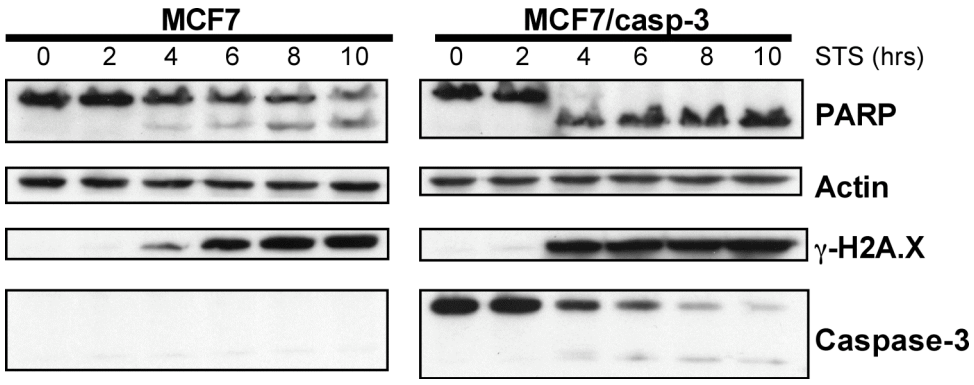

Figure 39: Phosphorylation of H2A.X in MCF7 cells during apoptosis. MCF7 and caspase-3 retransfected MCF7 (MCF7/casp-3) cells were treated with staurosporine (STS) for the indicated time durations. Whole cell extracts were analyzed for the proteins indicated on the right. PARP cleavage is considerably delayed in MCF7 cells due to absence of caspase-3. MCF7/casp-3 cells, on the other hand, show complete cleavage of PARP after only 4 hours of staurosporine treatment. H2A.X phosphorylation, however, occurs in MCF7 cells about the same time as MCF7/casp-3 cells though at lesser intensity.

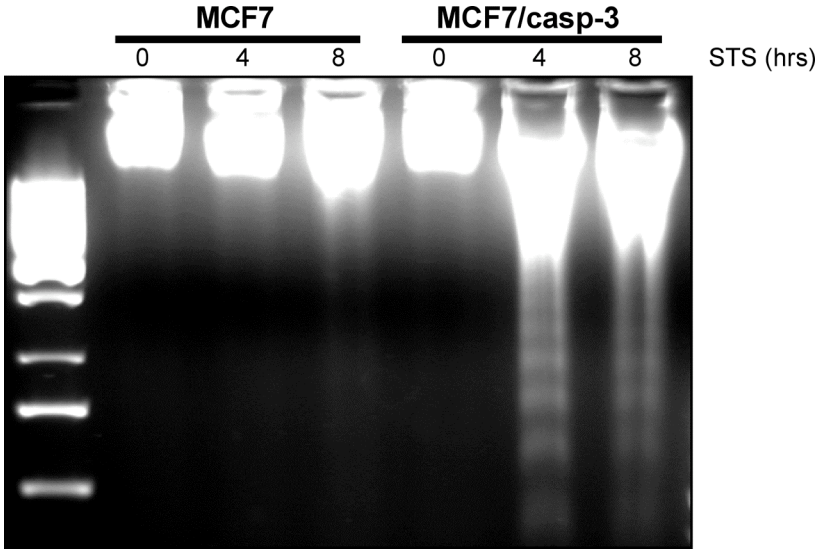

Figure 40: Oligonucleosomal DNA laddering in apoptotic MCF7 cells. Apoptosis was induced in MCF7 and MCF7/casp-3 cells by treatment with 1 µM staurosporine (STS) for 0, 4 and 8 hours. DNA was subsequently extracted from cells and analyzed on a 1 % agarose gel. Oligonucleosomal laddering is completely blocked in MCF7 cells but is restored in the caspase-3 retransfected cells.

VII. DISCUSSION

Activation of apoptosis in cells leads to certain morphological changes in the nucleus downstream of caspase activation. Although a variety of signals can trigger the initiation of the apoptotic process, the eventual molecular outcome of apoptosis includes chromatin condensation and fragmentation of the DNA. These biochemical changes in the dying cells have been considered hallmarks of apoptotic cell death. Evidence suggests the role of a caspase activated DNase (CAD) in both chromatin condensation and cleavage of the cellular DNA into oligonucleosomal fragments. Accordingly, inactivation of caspase-3, which is the major caspase involved in CAD activation, can delay cell death and largely abolish the type of advanced chromatin condensation that can be observed in most cells treated with apoptosis inducers such as staurosporine (STS) (Zheng et al., 1998). Similarly, inactivation of CAD function also prevents advanced chromatin condensation in different cell types (Liu et al., 1998). Caspases and CAD, however, are not the only effectors of chromatin condensation since condensation has been observed in lymphoid cells treated with STS and anti-CD2 (Deas et al., 1998), as well as fibroblasts overexpressing PML (Quignon et al., 1998), even when caspase activation is inhibited. Recently, apoptosis inducing factor (AIF), a mitochondrial intermembrane flavoprotein, has been reported to translocate to the nucleus in a caspase-independent fashion (Susin et al., 2000) and induce DNA degradation in apoptotic cells.

Among a multitude of target proteins cleaved by executioner caspases is a nuclear protein termed Acinus that has been proposed recently to be a sufficient as well as a necessary inducer of apoptotic chromatin condensation (Sahara et al., 1999). Acinus is expressed in different isoforms, Acinus-L, -S and -S', all of which are targets of caspase-3 cleavage during apoptosis. All known non-apoptotic isoforms of Acinus are cleaved during apoptosis by the combined action of caspase-3 and an unknown protease generating the active p23 fragment of Acinus implicated in apoptotic chromatin condensation (Sahara et al., 1999). To gain further insight into the physiological role of Acinus during apoptotic chromatin condensation, an inducible RNA interference (RNAi)

approach was employed to generate cells that can be induced to knock down Acinus.

VII.1. A STABLE, INDUCIBLE AND REVERSIBLE KNOCKDOWN OF ACINUS

Tet-inducible systems are widely used for mRNA expression driven by RNA polymerase promoter. Of the various tet-inducible systems available, the Pol III H1 RNA promoter based system stands out as the best for efficient expression of siRNAs since it is essential that transcription starts at the first nucleotide of the target sequence. Additionally, the H1 RNA promoter has a well-defined transcriptional termination site at the stretch of five thymidines and is ideal for the expression of short non-coding RNA molecules. Using a Pol III H1 RNA promoter-based tetracycline-inducible system a stable Acinus knockdown cell line was established.

shRNAs are known to be synthesized after 4 hours of RNAi induction approaching a more robust level after 24 hours of induction (van de Wetering et al., 2003). Furthermore, it was reported that after 48 hours of induction considerable loss-of-function of the concerned protein was observed. Reduction of a target protein by RNAi, however, depends on the protein turnover rate. Analysis of protein turnover rate of Acinus revealed that both isoforms of Acinus had a relatively slow turnover rate (Figure 11). At the mRNA level significant knockdown was observed after 48 to 72 hours of RNAi induction (Figure 10). Consistent with the slow protein turnover rate, significant knockdown of Acinus to an extent of >95% was achieved only when RNAi was induced with tetracycline for extended durations. Furthermore, tetracycline-induced knockdown of Acinus was completely reversible when tetracycline was removed from the growth media and the cells allowed to recover for a few days (Figure 13). Importantly, this inducible system for RNAi allows an unbiased and comparable analysis of loss-of-function phenotype by comparing a selected cell population at the induced and the uninduced level.

VII.2. CONSEQUENCE OF ACINUS KNOCKDOWN

VII.2.A. A NUCLEAR RNPS1-SAP18 INTERACTION PERSISTS IN THE ABSENCE OF ACINUS

Acinus has been identified to exist in a complex consisting of RNPS1 and SAP18, termed ASAP complex, with a prospective role in apoptosis and splicing (Schwerk et al., 2003). Although the knockdown resulted in a virtual absence of all isoforms of Acinus, fractionation of the cytoplasmic and nuclear extracts revealed that significant amounts of both RNPS1 and SAP18 still remained in the nucleus. Furthermore, it was established by immunoprecipitation experiments (Figure 14 and Figure 15) that RNPS1 and SAP18 continued to interact even when no Acinus was detectable. Acinus, RNPS1 and SAP18 have all been found to interact and co-purify with factors of the exon-junction complex (Tange et al., 2005). It is conceivable that these factors might stabilize the interaction between RNPS1 and SAP18. However, it is also possible that the interaction between RNPS1 and SAP18 in the ASAP complex might not require the participation of Acinus.

VII.2.B. KNOCKDOWN OF ACINUS RESULTS IN GROWTH SUPPRESSION

Analysis of HeLa cells after knockdown of Acinus revealed a reduced growth rate in these cells. Significant reduction in the growth of Acinus knockdown cells was observed in comparison to control cells during routine maintenance of the cell lines. This growth suppression was subsequently quantitated and confirmed by counting the cells over a period of 9 days (Figure 16) and also spectrometrically after serial dilution and staining with crystal violet after 8 days of growth (Figure 17).

Two distinct mechanisms by which higher organisms can suppress cell growth are apoptosis or programmed cell death and cellular senescence. Although originally used to describe proliferative arrest that occurs after the accumulation of cell generations (replicative senescence), the term senescence has come to include any permanent and irreversible growth arrest caused by varying factors such as DNA damaging agents and oxidative or chemical stress (Serrano and Blasco, 2001). Acinus knockdown cells, however, failed to stain for

senescence-induced β-galactosidase, suggesting that an alternative mechanism was probably responsible for the effect of growth suppression observed in the absence of Acinus. As discussed in the next section, this could be a result of sensitization of Acinus knockdown cells to apoptosis pointing to a plausible background apoptosis.

VII.2.C. EARLIER CASPASE ACTIVATION

Previous studies demonstrate a role for Acinus in the apoptotic process. Downstream caspases are the effectors of apoptotic changes occurring in the cells and activation of caspases is a distinctive feature of apoptosis. To further describe the role of Acinus during apoptosis, Acinus knockdown cells were analyzed for apoptotic markers such as caspase activation and cleavage. Staurosporine-induced apoptosis proceeded rapidly in the Acinus knockdown cell as observed by Western blot analysis of caspase cleavage. Western blot analysis of caspase substrates, such as PARP and ICAD-L, also pointed to an accelerated apoptosis in Acinus knockdown cells. PARP is probably one of the best-characterized caspase substrates, which is cleaved early during apoptosis in many systems and is indicative of the nuclear changes that occur in the apoptotic cell (Kaufmann, 1989; Kaufmann et al., 1993). Caspase-7 and caspase-3 can cleave the 116 kDa PARP (Cohen, 1997; Lazebnik et al., 1994) into a 24 kDa and an 89 kDa fragment representing the N-terminal DNA-binding domain and the C-terminal catalytic subunit, respectively. An *in vitro* substrate cleavage assay further confirmed that caspases were activated in Acinus knockdown cells. In fact, a closer inspection of the kinetics of caspase activation and that of substrate cleavage indicated that caspases were indeed activated earlier and that apoptosis in general was expedited in the absence of Acinus. Accelerated apoptosis in Acinus-depleted cells might promote a higher background rate of spontaneous apoptosis, which can plausibly contribute to the decreased growth rate observed in these cells. Taken together, these results indicate that apoptotic events upstream of caspase-dependent substrate cleavage are not affected by the absence of Acinus and point to an increased sensitization of Acinus knockdown cells to apoptosis.

VII.3. CHROMATIN CONDENSATION IS UNAFFECTED BY THE ABSENCE OF ACINUS

Because Acinus has been implicated in the process of apoptotic chromatin condensation, Acinus knockdown cells were analyzed for alterations in condensed chromatin during STS and TNF-α-induced apoptosis. The extent of apoptotic chromatin condensation in Acinus knockdown cells paralleled the activation of caspases and the cleavage of caspase substrates such as PARP and ICAD-L. Significant chromatin condensation could be observed after induction of apoptosis by either STS or TNF-α and cycloheximide even when Acinus had been depleted from the cells. Notably, a similar acceleration of chromatin condensation was observed in Acinus knockdown cells at various concentrations of STS used. As expected, at lower concentrations of STS a general delay in apoptosis was observed in all cells tested, although Acinus knockdown cells displayed accelerated chromatin condensation compared to control cells at any particular STS concentration.

An *in vitro* chromatin condensation assay, similar to the one described in the original Acinus report (Sahara et al., 1999), was also performed. Permeabilized Acinus knockdown cells were incubated with HeLa cell cytoplasmic extract in the presence or absence of active recombinant caspase-3. Due to nuclear localization of Acinus, the HeLa cytoplasmic extracts are virtually devoid of any detectable Acinus. Nuclei from Acinus knockdown cells did not demonstrate any repression of chromatin condensation in the *in vitro* cell-free system. Subsequently, a similar *in vitro* cell-free chromatin condensation assay was performed employing recombinant Acinus proteins. However, the addition of wild-type Acinus-L into such an assay did not affect the extent or rate of chromatin condensation observed in the presence of active caspase-3. As expected, the addition of a caspase-3 non-cleavable Acinus-L mutant had no effect of chromatin condensation either.

A role for Acinus in chromatin condensation during apoptosis was proposed previously based on the ability of a recombinant fragment of Acinus, resembling a 23 kDa cleavage fragment of Acinus generated during apoptosis, to induce

chromatin condensation in an *in vitro* chromatin condensation assay (Sahara et al., 1999). Additionally, in the same study, depletion of Acinus by an antisense construct lead to delayed chromatin condensation in response to anti-Fas and STS-induced apoptosis. Moreover, a recent study reported that apoptotic chromatin condensation in STS/etoposide treated rat PC12 cells was diminished after knockdown of endogenous Acinus by RNAi (Hu et al., 2005). The results presented here are at variance with those presented in these reports. Although it is difficult to rule out that trace amounts of Acinus present in the knockdown cells were sufficient to mediate chromatin condensation, the absence of any alterations and an indeed accelerated chromatin condensation despite a virtually thorough depletion of Acinus in the knockdown cells questions the role of Acinus, if any, in apoptotic chromatin condensation in the system employed. The reason for the discrepancies in the results presented here compared to the published data might be due to diverse experimental setup and/or cell types employed in these studies.

The mechanism of chromatin condensation is still controversial because the relationship between chromatin condensation and DNA fragmentation has remained unclear. It has been suggested that DNA fragmentation could induce chromatin condensation, because activated CAD, the key enzyme involved in oligonucleosomal DNA fragmentation, can by itself induce chromatin condensation when incubated with the nuclei. Additionally, cells from CAD knockout mice display an inhibition of chromatin condensation (Liu et al., 1998). Importantly, Acinus knockdown also resulted in the suppression of oligonucleosomal DNA fragmentation (Figure 35 and Figure 36; discussed further in section VI.4.A.). This observation could explain the reduction of DNA condensation observed when Acinus was downregulated in the experiments performed by Sahara et al. and Hu et al. but not the rather accelerated chromatin condensation observed in the results presented in this thesis (Figure 22 and Figure 23).

Furthermore, it should be noted that numerous other proteins have also been implicated in the process of apoptotic chromatin condensation. Cleavage of two structural proteins, lamin and NuMA, has been reported to be involved in the

structural disassembly and condensation of the nuclear envelop during apoptosis (Robertson et al., 2000). Additionally, caspase-6-mediated cleavage of lamin A in particular has been shown to be essential for apoptotic chromatin condensation in cells that express lamin A (Ruchaud et al., 2002). Cleavage of yet another caspase substrate, mammalian STE20-like kinase 1 (MST1), separates the nuclear export signal (NES) containing C-terminal of MST1 from the N-terminal catalytic domain, resulting in the nuclear translocation of the N-terminal domain which can then facilitate chromatin condensation by phosphorylating histone H2B at serine 14 in a CAD-independent manner (Cheung et al., 2003; Ura et al., 2001). A separate report suggests the involvement of nucleoplasmin in apoptotic chromatin condensation. Nucleoplasmin is an acidic, thermo-resistant protein found in large amounts in the oocytes and unfertilized eggs of Xenopus and other amphibians. Homologs of Xenopus nucleoplasmin are also found in humans and rats. During apoptosis, nucleoplasmin is dephosphorylated at tyrosine 124, which is essential for chromatin condensation. Inhibition of tyrosine dephosphorylation of nucleoplasmin impedes condensation but does not obstruct DNA fragmentation (Lu et al., 2005). It is conceivable that these processes might not be affected in the Acinus knockdown cells and therefore could contribute to normal apoptotic chromatin condensation that is observed in the absence of Acinus.

Moreover, it has also been suggested that, in a caspase-independent manner, AIF released from the mitochondria could translocate to the nucleus and induce HMW DNA fragmentation and chromatin condensation (Susin et al., 1999). The observation that HMW fragmentation is unaffected in the absence of Acinus (Figure 37; discussed further in section IV.4.B), could therefore, at least partly, explain the presence of chromatin condensation in these cells.

VII.4. DNA FRAGMENTATION IN ACINUS KNOCKDOWN CELLS

Nuclear changes in an apoptotic cell are the result of two distinct parallel and redundant pathways that occur downstream of mitochondrial membrane permeabilization and caspase activation. One of these pathways results in the cleavage of DNA into high molecular weight fragments of about 50-300 kb. The

executors of this pathway include AIF, endonuclease G, topoisomerase II and cyclophilins and are largely caspase-independent although activation of caspases during apoptosis and subsequent mitochondrial membrane permeabilization can append the effects of some of these factors (Samejima and Earnshaw, 2005). The cleavage of HMW fragments also coincides with the appearance of stage I chromatin condensation at the nuclear periphery (Susin et al., 2000). The second, caspase-dependent pathway, involves the major apoptotic nuclease CAD and leads to oligonucleosomal DNA fragmentation or LMW fragmentation (Enari et al., 1998). Caspase-3-mediated cleavage of the CAD inhibitor ICAD releases the active nuclease, which then cleaves DNA into oligonucleosomal fragments. Although these pathways may operate in parallel, it is also plausible that they might function in a stepwise fashion with HMW fragmentation preceding LMW fragmentation. However, HMW fragmentation can exclusively manifest under certain conditions and in some cell types even in the absence of oligonucleosomal fragmentation (Brown et al., 1993).

VII.4.A. OLIGONUCLEOSOMAL DNA FRAGMENTATION IS IMPAIRED

Analysis of Acinus knockdown cells after induction of apoptosis by either STS (Figure 32) or by TNF-α and cycloheximide (Figure 33) by FACS measurement indicated a reduced sub-G_1 peak suggesting impairment in the DNA degradation pathway in these cells. Subsequently, cells that have been induced to knockdown Acinus were analyzed for oligonucleosomal DNA laddering on an agarose gel (Figure 35 and Figure 36). All three Acinus knockdown clones analyzed displayed hindered oligonucleosomal DNA fragmentation. Because the major apoptotic nuclease known to cause oligonucleosomal DNA cleavage is CAD, this diminution is conceivably the result of inhibition of the nucleolytic activity of CAD. Importantly, the inhibition of LMW fragmentation was not a result of a general obstruction or delay of apoptosis since upstream events such as caspase activation and substrate cleavage were not delayed, but rather accelerated, in the Acinus knockdown cells. Together, these observations further support the inference that the diminution of oligonucleosomal DNA fragmentation in Acinus knockdown cells might signify the inhibition of CAD

activity possibly by limiting the access of CAD to the internucleosomal DNA.

In eukaryotic cells, chromosomal DNA is organized into a hierarchy of supercoiled structures resulting in at least a 10,000 fold compaction of the DNA within the nucleus. The most basic level of organization consists of the folding of the DNA into 50 to 100 kb loops which are further wound into nucleosomes (Pienta and Coffey, 1984). Microscopic and biochemical studies have shown that these 50-100 kb DNA loops are attached to the nuclear matrix mediated by DNA sequence motifs termed matrix attachment regions (MARs) (Cockerill and Garrard, 1986; Gasser and Laemmli, 1986). The MARs also contain one or more matches to the topoisomerase II consensus sequence (Cockerill and Garrard, 1986) which is the major protein isolated from the nuclear matrix (Danks et al., 1994). Furthermore, topoisomerase IIα along with histone H1, high mobility group protein (HMG)-1 and HMG-2 and heat shock protein are known to directly bind CAD and activate its nucleolytic activity (Durrieu et al., 2000; Liu et al., 1998; Liu et al., 1999).

Heterodimeric CAD-ICAD complexes have been shown to associate with chromatin, which enhances the nucleolytic activity of CAD once it is activated during apoptosis in this DNA bound state (Korn et al., 2005). A number of reports indicate that the CAD-ICAD heterodimer resides predominantly in the nucleus of non-apoptotic cells. CAD is known to cleave dsDNA with a preference for A/T-rich regions (Widlak et al., 2000) and most notably, DNA at the nuclear matrix is most exposed and A/T-rich. Interestingly, the long isoform of Acinus (Acinus-L) harbors a SAP domain at its N-terminus which constitutes a putative DNA-binding domain (Aravind and Koonin, 2000). SAP (for SAF-A /B (scaffold attachment factors A/B), Acinus and PIAS) domain has also been identified in several other proteins with known sequence or structure-specific DNA binding abilities and particularly targets them to specific chromosomal locations especially at the A/T-rich MARs. It is therefore conceivable, on the basis of such close proximity between Acinus and CAD at their nuclear locations, that Acinus might influence CAD nucleolytic activity by direct or indirect protein-protein interaction in a manner comparable to topoisomerase II or histone H1.

VII.4.B. HMW FRAGMENTATION IS UNAFFECTED

The formation of HMW DNA fragments is considered to be an early critical event during apoptotic DNA disintegration (Oberhammer et al., 1993). As mentioned earlier, DNA is organized as 50-100 kb loops attached to the nuclear matrix through the MARs. Topoisomerase II, which binds to the MAR sequences, can mediate the excision of DNA loop domains during apoptosis (Lagarkova et al., 1995; Li et al., 1999). Additionally, AIF and cyclophilins can also generate HMW fragments during apoptosis resulting in DNA double strand breaks. Introduction of dsDNA breaks can prompt the phosphorylation of H2A.X at serine 139 (Rogakou et al., 2000; Rogakou et al., 1998).

Consistent with activation of caspases and other markers of apoptosis, such as substrate cleavage, analysis of DNA from apoptotic Acinus knockdown cells by pulsed-field gel electrophoresis revealed that the appearance of HMW cleavage fragments was somewhat expedited (Figure 37). Moreover, significant H2A.X phosphorylation was also observed in the Acinus knockdown cells after the induction of cell death (Figure 38). Notably, in MCF7 cells, which lack an active caspase-3, the principle caspase involved in CAD activation, oligonucleosomal fragmentation was also blocked as a consequence of inhibition of CAD activity (Figure 40), although significant HMW cleavage comparable to a caspase-3 retransfected MCF7 cell line was observed as demonstrated by H2A.X phosphorylation (Figure 39). Furthermore, particularly interesting was the observation that although H2A.X phosphorylation was slightly delayed in MCF7 cells, it paralleled PARP cleavage, indicating a correlation between apoptotic nuclear changes and HMW fragmentation. Importantly, due to the absence of caspase-3 in MCF7 cells, Acinus cannot be cleaved and thereby, the active p23 fragment of Acinus cannot be generated. Therefore, HMW fragmentation observed in the MCF7 cells is essentially independent of Acinus. Together these results implicate a role for Acinus in oligonucleosomal DNA fragmentation without influencing HMW fragmentation during apoptosis.

VII.4.C. IMPLICATIONS OF ACINUS IN NUCLEAR APOPTOSIS

DNA degradation pathways that operate as part of nuclear changes during apoptosis have turned out to be surprisingly complex. Numerous nucleases and factors have been identified to play a part during this intricate operation. The wide diversity of these apoptotic nucleases and factors suggests differential activation and roles at various stages of cell differentiation and development. Therefore, a particular apoptotic stimulus might activate a different set of apoptotic nucleases in different cell types (Bortner et al., 1995). On the other hand, a particular cell type might also prompt a distinct selection of nucleolytic enzymes depending on the type of apoptotic stimuli (Solovyan et al., 1999). Consequently, the interplay of these diverse nucleases also necessitates regulation at various levels. Acinus, on account of its involvement in pre-mRNA splicing could provide one such regulatory function. Acinus was identified as a component of the ASAP complex, in association with SAP18 (Schwerk et al., 2003) and RNPS1, a general splicing activator (Mayeda et al., 1999). Identification of Acinus and RNPS1 as a component of functional spliceosomes (Rappsilber et al., 2002; Zhou et al., 2002) and their presence in the exon junction complex further substantiates the role of Acinus in splicing regulation (Tange et al., 2005). Additionally, various components of the apoptotic machinery are regulated by alternative splicing (Schwerk and Schulze-Osthoff, 2005), including the inhibitor of CAD, ICAD, which is expressed in two isoforms, ICAD-L and ICAD-S. Both these isoforms exhibit similar inhibitory activity but only ICAD-L is capable of assisting proper folding of the CAD polypeptide during its synthesis. Correspondingly, a recent study provided *in vivo* evidence in line with those presented here, illustrating the significance of splicing regulation of ICAD pre-mRNA in the process of apoptotic DNA fragmentation (Li et al., 2005). Essentially, the depletion of a splicing factor, an SR protein termed ASF/SF2, in a chicken cell line resulted in cell death with the cells displaying characteristic features of apoptosis except oligonucleosomal DNA fragmentation (Li et al., 2005) although HMW fragmentation and H2A.X phosphorylation was unaffected (Li and Manley, 2005). Subsequently, the loss of apoptotic DNA laddering was traced to a reversal in the ratio of long to short isoforms of ICAD. The reduced

levels of large isoform brought about by the switch in ICAD pre-mRNA alternative splicing plausibly resulted in the synthesis of improperly folded CAD thereby inhibiting oligonucleosomal DNA fragmentation. Depletion of Acinus could have a similar influence on the splicing patterns of factors involved in nuclear apoptotic changes. It is conceivable that, due to its presence in the ASAP complex, Acinus might regulate the splicing-activating function of its ASAP counterpart, RNPS1, which is a well-known general activator of pre-mRNA splicing. Alternatively, Acinus might itself act as a splicing regulator. Additionally, as a component of the EJC, Acinus and the ASAP components might also influence the later steps in gene expression such as mRNA export and nonsense-mediated mRNA decay (NMD) (Tange et al., 2005).

Regulation of the process of splicing enables a cell to progress smoothly through the cell cycle. Dysfunction of the splicing machinery, on the other hand, can severely influence not only the viability of the concerned cell but also the general survival of the organism. In *Caenorhabditis elegans*, gene targeting of certain splicing factors or a combination of them resulted in lethality (Longman et al., 2000). Similarly in Drosophila, a null allele of a gene encoding an SR protein resulted in lethality (Ring and Lis, 1994). A recent study (Li and Manley, 2005) on the effect of inactivation of the SR protein ASF/SF2 in chicken DT40 cells revealed a novel link between splicing and genomic stability. Depletion of ASF/SF2 caused nascent transcripts to anneal with the DNA forming DNA/RNA hybrid R loop structures which resulted in dsDNA breaks (Li and Manley, 2005). Therefore, one could speculate that DNA damage acquired in the absence of Acinus could activate the intrinsic apoptotic pathway resulting in an earlier activation of caspases in these cells.

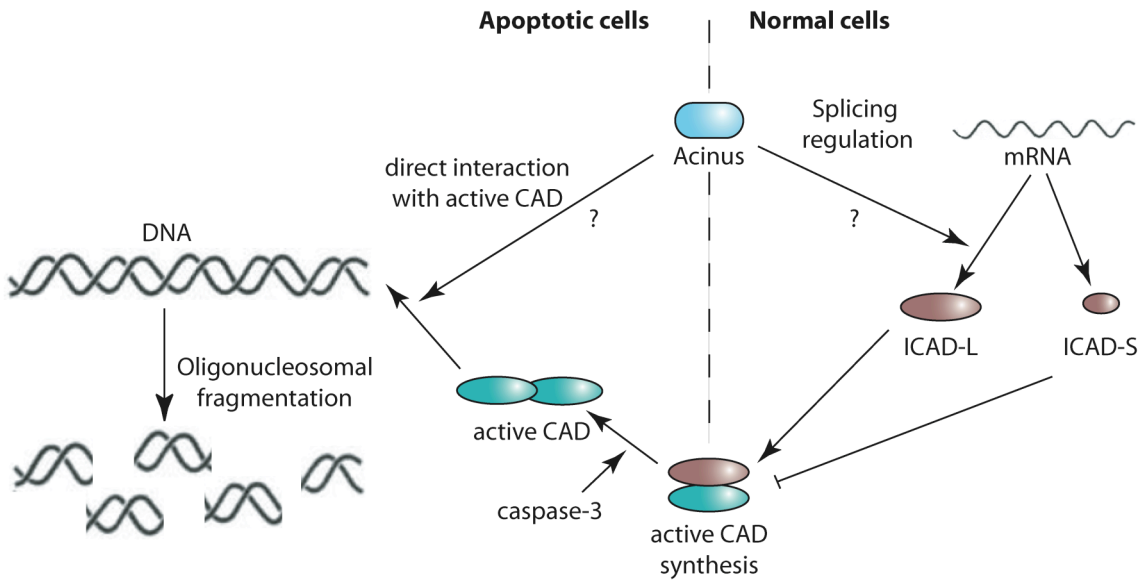

Figure 41: Scenario for the role of Acinus in nuclear apoptosis. In vivo knockdown of Acinus results in a severe impairment of apoptotic oligonucleosomal fragmentation. Two possible mechanisms by which Acinus could mediate this effect is described here. In the normal cell, Acinus could regulate synthesis of functional CAD by positively regulating ICAD-L splicing. Alternatively, Acinus could influence the access of CAD to DNA in an apoptotic cell thereby enhancing CADs nucleolytic activity.

Although the exact role of Acinus in apoptotic chromatin condensation and RNA splicing regulation, especially of apoptotic factors, remains to be established, these results point to a novel function of Acinus in the execution and possibly the regulation of apoptotic DNA fragmentation, particularly oligonucleosomal DNA laddering. In spite of the fact that Acinus influences the final stages of the 'execution' phase of the apoptotic process, the significance of such an involvement on the eventual death of the cell still has to be considered. Two separate reports have indicated that processes at the final stages of the death execution, such as the eventual engulfment of apoptotic bodies by phagocytes could influence the overall death rate (Hoeppner et al., 2001; Reddien et al., 2001). Moreover, a recent study presented evidence suggesting a role for CAD in maintaining genetic stability and preventing tumorigenesis (Yan et al., 2006). Therefore, it is plausible that Acinus, by virtue of its influence on DNA fragmentation and CAD function, may even influence the eventual cell death decision.

VIII. SUMMARY

Apoptosis is a morphologically distinct form of cell death that is characterized by the activation of caspases that execute, among other actions, the nuclear hallmarks of apoptosis. These nuclear changes that take place during the course of apoptosis are characterized by nuclear condensation and oligonucleosomal DNA fragmentation. An increased understanding of the nuclear events in apoptosis continues to be a prominent research focus within this field. Although significant progress has been made to specifically define and characterize the nuclear changes that occur in an apoptotic cell, events that essentially elicit and regulate nuclear condensation and fragmentation are largely unknown. A number of caspase-dependent and independent mechanisms have come to light in recent times. Amidst a myriad of other proteins that have been implicated during these last stages of apoptosis, is a protein of about 220 kDa called apoptotic chromatin condensation inducer in the nucleus (Acinus). A proteolytic fragment of Acinus, which is generated by cleavage of caspases and an unknown protease, has been implicated in mediating apoptotic chromatin condensation.

Stable cell lines in which Acinus isoforms were knocked down by inducible and reversible RNA interference (RNAi) were analyzed. Knockdown of Acinus resulted in reduced cell growth likely due to sensitization to apoptosis. In correlation with this, caspase activation was accelerated in the absence of Acinus. In contrast to published data, cells knocked-down for Acinus did not display any impairment in chromatin condensation. However, flow cytometric analysis of apoptotic Acinus knockdown cells showed reduced DNA processing. Subsequent analysis of oligonucleosomal DNA laddering during staurosporine-induced apoptosis in Acinus knockdown cells confirmed this result. High molecular weight (HMW) cleavage of DNA, another significant feature of the early nuclear changes during apoptosis, was not affected in apoptotic Acinus knockdown cells. Furthermore, analysis of phosphorylation of the histone variant, H2A.X as a marker of DNA double strand breaks confirmed an equally robust DNA cleavage in Acinus knockdown cells.

These results therefore question the direct involvement of Acinus in DNA condensation, but rather point to a role for Acinus in internucleosomal DNA cleavage during programmed cell death. Because the major nuclease implicated in oligonucleosomal DNA cleavage in apoptotic cells is CAD and since HMW DNA cleavage is not affected in Acinus knockdown cells, Acinus plausibly regulates oligonucleosomal DNA fragmentation by influencing the nucleolytic function of CAD. Although the exact mechanism by which this is attained remains to be deciphered, the results of this study points to a novel function of Acinus in DNA degradation during nuclear apoptosis.

IX. BIBLIOGRAPHY

Adam, S. A., Marr, R. S., and Gerace, L. (1990). Nuclear protein import in permeabilized mammalian cells requires soluble cytoplasmic factors. J Cell Biol *111*, 807-816.

Adams, J. M. (2003). Ways of dying: multiple pathways to apoptosis. Genes Dev *17*, 2481-2495.

Akgul, C., Moulding, D. A., and Edwards, S. W. (2004). Alternative splicing of Bcl-2-related genes: functional consequences and potential therapeutic applications. Cell Mol Life Sci *61*, 2189-2199.

Alberts, B. (2002). Molecular biology of the cell, 4th ed / Bruce Alberts ... [et al.] edn (New York, Garland Science).

Alnemri, E. S. (1997). Mammalian cell death proteases: a family of highly conserved aspartate specific cysteine proteases. J Cell Biochem *64*, 33-42.

Ambros, V. (2003). MicroRNA pathways in flies and worms: growth, death, fat, stress, and timing. Cell *113*, 673-676.

Ambros, V., Bartel, B., Bartel, D. P., Burge, C. B., Carrington, J. C., Chen, X., Dreyfuss, G., Eddy, S. R., Griffiths-Jones, S., Marshall, M.*, et al.* (2003). A uniform system for microRNA annotation. RNA *9*, 277-279.

Andrade, F., Roy, S., Nicholson, D., Thornberry, N., Rosen, A., and Casciola-Rosen, L. (1998). Granzyme B directly and efficiently cleaves several downstream caspase substrates: implications for CTL-induced apoptosis. Immunity *8*, 451-460.

Aravin, A. A., Lagos-Quintana, M., Yalcin, A., Zavolan, M., Marks, D., Snyder, B., Gaasterland, T., Meyer, J., and Tuschl, T. (2003). The small RNA profile during Drosophila melanogaster development. Dev Cell *5*, 337-350.

Aravind, L., Dixit, V. M., and Koonin, E. V. (1999). The domains of death: evolution of the apoptosis machinery. Trends Biochem Sci *24*, 47-53.

Aravind, L., and Koonin, E. V. (2000). SAP - a putative DNA-binding motif involved in chromosomal organization. Trends Biochem Sci *25*, 112-114.

Arnoult, D., Gaume, B., Karbowski, M., Sharpe, J. C., Cecconi, F., and Youle, R. J. (2003). Mitochondrial release of AIF and EndoG requires caspase activation downstream of Bax/Bak-mediated permeabilization. EMBO J *22*, 4385-4399.

Ashkenazi, A., and Dixit, V. M. (1999). Apoptosis control by death and decoy receptors. Curr Opin Cell Biol *11*, 255-260.

Baer, M., Nilsen, T. W., Costigan, C., and Altman, S. (1990). Structure and transcription of a human gene for H1 RNA, the RNA component of human RNase P. Nucleic Acids Res *18*,

97-103.

Barbieri, D., Troiano, L., Grassilli, E., Agnesini, C., Cristofalo, E. A., Monti, D., Capri, M., Cossarizza, A., and Franceschi, C. (1992). Inhibition of apoptosis by zinc: a reappraisal. Biochem Biophys Res Commun *187*, 1256-1261.

Bartel, D. P. (2004). MicroRNAs: genomics, biogenesis, mechanism, and function. Cell *116*, 281-297.

Benard, J., and Douc-Rasy, S. (2005). [Micro-RNA and oncogenesis]. Bull Cancer *92*, 757-762.

Bernstein, E., Caudy, A. A., Hammond, S. M., and Hannon, G. J. (2001). Role for a bidentate ribonuclease in the initiation step of RNA interference. Nature *409*, 363-366.

Black, D. L. (2003). Mechanisms of alternative pre-messenger RNA splicing. Annu Rev Biochem *72*, 291-336.

Boatright, K. M., Renatus, M., Scott, F. L., Sperandio, S., Shin, H., Pedersen, I. M., Ricci, J. E., Edris, W. A., Sutherlin, D. P., Green, D. R., and Salvesen, G. S. (2003). A unified model for apical caspase activation. Mol Cell *11*, 529-541.

Boatright, K. M., and Salvesen, G. S. (2003). Mechanisms of caspase activation. Curr Opin Cell Biol *15*, 725-731.

Boix, J., Llecha, N., Yuste, V. J., and Comella, J. X. (1997). Characterization of the cell death process induced by staurosporine in human neuroblastoma cell lines. Neuropharmacology *36*, 811-821.

Bortner, C. D., Oldenburg, N. B., and Cidlowski, J. A. (1995). The role of DNA fragmentation in apoptosis. Trends Cell Biol *5*, 21-26.

Bringold, F., and Serrano, M. (2000). Tumor suppressors and oncogenes in cellular senescence. Exp Gerontol *35*, 317-329.

Brown, D. G., Sun, X. M., and Cohen, G. M. (1993). Dexamethasone-induced apoptosis involves cleavage of DNA to large fragments prior to internucleosomal fragmentation. J Biol Chem *268*, 3037-3039.

Brummelkamp, T. R., Bernards, R., and Agami, R. (2002). A system for stable expression of short interfering RNAs in mammalian cells. Science *296*, 550-553.

Budihardjo, I., Oliver, H., Lutter, M., Luo, X., and Wang, X. (1999). Biochemical pathways of caspase activation during apoptosis. Annu Rev Cell Dev Biol *15*, 269-290.

Castedo, M., Hirsch, T., Susin, S. A., Zamzami, N., Marchetti, P., Macho, A., and Kroemer, G. (1996). Sequential acquisition of mitochondrial and plasma membrane alterations during early lymphocyte apoptosis. J Immunol *157*, 512-521.

Chai, J., Wu, Q., Shiozaki, E., Srinivasula, S. M., Alnemri, E. S., and Shi, Y. (2001). Crystal structure of a procaspase-7 zymogen: mechanisms of activation and substrate binding. Cell *107*, 399-407.

Chang, H. S., Lin, C. H., Chen, Y. C., and Yu, W. C. (2004). Using siRNA technique to generate transgenic animals with spatiotemporal and conditional gene knockdown. Am J Pathol *165*, 1535-1541.

Chen, C. Z., and Lodish, H. F. (2005). MicroRNAs as regulators of mammalian hematopoiesis. Semin Immunol *17*, 155-165.

Chen, Y., Stamatoyannopoulos, G., and Song, C. Z. (2003). Down-regulation of CXCR4 by inducible small interfering RNA inhibits breast cancer cell invasion in vitro. Cancer Res *63*, 4801-4804.

Cheung, W. L., Ajiro, K., Samejima, K., Kloc, M., Cheung, P., Mizzen, C. A., Beeser, A., Etkin, L. D., Chernoff, J., Earnshaw, W. C., and Allis, C. D. (2003). Apoptotic phosphorylation of histone H2B is mediated by mammalian sterile twenty kinase. Cell *113*, 507-517.

Cockerill, P. N., and Garrard, W. T. (1986). Chromosomal loop anchorage of the kappa immunoglobulin gene occurs next to the enhancer in a region containing topoisomerase II sites. Cell *44*, 273-282.

Cogoni, C., Irelan, J. T., Schumacher, M., Schmidhauser, T. J., Selker, E. U., and Macino, G. (1996). Transgene silencing of the al-1 gene in vegetative cells of Neurospora is mediated by a cytoplasmic effector and does not depend on DNA-DNA interactions or DNA methylation. EMBO J *15*, 3153-3163.

Cohen, G. M. (1997). Caspases: the executioners of apoptosis. Biochem J *326*, 1-16.

Coumoul, X., Li, W., Wang, R. H., and Deng, C. (2004). Inducible suppression of Fgfr2 and Survivin in ES cells using a combination of the RNA interference (RNAi) and the Cre-LoxP system. Nucleic Acids Res *32*, e85.

Croce, C. M., and Calin, G. A. (2005). miRNAs, cancer, and stem cell division. Cell *122*, 6-7.

Czauderna, F., Santel, A., Hinz, M., Fechtner, M., Durieux, B., Fisch, G., Leenders, F., Arnold, W., Giese, K., Klippel, A., and Kaufmann, J. (2003). Inducible shRNA expression for application in a prostate cancer mouse model. Nucleic Acids Res *31*, e127.

Danks, M. K., Qiu, J., Catapano, C. V., Schmidt, C. A., Beck, W. T., and Fernandes, D. J. (1994). Subcellular distribution of the alpha and beta topoisomerase II-DNA complexes stabilized by VM-26. Biochem Pharmacol *48*, 1785-1795.

Daugas, E., Nochy, D., Ravagnan, L., Loeffler, M., Susin, S. A., Zamzami, N., and Kroemer, G. (2000). Apoptosis-inducing factor (AIF): a ubiquitous mitochondrial oxidoreductase involved

in apoptosis. FEBS Lett *476*, 118-123.

Deas, O., Dumont, C., MacFarlane, M., Rouleau, M., Hebib, C., Harper, F., Hirsch, F., Charpentier, B., Cohen, G. M., and Senik, A. (1998). Caspase-independent cell death induced by anti-CD2 or staurosporine in activated human peripheral T lymphocytes. J Immunol *161*, 3375-3383.

Denault, J. B., and Salvesen, G. S. (2002). Caspases: keys in the ignition of cell death. Chem Rev *102*, 4489-4500.

Desagher, S., Osen-Sand, A., Nichols, A., Eskes, R., Montessuit, S., Lauper, S., Maundrell, K., Antonsson, B., and Martinou, J. C. (1999). Bid-induced conformational change of Bax is responsible for mitochondrial cytochrome c release during apoptosis. J Cell Biol *144*, 891-901.

Di Leonardo, A., Linke, S. P., Clarkin, K., and Wahl, G. M. (1994). DNA damage triggers a prolonged p53-dependent G1 arrest and long-term induction of Cip1 in normal human fibroblasts. Genes Dev *8*, 2540-2551.

Dimri, G. P., Lee, X., Basile, G., Acosta, M., Scott, G., Roskelley, C., Medrano, E. E., Linskens, M., Rubelj, I., Pereira-Smith, O., and et al. (1995). A biomarker that identifies senescent human cells in culture and in aging skin in vivo. Proc Natl Acad Sci U S A *92*, 9363-9367.

Doench, J. G., Petersen, C. P., and Sharp, P. A. (2003). siRNAs can function as miRNAs. Genes Dev *17*, 438-442.

Doench, J. G., and Sharp, P. A. (2004). Specificity of microRNA target selection in translational repression. Genes Dev *18*, 504-511.

Dunn, W. A., Jr. (1990a). Studies on the mechanisms of autophagy: formation of the autophagic vacuole. J Cell Biol *110*, 1923-1933.

Dunn, W. A., Jr. (1990b). Studies on the mechanisms of autophagy: maturation of the autophagic vacuole. J Cell Biol *110*, 1935-1945.

Dunn, W. A., Jr. (1994). Autophagy and related mechanisms of lysosome-mediated protein degradation. Trends Cell Biol *4*, 139-143.

Durrieu, F., Samejima, K., Fortune, J. M., Kandels-Lewis, S., Osheroff, N., and Earnshaw, W. C. (2000). DNA topoisomerase IIalpha interacts with CAD nuclease and is involved in chromatin condensation during apoptotic execution. Curr Biol *10*, 923-926.

Earnshaw, W. C., Martins, L. M., and Kaufmann, S. H. (1999). Mammalian caspases: structure, activation, substrates, and functions during apoptosis. Annu Rev Biochem *68*, 383-424.

Elbashir, S. M., Harborth, J., Lendeckel, W., Yalcin, A., Weber, K., and Tuschl, T. (2001a). Duplexes of 21-nucleotide RNAs mediate RNA interference in cultured mammalian cells.

Nature *411*, 494-498.

Elbashir, S. M., Harborth, J., Weber, K., and Tuschl, T. (2002). Analysis of gene function in somatic mammalian cells using small interfering RNAs. Methods *26*, 199-213.

Elbashir, S. M., Lendeckel, W., and Tuschl, T. (2001b). RNA interference is mediated by 21- and 22-nucleotide RNAs. Genes Dev *15*, 188-200.

Enari, M., Sakahira, H., Yokoyama, H., Okawa, K., Iwamatsu, A., and Nagata, S. (1998). A caspase-activated DNase that degrades DNA during apoptosis, and its inhibitor ICAD. Nature *391*, 43-50.

Ettorre, A., Andreassi, M., Anselmi, C., Neri, P., Andreassi, L., and Di Stefano, A. (2003). Involvement of oxidative stress in apoptosis induced by a mixture of isothiazolinones in normal human keratinocytes. J Invest Dermatol *121*, 328-336.

Filipski, J., Leblanc, J., Youdale, T., Sikorska, M., and Walker, P. R. (1990). Periodicity of DNA folding in higher order chromatin structures. EMBO J *9*, 1319-1327.

Fire, A., Xu, S., Montgomery, M. K., Kostas, S. A., Driver, S. E., and Mello, C. C. (1998). Potent and specific genetic interference by double-stranded RNA in Caenorhabditis elegans. Nature *391*, 806-811.

Fischer, U., Janicke, R. U., and Schulze-Osthoff, K. (2003). Many cuts to ruin: a comprehensive update of caspase substrates. Cell Death Differ *10*, 76-100.

Fisher, D. Z., Chaudhary, N., and Blobel, G. (1986). cDNA sequencing of nuclear lamins A and C reveals primary and secondary structural homology to intermediate filament proteins. Proc Natl Acad Sci U S A *83*, 6450-6454.

Formichi, P., Radi, E., Battisti, C., Tarquini, E., Leonini, A., Di Stefano, A., and Federico, A. (2006). Human fibroblasts undergo oxidative stress-induced apoptosis without internucleosomal DNA fragmentation. J Cell Physiol *208*, 289-297.

Formigli, L., Papucci, L., Tani, A., Schiavone, N., Tempestini, A., Orlandini, G. E., Capaccioli, S., and Orlandini, S. Z. (2000). Aponecrosis: morphological and biochemical exploration of a syncretic process of cell death sharing apoptosis and necrosis. J Cell Physiol *182*, 41-49.

Gasser, S. M., and Laemmli, U. K. (1986). The organisation of chromatin loops: characterization of a scaffold attachment site. EMBO J *5*, 511-518.

Gossen, M., and Bujard, H. (1992). Tight control of gene expression in mammalian cells by tetracycline-responsive promoters. Proc Natl Acad Sci U S A *89*, 5547-5551.

Gossen, M., Freundlieb, S., Bender, G., Muller, G., Hillen, W., and Bujard, H. (1995). Transcriptional activation by tetracyclines in mammalian cells. Science *268*, 1766-1769.

Greenberg, A. H. (1996). Granzyme B-induced apoptosis. Adv Exp Med Biol *406*, 219-228.

Griffiths, G. J., Dubrez, L., Morgan, C. P., Jones, N. A., Whitehouse, J., Corfe, B. M., Dive, C., and Hickman, J. A. (1999). Cell damage-induced conformational changes of the pro-apoptotic protein Bak in vivo precede the onset of apoptosis. J Cell Biol *144*, 903-914.

Gu, J., Dong, R. P., Zhang, C., McLaughlin, D. F., Wu, M. X., and Schlossman, S. F. (1999). Functional interaction of DFF35 and DFF45 with caspase-activated DNA fragmentation nuclease DFF40. J Biol Chem *274*, 20759-20762.

Guilly, M. N., Bensussan, A., Bourge, J. F., Bornens, M., and Courvalin, J. C. (1987). A human T lymphoblastic cell line lacks lamins A and C. EMBO J *6*, 3795-3799.

Guo, S., and Kemphues, K. J. (1995). par-1, a gene required for establishing polarity in C. elegans embryos, encodes a putative Ser/Thr kinase that is asymmetrically distributed. Cell *81*, 611-620.

Haanen, C., and Vermes, I. (1996). Apoptosis: programmed cell death in fetal development. Eur J Obstet Gynecol Reprod Biol *64*, 129-133.

Haase, A. D., Jaskiewicz, L., Zhang, H., Laine, S., Sack, R., Gatignol, A., and Filipowicz, W. (2005). TRBP, a regulator of cellular PKR and HIV-1 virus expression, interacts with Dicer and functions in RNA silencing. EMBO Rep *6*, 961-967.

Haley, B., and Zamore, P. D. (2004). Kinetic analysis of the RNAi enzyme complex. Nat Struct Mol Biol *11*, 599-606.

Hamilton, A. J., and Baulcombe, D. C. (1999). A species of small antisense RNA in posttranscriptional gene silencing in plants. Science *286*, 950-952.

Hammond, S. M., Bernstein, E., Beach, D., and Hannon, G. J. (2000). An RNA-directed nuclease mediates post-transcriptional gene silencing in Drosophila cells. Nature *404*, 293-296.

Hammond, S. M., Boettcher, S., Caudy, A. A., Kobayashi, R., and Hannon, G. J. (2001). Argonaute2, a link between genetic and biochemical analyses of RNAi. Science *293*, 1146-1150.

Han, J., Lee, Y., Yeom, K. H., Kim, Y. K., Jin, H., and Kim, V. N. (2004). The Drosha-DGCR8 complex in primary microRNA processing. Genes Dev *18*, 3016-3027.

Hernandez, N. (2001). Small nuclear RNA genes: a model system to study fundamental mechanisms of transcription. J Biol Chem *276*, 26733-26736.

Hillen, W., Gatz, C., Altschmied, L., Schollmeier, K., and Meier, I. (1983). Control of expression of the Tn10-encoded tetracycline resistance genes. Equilibrium and kinetic investigation of the regulatory reactions. J Mol Biol *169*, 707-721.

Hirata, H., Takahashi, A., Kobayashi, S., Yonehara, S., Sawai, H., Okazaki, T., Yamamoto, K.,

and Sasada, M. (1998). Caspases are activated in a branched protease cascade and control distinct downstream processes in Fas-induced apoptosis. J Exp Med *187*, 587-600.

Hirt, B. (1967). Selective extraction of polyoma DNA from infected mouse cell cultures. J Mol Biol *26*, 365-369.

Hoeppner, D. J., Hengartner, M. O., and Schnabel, R. (2001). Engulfment genes cooperate with ced-3 to promote cell death in Caenorhabditis elegans. Nature *412*, 202-206.

Hu, Y., Yao, J., Liu, Z., Liu, X., Fu, H., and Ye, K. (2005). Akt phosphorylates acinus and inhibits its proteolytic cleavage, preventing chromatin condensation. EMBO J *24*, 3543-3554.

Hutvagner, G. (2005). Small RNA asymmetry in RNAi: function in RISC assembly and gene regulation. FEBS Lett *579*, 5850-5857.

Ishigaki, Y., Li, X., Serin, G., and Maquat, L. E. (2001). Evidence for a pioneer round of mRNA translation: mRNAs subject to nonsense-mediated decay in mammalian cells are bound by CBP80 and CBP20. Cell *106*, 607-617.

Jacobs, J. J., Kieboom, K., Marino, S., DePinho, R. A., and van Lohuizen, M. (1999). The oncogene and Polycomb-group gene bmi-1 regulates cell proliferation and senescence through the ink4a locus. Nature *397*, 164-168.

Jacobson, M. D., Burne, J. F., and Raff, M. C. (1994). Programmed cell death and Bcl-2 protection in the absence of a nucleus. EMBO J *13*, 1899-1910.

Janicke, R. U., Sprengart, M. L., Wati, M. R., and Porter, A. G. (1998). Caspase-3 is required for DNA fragmentation and morphological changes associated with apoptosis. J Biol Chem *273*, 9357-9360.

Jiang, Z. H., and Wu, J. Y. (1999). Alternative splicing and programmed cell death. Proc Soc Exp Biol Med *220*, 64-72.

Kanellopoulou, C., Muljo, S. A., Kung, A. L., Ganesan, S., Drapkin, R., Jenuwein, T., Livingston, D. M., and Rajewsky, K. (2005). Dicer-deficient mouse embryonic stem cells are defective in differentiation and centromeric silencing. Genes Dev *19*, 489-501.

Kaufmann, S. H. (1989). Induction of endonucleolytic DNA cleavage in human acute myelogenous leukemia cells by etoposide, camptothecin, and other cytotoxic anticancer drugs: a cautionary note. Cancer Res *49*, 5870-5878.

Kaufmann, S. H., Desnoyers, S., Ottaviano, Y., Davidson, N. E., and Poirier, G. G. (1993). Specific proteolytic cleavage of poly(ADP-ribose) polymerase: an early marker of chemotherapy-induced apoptosis. Cancer Res *53*, 3976-3985.

Kaufmann, S. H., and Earnshaw, W. C. (2000). Induction of apoptosis by cancer chemotherapy. Exp Cell Res *256*, 42-49.

Kerr, J. F., Wyllie, A. H., and Currie, A. R. (1972). Apoptosis: a basic biological phenomenon with wide-ranging implications in tissue kinetics. Br J Cancer *26*, 239-257.

Korn, C., Scholz, S. R., Gimadutdinow, O., Lurz, R., Pingoud, A., and Meiss, G. (2005). Interaction of DNA fragmentation factor (DFF) with DNA reveals an unprecedented mechanism for nuclease inhibition and suggests that DFF can be activated in a DNA-bound state. J Biol Chem *280*, 6005-6015.

Kunath, T., Gish, G., Lickert, H., Jones, N., Pawson, T., and Rossant, J. (2003). Transgenic RNA interference in ES cell-derived embryos recapitulates a genetic null phenotype. Nat Biotechnol *21*, 559-561.

Kurz, D. J., Decary, S., Hong, Y., and Erusalimsky, J. D. (2000). Senescence-associated (beta)-galactosidase reflects an increase in lysosomal mass during replicative ageing of human endothelial cells. J Cell Sci *113 (Pt 20)*, 3613-3622.

Lagarkova, M. A., Iarovaia, O. V., and Razin, S. V. (1995). Large-scale fragmentation of mammalian DNA in the course of apoptosis proceeds via excision of chromosomal DNA loops and their oligomers. J Biol Chem *270*, 20239-20241.

Lai, E. C., Tam, B., and Rubin, G. M. (2005). Pervasive regulation of Drosophila Notch target genes by GY-box-, Brd-box-, and K-box-class microRNAs. Genes Dev *19*, 1067-1080.

Lazebnik, Y. A., Kaufmann, S. H., Desnoyers, S., Poirier, G. G., and Earnshaw, W. C. (1994). Cleavage of poly(ADP-ribose) polymerase by a proteinase with properties like ICE. Nature *371*, 346-347.

Le Hir, H., Gatfield, D., Izaurralde, E., and Moore, M. J. (2001). The exon-exon junction complex provides a binding platform for factors involved in mRNA export and nonsense-mediated mRNA decay. EMBO J *20*, 4987-4997.

Le Hir, H., Izaurralde, E., Maquat, L. E., and Moore, M. J. (2000). The spliceosome deposits multiple proteins 20-24 nucleotides upstream of mRNA exon-exon junctions. EMBO J *19*, 6860-6869.

Lechardeur, D., Drzymala, L., Sharma, M., Zylka, D., Kinach, R., Pacia, J., Hicks, C., Usmani, N., Rommens, J. M., and Lukacs, G. L. (2000). Determinants of the nuclear localization of the heterodimeric DNA fragmentation factor (ICAD/CAD). J Cell Biol *150*, 321-334.

Lechardeur, D., Xu, M., and Lukacs, G. L. (2004). Contrasting nuclear dynamics of the caspase-activated DNase (CAD) in dividing and apoptotic cells. J Cell Biol *167*, 851-862.

Lecoeur, H. (2002). Nuclear apoptosis detection by flow cytometry: influence of endogenous endonucleases. Exp Cell Res *277*, 1-14.

Lee, Y., Ahn, C., Han, J., Choi, H., Kim, J., Yim, J., Lee, J., Provost, P., Radmark, O., Kim, S.,

and Kim, V. N. (2003). The nuclear RNase III Drosha initiates microRNA processing. Nature *425*, 415-419.

Leist, M., and Jaattela, M. (2001). Four deaths and a funeral: from caspases to alternative mechanisms. Nat Rev Mol Cell Biol *2*, 589-598.

Lejeune, F., and Maquat, L. E. (2005). Mechanistic links between nonsense-mediated mRNA decay and pre-mRNA splicing in mammalian cells. Curr Opin Cell Biol *17*, 309-315.

Lewis, B. P., Burge, C. B., and Bartel, D. P. (2005). Conserved seed pairing, often flanked by adenosines, indicates that thousands of human genes are microRNA targets. Cell *120*, 15-20.

Li, P., Nijhawan, D., Budihardjo, I., Srinivasula, S. M., Ahmad, M., Alnemri, E. S., and Wang, X. (1997). Cytochrome c and dATP-dependent formation of Apaf-1/caspase-9 complex initiates an apoptotic protease cascade. Cell *91*, 479-489.

Li, T. K., Chen, A. Y., Yu, C., Mao, Y., Wang, H., and Liu, L. F. (1999). Activation of topoisomerase II-mediated excision of chromosomal DNA loops during oxidative stress. Genes Dev *13*, 1553-1560.

Li, X., and Manley, J. L. (2005). Inactivation of the SR protein splicing factor ASF/SF2 results in genomic instability. Cell *122*, 365-378.

Li, X., Wang, J., and Manley, J. L. (2005). Loss of splicing factor ASF/SF2 induces G2 cell cycle arrest and apoptosis, but inhibits internucleosomal DNA fragmentation. Genes Dev *19*, 2705-2714.

Liu, X., Li, P., Widlak, P., Zou, H., Luo, X., Garrard, W. T., and Wang, X. (1998). The 40-kDa subunit of DNA fragmentation factor induces DNA fragmentation and chromatin condensation during apoptosis. Proc Natl Acad Sci U S A *95*, 8461-8466.

Liu, X., Zou, H., Slaughter, C., and Wang, X. (1997). DFF, a heterodimeric protein that functions downstream of caspase-3 to trigger DNA fragmentation during apoptosis. Cell *89*, 175-184.

Liu, X., Zou, H., Widlak, P., Garrard, W., and Wang, X. (1999). Activation of the apoptotic endonuclease DFF40 (caspase-activated DNase or nuclease). Oligomerization and direct interaction with histone H1. J Biol Chem *274*, 13836-13840.

Longman, D., Johnstone, I. L., and Caceres, J. F. (2000). Functional characterization of SR and SR-related genes in Caenorhabditis elegans. EMBO J *19*, 1625-1637.

Lorenzo, H. K., Susin, S. A., Penninger, J., and Kroemer, G. (1999). Apoptosis inducing factor (AIF): a phylogenetically old, caspase-independent effector of cell death. Cell Death Differ *6*, 516-524.

Los, M., Wesselborg, S., and Schulze-Osthoff, K. (1999). The role of caspases in development,

immunity, and apoptotic signal transduction: lessons from knockout mice. Immunity *10*, 629-639.

Loyer, P., Trembley, J. H., Lahti, J. M., and Kidd, V. J. (1998). The RNP protein, RNPS1, associates with specific isoforms of the p34cdc2-related PITSLRE protein kinase in vivo. J Cell Sci *111 (Pt 11)*, 1495-1506.

Lu, Z., Zhang, C., and Zhai, Z. (2005). Nucleoplasmin regulates chromatin condensation during apoptosis. Proc Natl Acad Sci U S A *102*, 2778-2783.

Lydersen, B. K., and Pettijohn, D. E. (1980). Human-specific nuclear protein that associates with the polar region of the mitotic apparatus: distribution in a human/hamster hybrid cell. Cell *22*, 489-499.

Lykke-Andersen, J., Shu, M. D., and Steitz, J. A. (2000). Human Upf proteins target an mRNA for nonsense-mediated decay when bound downstream of a termination codon. Cell *103*, 1121-1131.

Mayeda, A., Badolato, J., Kobayashi, R., Zhang, M. Q., Gardiner, E. M., and Krainer, A. R. (1999). Purification and characterization of human RNPS1: a general activator of pre-mRNA splicing. EMBO J *18*, 4560-4570.

McConkey, D. J. (1996). Calcium-dependent, interleukin 1-converting enzyme inhibitor-insensitive degradation of lamin B1 and DNA fragmentation in isolated thymocyte nuclei. J Biol Chem *271*, 22398-22406.

Medema, J. P., Scaffidi, C., Kischkel, F. C., Shevchenko, A., Mann, M., Krammer, P. H., and Peter, M. E. (1997). FLICE is activated by association with the CD95 death-inducing signaling complex (DISC). EMBO J *16*, 2794-2804.

Modjtahedi, N., Giordanetto, F., Madeo, F., and Kroemer, G. (2006). Apoptosis-inducing factor: vital and lethal. Trends Cell Biol *16*, 264-272.

Morreau, H., Galjart, N. J., Gillemans, N., Willemsen, R., van der Horst, G. T., and d'Azzo, A. (1989). Alternative splicing of beta-galactosidase mRNA generates the classic lysosomal enzyme and a beta-galactosidase-related protein. J Biol Chem *264*, 20655-20663.

Nagata, S. (2005). DNA degradation in development and programmed cell death. Annu Rev Immunol *23*, 853-875.

Nagata, S., Nagase, H., Kawane, K., Mukae, N., and Fukuyama, H. (2003). Degradation of chromosomal DNA during apoptosis. Cell Death Differ *10*, 108-116.

Nagata, T., Kishi, H., Liu, Q. L., Matsuda, T., Imanaka, T., Tsukada, K., Kang, D., and Muraguchi, A. (2002). The regulation of DNAse activities in subcellular compartments of activated thymocytes. Immunology *105*, 399-406.

Napoli, C., Lemieux, C., and Jorgensen, R. (1990). Introduction of a Chimeric Chalcone Synthase Gene into Petunia Results in Reversible Co-Suppression of Homologous Genes in trans. Plant Cell *2*, 279-289.

Nicholson, D. W., and Thornberry, N. A. (1997). Caspases: killer proteases. Trends Biochem Sci *22*, 299-306.

Nicoletti, I., Migliorati, G., Pagliacci, M. C., Grignani, F., and Riccardi, C. (1991). A rapid and simple method for measuring thymocyte apoptosis by propidium iodide staining and flow cytometry. J Immunol Methods *139*, 271-279.

Oberhammer, F., Wilson, J. W., Dive, C., Morris, I. D., Hickman, J. A., Wakeling, A. E., Walker, P. R., and Sikorska, M. (1993). Apoptotic death in epithelial cells: cleavage of DNA to 300 and/or 50 kb fragments prior to or in the absence of internucleosomal fragmentation. EMBO J *12*, 3679-3684.

Oppenheim, R. W. (1991). Cell death during development of the nervous system. Annu Rev Neurosci *14*, 453-501.

Patel, T., Gores, G. J., and Kaufmann, S. H. (1996). The role of proteases during apoptosis. Faseb J *10*, 587-597.

Pienta, K. J., and Coffey, D. S. (1984). A structural analysis of the role of the nuclear matrix and DNA loops in the organization of the nucleus and chromosome. J Cell Sci Suppl *1*, 123-135.

Quignon, F., De Bels, F., Koken, M., Feunteun, J., Ameisen, J. C., and de The, H. (1998). PML induces a novel caspase-independent death process. Nat Genet *20*, 259-265.

Rao, L., Perez, D., and White, E. (1996). Lamin proteolysis facilitates nuclear events during apoptosis. J Cell Biol *135*, 1441-1455.

Rappsilber, J., Ryder, U., Lamond, A. I., and Mann, M. (2002). Large-scale proteomic analysis of the human spliceosome. Genome Res *12*, 1231-1245.

Reddien, P. W., Cameron, S., and Horvitz, H. R. (2001). Phagocytosis promotes programmed cell death in C. elegans. Nature *412*, 198-202.

Riedl, S. J., Fuentes-Prior, P., Renatus, M., Kairies, N., Krapp, S., Huber, R., Salvesen, G. S., and Bode, W. (2001). Structural basis for the activation of human procaspase-7. Proc Natl Acad Sci U S A *98*, 14790-14795.

Ring, H. Z., and Lis, J. T. (1994). The SR protein B52/SRp55 is essential for Drosophila development. Mol Cell Biol *14*, 7499-7506.

Robertson, J. D., Orrenius, S., and Zhivotovsky, B. (2000). Review: nuclear events in apoptosis. J Struct Biol *129*, 346-358.

Rodriguez, J., and Lazebnik, Y. (1999). Caspase-9 and APAF-1 form an active holoenzyme.

Genes Dev *13*, 3179-3184.

Rogakou, E. P., Nieves-Neira, W., Boon, C., Pommier, Y., and Bonner, W. M. (2000). Initiation of DNA fragmentation during apoptosis induces phosphorylation of H2AX histone at serine 139. J Biol Chem *275*, 9390-9395.

Rogakou, E. P., Pilch, D. R., Orr, A. H., Ivanova, V. S., and Bonner, W. M. (1998). DNA double-stranded breaks induce histone H2AX phosphorylation on serine 139. J Biol Chem *273*, 5858-5868.

Roopra, A., Sharling, L., Wood, I. C., Briggs, T., Bachfischer, U., Paquette, A. J., and Buckley, N. J. (2000). Transcriptional repression by neuron-restrictive silencer factor is mediated via the Sin3-histone deacetylase complex. Mol Cell Biol *20*, 2147-2157.

Ruchaud, S., Korfali, N., Villa, P., Kottke, T. J., Dingwall, C., Kaufmann, S. H., and Earnshaw, W. C. (2002). Caspase-6 gene disruption reveals a requirement for lamin A cleavage in apoptotic chromatin condensation. EMBO J *21*, 1967-1977.

Sahara, S., Aoto, M., Eguchi, Y., Imamoto, N., Yoneda, Y., and Tsujimoto, Y. (1999). Acinus is a caspase-3-activated protein required for apoptotic chromatin condensation. Nature *401*, 168-173.

Sakahira, H., Enari, M., and Nagata, S. (1998). Cleavage of CAD inhibitor in CAD activation and DNA degradation during apoptosis. Nature *391*, 96-99.

Samejima, K., and Earnshaw, W. C. (1998). ICAD/DFF regulator of apoptotic nuclease is nuclear. Exp Cell Res *243*, 453-459.

Samejima, K., and Earnshaw, W. C. (2000). Differential localization of ICAD-L and ICAD-S in cells due to removal of a C-terminal NLS from ICAD-L by alternative splicing. Exp Cell Res *255*, 314-320.

Samejima, K., and Earnshaw, W. C. (2005). Trashing the genome: the role of nucleases during apoptosis. Nat Rev Mol Cell Biol *6*, 677-688.

Schulze-Osthoff, K., Walczak, H., Droge, W., and Krammer, P. H. (1994). Cell nucleus and DNA fragmentation are not required for apoptosis. J Cell Biol *127*, 15-20.

Schwerk, C., Prasad, J., Degenhardt, K., Erdjument-Bromage, H., White, E., Tempst, P., Kidd, V. J., Manley, J. L., Lahti, J. M., and Reinberg, D. (2003). ASAP, a novel protein complex involved in RNA processing and apoptosis. Mol Cell Biol *23*, 2981-2990.

Schwerk, C., and Schulze-Osthoff, K. (2005). Regulation of apoptosis by alternative pre-mRNA splicing. Mol Cell *19*, 1-13.

Serrano, M., and Blasco, M. A. (2001). Putting the stress on senescence. Curr Opin Cell Biol *13*, 748-753.

Serrano, M., Lin, A. W., McCurrach, M. E., Beach, D., and Lowe, S. W. (1997). Oncogenic ras provokes premature cell senescence associated with accumulation of p53 and p16INK4a. Cell *88*, 593-602.

Sharif-Askari, E., Alam, A., Rheaume, E., Beresford, P. J., Scotto, C., Sharma, K., Lee, D., DeWolf, W. E., Nuttall, M. E., Lieberman, J., and Sekaly, R. P. (2001). Direct cleavage of the human DNA fragmentation factor-45 by granzyme B induces caspase-activated DNase release and DNA fragmentation. EMBO J *20*, 3101-3113.

Solovyan, V., Bezvenyuk, Z., Huotari, V., Tapiola, T., and Salminen, A. (1999). Distinct mechanisms underlay DNA disintegration during apoptosis induced by genotoxic and nongenotoxic agents in neuroblastoma cells. Neurochem Int *34*, 465-472.

Stennicke, H. R., Deveraux, Q. L., Humke, E. W., Reed, J. C., Dixit, V. M., and Salvesen, G. S. (1999). Caspase-9 can be activated without proteolytic processing. J Biol Chem *274*, 8359-8362.

Stewart, C., and Burke, B. (1987). Teratocarcinoma stem cells and early mouse embryos contain only a single major lamin polypeptide closely resembling lamin B. Cell *51*, 383-392.

Strack, S., Cribbs, J. T., and Gomez, L. (2004). Critical role for protein phosphatase 2A heterotrimers in mammalian cell survival. J Biol Chem *279*, 47732-47739.

Stroh, C., and Schulze-Osthoff, K. (1998). Death by a thousand cuts: an ever increasing list of caspase substrates. Cell Death Differ *5*, 997-1000.

Sun, Z. W., and Hampsey, M. (1999). A general requirement for the Sin3-Rpd3 histone deacetylase complex in regulating silencing in Saccharomyces cerevisiae. Genetics *152*, 921-932.

Susin, S. A., Daugas, E., Ravagnan, L., Samejima, K., Zamzami, N., Loeffler, M., Costantini, P., Ferri, K. F., Irinopoulou, T., Prevost, M. C.*, et al.* (2000). Two distinct pathways leading to nuclear apoptosis. J Exp Med *192*, 571-580.

Susin, S. A., Lorenzo, H. K., Zamzami, N., Marzo, I., Snow, B. E., Brothers, G. M., Mangion, J., Jacotot, E., Costantini, P., Loeffler, M.*, et al.* (1999). Molecular characterization of mitochondrial apoptosis-inducing factor. Nature *397*, 441-446.

Tabara, H., Sarkissian, M., Kelly, W. G., Fleenor, J., Grishok, A., Timmons, L., Fire, A., and Mello, C. C. (1999). The rde-1 gene, RNA interference, and transposon silencing in C. elegans. Cell *99*, 123-132.

Tange, T. O., Shibuya, T., Jurica, M. S., and Moore, M. J. (2005). Biochemical analysis of the EJC reveals two new factors and a stable tetrameric protein core. RNA *11*, 1869-1883.

Thomas, D. A., Du, C., Xu, M., Wang, X., and Ley, T. J. (2000). DFF45/ICAD can be directly

processed by granzyme B during the induction of apoptosis. Immunity *12*, 621-632.

Thornberry, N. A., and Lazebnik, Y. (1998). Caspases: enemies within. Science *281*, 1312-1316.

Toussaint, O., Medrano, E. E., and von Zglinicki, T. (2000). Cellular and molecular mechanisms of stress-induced premature senescence (SIPS) of human diploid fibroblasts and melanocytes. Exp Gerontol *35*, 927-945.

Tschopp, J., Martinon, F., and Burns, K. (2003). NALPs: a novel protein family involved in inflammation. Nat Rev Mol Cell Biol *4*, 95-104.

Tuschl, T. (2002). Expanding small RNA interference. Nat Biotechnol *20*, 446-448.

Ucker, D. S., Obermiller, P. S., Eckhart, W., Apgar, J. R., Berger, N. A., and Meyers, J. (1992). Genome digestion is a dispensable consequence of physiological cell death mediated by cytotoxic T lymphocytes. Mol Cell Biol *12*, 3060-3069.

Ura, S., Masuyama, N., Graves, J. D., and Gotoh, Y. (2001). Caspase cleavage of MST1 promotes nuclear translocation and chromatin condensation. Proc Natl Acad Sci U S A *98*, 10148-10153.

Van Criekinge, W., Beyaert, R., Van de Craen, M., Vandenabeele, P., Schotte, P., De Valck, D., and Fiers, W. (1996). Functional characterization of the prodomain of interleukin-1beta-converting enzyme. J Biol Chem *271*, 27245-27248.

van de Wetering, M., Oving, I., Muncan, V., Pon Fong, M. T., Brantjes, H., van Leenen, D., Holstege, F. C., Brummelkamp, T. R., Agami, R., and Clevers, H. (2003). Specific inhibition of gene expression using a stably integrated, inducible small-interfering-RNA vector. EMBO Rep *4*, 609-615.

Walker, P. R., Leblanc, J., Carson, C., Ribecco, M., and Sikorska, M. (1999). Neither caspase-3 nor DNA fragmentation factor is required for high molecular weight DNA degradation in apoptosis. Ann N Y Acad Sci *887*, 48-59.

Wang, X. (2001). The expanding role of mitochondria in apoptosis. Genes Dev *15*, 2922-2933.

Wesselborg, S., Engels, I. H., Rossmann, E., Los, M., and Schulze-Osthoff, K. (1999). Anticancer drugs induce caspase-8/FLICE activation and apoptosis in the absence of CD95 receptor/ligand interaction. Blood *93*, 3053-3063.

Widlak, P., Li, P., Wang, X., and Garrard, W. T. (2000). Cleavage preferences of the apoptotic endonuclease DFF40 (caspase-activated DNase or nuclease) on naked DNA and chromatin substrates. J Biol Chem *275*, 8226-8232.

Wieder, T., Geilen, C. C., Kolter, T., Sadeghlar, F., Sandhoff, K., Brossmer, R., Ihrig, P., Perry, D., Orfanos, C. E., and Hannun, Y. A. (1997). Bcl-2 antagonizes apoptotic cell death induced by two new ceramide analogues. FEBS Lett *411*, 260-264.

Wolf, B. B., Schuler, M., Echeverri, F., and Green, D. R. (1999). Caspase-3 is the primary activator of apoptotic DNA fragmentation via DNA fragmentation factor-45/inhibitor of caspase-activated DNase inactivation. J Biol Chem *274*, 30651-30656.

Woo, M., Hakem, R., Soengas, M. S., Duncan, G. S., Shahinian, A., Kagi, D., Hakem, A., McCurrach, M., Khoo, W., Kaufman, S. A*., et al.* (1998). Essential contribution of caspase 3/CPP32 to apoptosis and its associated nuclear changes. Genes Dev *12*, 806-819.

Wyllie, A. H., Kerr, J. F., and Currie, A. R. (1980). Cell death: the significance of apoptosis. Int Rev Cytol *68*, 251-306.

Xia, H., Mao, Q., Paulson, H. L., and Davidson, B. L. (2002). siRNA-mediated gene silencing in vitro and in vivo. Nat Biotechnol *20*, 1006-1010.

Yan, B., Wang, H., Peng, Y., Hu, Y., Wang, H., Zhang, X., Chen, Q., Bedford, J. S., Dewhirst, M. W., and Li, C. Y. (2006). A unique role of the DNA fragmentation factor in maintaining genomic stability. Proc Natl Acad Sci U S A *103*, 1504-1509.

Yao, F., Svensjo, T., Winkler, T., Lu, M., Eriksson, C., and Eriksson, E. (1998). Tetracycline repressor, tetR, rather than the tetR-mammalian cell transcription factor fusion derivatives, regulates inducible gene expression in mammalian cells. Hum Gene Ther *9*, 1939-1950.

Yuste, V. J., Bayascas, J. R., Llecha, N., Sanchez-Lopez, I., Boix, J., and Comella, J. X. (2001). The absence of oligonucleosomal DNA fragmentation during apoptosis of IMR-5 neuroblastoma cells: disappearance of the caspase-activated DNase. J Biol Chem *276*, 22323-22331.

Zamore, P. D., and Haley, B. (2005). Ribo-gnome: the big world of small RNAs. Science *309*, 1519-1524.

Zamore, P. D., Tuschl, T., Sharp, P. A., and Bartel, D. P. (2000). RNAi: double-stranded RNA directs the ATP-dependent cleavage of mRNA at 21 to 23 nucleotide intervals. Cell *101*, 25-33.

Zamzami, N., and Kroemer, G. (1999). Condensed matter in cell death. Nature *401*, 127-128.

Zhang, J., Liu, X., Scherer, D. C., van Kaer, L., Wang, X., and Xu, M. (1998). Resistance to DNA fragmentation and chromatin condensation in mice lacking the DNA fragmentation factor 45. Proc Natl Acad Sci U S A *95*, 12480-12485.

Zhang, J., Wang, X., Bove, K. E., and Xu, M. (1999). DNA fragmentation factor 45-deficient cells are more resistant to apoptosis and exhibit different dying morphology than wild-type control cells. J Biol Chem *274*, 37450-37454.

Zhang, Y., Iratni, R., Erdjument-Bromage, H., Tempst, P., and Reinberg, D. (1997). Histone deacetylases and SAP18, a novel polypeptide, are components of a human Sin3 complex.

Cell *89*, 357-364.

Zheng, T. S., Hunot, S., Kuida, K., and Flavell, R. A. (1999). Caspase knockouts: matters of life and death. Cell Death Differ *6*, 1043-1053.

Zheng, T. S., Schlosser, S. F., Dao, T., Hingorani, R., Crispe, I. N., Boyer, J. L., and Flavell, R. A. (1998). Caspase-3 controls both cytoplasmic and nuclear events associated with Fas-mediated apoptosis in vivo. Proc Natl Acad Sci U S A *95*, 13618-13623.

Zhivotovsky, B., Gahm, A., and Orrenius, S. (1997). Two different proteases are involved in the proteolysis of lamin during apoptosis. Biochem Biophys Res Commun *233*, 96-101.

Zhou, Z., Licklider, L. J., Gygi, S. P., and Reed, R. (2002). Comprehensive proteomic analysis of the human spliceosome. Nature *419*, 182-185.

Erklärung

Die hier vorgelegte Dissertation habe ich eigenständig und ohne unerlaubte Hilfe angefertigt. Die Dissertation wurde in der vorgelegten oder in ähnlicher Form noch bei keiner anderen Institution eingereicht. Ich habe bisher keine erfolglosen Promotionsversuche unternommen.

Düsseldorf, den 20 Nov 2006

Alvin Paul Joselin